



Naturally inspired chimeric quinolone derivatives to reverse bacterial drug resistance

Qi Wen^{a,1}, Yuhang He^{b,1}, Jiaying Chi^{c,1}, Luyao Wang^d, Yixuan Ren^b, Xiaoke Niu^d, Yanqing Yang^f, Kang Chen^a, Qi Zhu^a, Juncheng Lin^a, Yanghui Xiang^e, Junqiu Xie^b, Wenteng Chen^a, Yongping Yu^a, Baohong Wang^e, Bo Wang^{d,*}, Ying Zhang^{e,**}, Chao Lu^{c,***}, Kairong Wang^{b,****}, Peng Teng^{a,j,*****} Ruhong Zhou^{f,g,h,i}

^a Institute of Drug Discovery and Design, College of Pharmaceutical Sciences, Zhejiang University, 866 Yuhangtang Rd, Hangzhou, 310058, Zhejiang, China

^b Key Laboratory of Preclinical Study for New Drugs of Gansu Province, Institute of Biochemistry and Molecular Biology, School of Basic Medical Sciences, Lanzhou University, West Donggang Road 199, Lanzhou, 730000, China

^c State Key Laboratory of Bioactive Molecules and Druggability Assessment, Guangdong Basic Research Center of Excellence for Natural Bioactive Molecules and Discovery of Innovative Drugs, College of Pharmacy, Jinan University, Guangzhou, 511436, China

^d School of Pharmacy, Nanjing University of Chinese Medicine, Nanjing, China

^e State Key Laboratory for Diagnosis and Treatment of Infectious Diseases, National Clinical Research Center for Infectious Diseases, The First Affiliated Hospital, Zhejiang University School of Medicine, Hangzhou, 310003, China

^f Zhejiang Key Laboratory of Cell and Molecular Intelligent Design and Development, Institute of Quantitative Biology, College of Life Sciences, Zhejiang University, Hangzhou, 310058, China

^g Shanghai Institute for Advanced Study, Zhejiang University, Shanghai, China

^h Cancer Center, Zhejiang University, Hangzhou, Zhejiang, China

ⁱ Department of Chemistry, Columbia University, New York, NY, USA

^j National Key Laboratory of Advanced Drug Delivery and Release Systems, Zhejiang University, Hangzhou, 310058, China

ARTICLE INFO

Keywords:

Antimicrobial resistance
Host defense peptide
Chimeric quinolone antibiotic
Membrane disruption
Reverse drug resistance
In vivo antimicrobial activity

ABSTRACT

Antimicrobial resistance poses an urgent threat to global health, underscoring the critical need for new antibacterial drugs. Ciprofloxacin, a third-generation quinolone antibiotic, is used to treat different types of bacterial infections; however, it often results in the rapid emergence of resistance in clinical settings. Inspired by low susceptibility to antimicrobial resistance of natural antimicrobial peptides, we herein propose a host defense peptide-mimicking strategy for designing chimeric quinolone derivatives which may reduce the likelihood of antibacterial resistance. This strategy involves the incorporation of deliberately designed amphiphilic moieties into ciprofloxacin to mimic the structural characteristics and resistance-evading properties of host defense peptides. A resulting chimeric compound **IPMCL-28b**, carrying a rigid linker and three cationic amino acids along with a lipophilic acyl n-decanoyl tail, exhibited potent activity against a panel of multidrug-resistant bacterial strains by endowing the ciprofloxacin derivatives with additional ability to disrupt bacterial cell membranes. Molecular dynamics simulations showed that **IPMCL-28b** demonstrates significantly stronger disruptive interactions with cell membranes than ciprofloxacin. This compound not only demonstrated high selectivity with low hemolysis side effect, but also significantly reduced the likelihood of resistance development compared with ciprofloxacin. Excitingly, **IPMCL-28b** demonstrated highly enhanced *in vivo* antimicrobial activity against methicillin-resistant *Staphylococcus aureus* (MRSA) with a 99.99 % (4.4 log) reduction in skin

This article is part of a special issue entitled: Antibacterial Agents published in European Journal of Medicinal Chemistry.

* Corresponding authors.

** Corresponding authors.

*** Corresponding authors.

**** Corresponding author.

***** Corresponding author. Institute of Drug Discovery and Design, College of Pharmaceutical Sciences, Zhejiang University, 866 Yuhangtang Rd, Hangzhou, 310058, Zhejiang, China.

E-mail addresses: bwang@njucm.edu.cn (B. Wang), yzhang207@zju.edu.cn (Y. Zhang), chaolu@jnu.edu.cn (C. Lu), wangkr@lzu.edu.cn (K. Wang), pengteng@zju.edu.cn (P. Teng).

¹ These authors contributed equally to this work.

<https://doi.org/10.1016/j.ejmech.2025.117496>

Received 6 February 2025; Received in revised form 5 March 2025; Accepted 8 March 2025

Available online 12 March 2025

0223-5234/© 2025 Elsevier Masson SAS. All rights are reserved, including those for text and data mining, AI training, and similar technologies.

bacterial load after a single dose. These findings highlight the potential of host defense peptides-mimicking amphiphilic ciprofloxacin derivatives to reverse antibiotic resistance and mitigate the development of antimicrobial resistance.

1. Introduction

Multidrug-resistant bacterial infections pose a significant global health threat, accounting for the majority of hospital-acquired infections and contributing to substantial morbidity and mortality in healthcare systems worldwide [1–3]. The third-generation fluoroquinolone ciprofloxacin, introduced into clinical practice nearly three decades ago, has been widely used to treat various bacterial infections due to its excellent antimicrobial activity, favorable pharmacokinetics, and minimal side effects [4–6]. Ciprofloxacin exerts its antimicrobial effects by inhibiting bacterial DNA synthesis through disruption of the enzymes DNA gyrase and topoisomerase IV, leading to chromosome breakage in bacteria [7, 8]. However, the widespread emergence and dissemination of antibiotic-resistant pathogens have significantly compromised its effectiveness [3,9]. Resistance mechanisms against quinolones include chromosomal mutations and/or the acquisition of plasmid-borne resistance genes, which alter topoisomerase targets, chemically modify quinolones, and/or reduce drug accumulation via decreased uptake or increased efflux [10–12]. To combat ciprofloxacin resistance, researchers have been exploring new strategies, including the development of ciprofloxacin prodrugs and co-drugs, as illustrated in Fig. 1a

[13–20]. These strategies aimed to increase the selectivity of ciprofloxacin and improve treatment efficacy while reducing the side effects and preserving the microbiota, which in turn helps reduce secondary infections and the subsequent need for additional antibiotic use. Despite these progress, new approaches to address the resistance of ciprofloxacin remain unmet.

Host defense peptides (HDPs), also known as antimicrobial peptides (AMPs), are a class of natural peptides derived from living organisms that have shown promise as antibacterial agents due to their broad-spectrum activity and low susceptibility to antimicrobial resistance [21–28]. The amphiphilic structures of HDPs comprise cationic, hydrophilic and hydrophobic regions, which imparts selectivity for bacterial cells over mammalian cells [29,30]. The cationic residues of HDPs are attracted to the negatively charged bacterial membranes, enabling their lipophilic side chains to insert into the lipid bilayer and disrupt membrane stability and integrity, ultimately leading to bacterial cell death [31–34]. This mode of action also underlies the reduced tendency of HDPs to induce resistance in bacteria [35,36]. Despite their potential, clinical applications of HDPs have been limited. Of the more than 3300 HDPs identified, only a few have made it to market (such as bacitracin [37], dalbavancin [27], and cepeleganan [27]) due to challenges such as

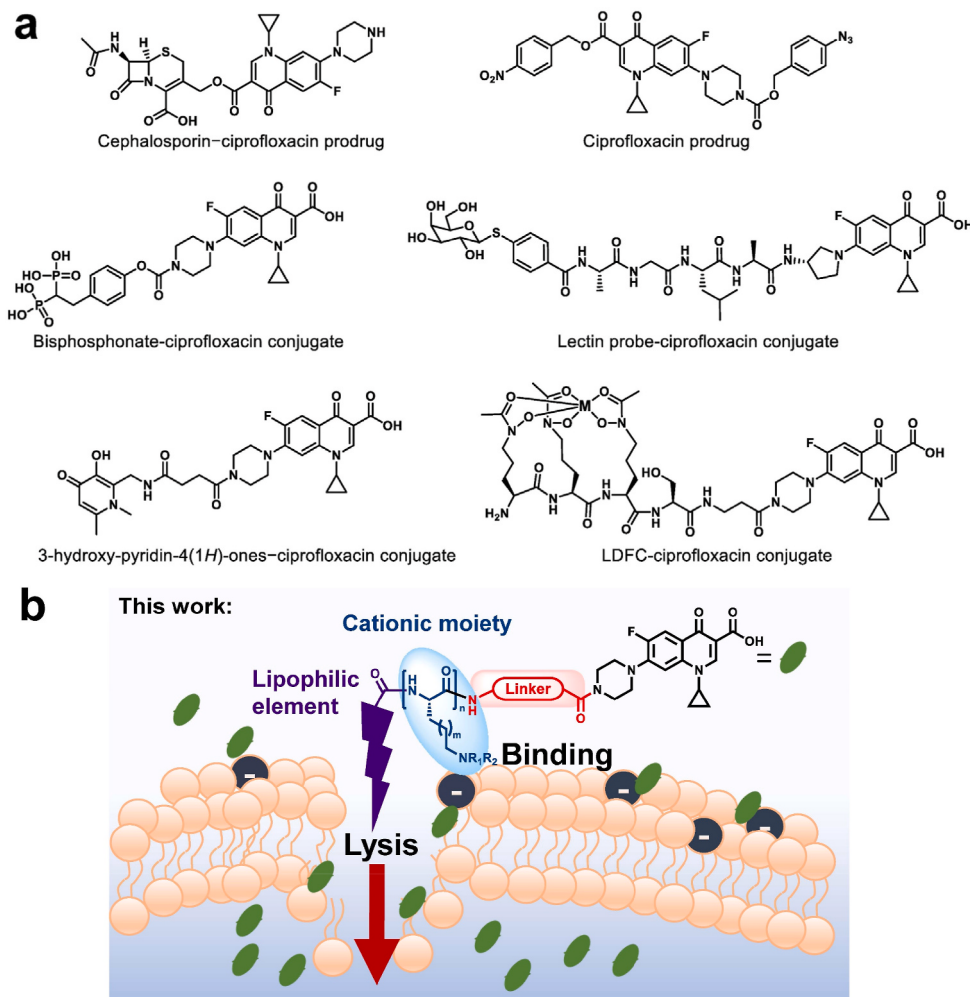


Fig. 1. (a) Selected representative examples of ciprofloxacin prodrugs and co-drugs. (b) Chimeric ciprofloxacin derivatives investigated in this work.

enzymatic instability *in vivo*, moderate efficacy, potential immunogenicity, and high production costs [25,38–41]. To address these limitations, researchers have focused on developing structurally simpler small-molecule HDP mimetics that retain the beneficial properties of HDPs while overcoming their drawbacks, such as stability and cost issues. Over the past three decades, persistent efforts have been made which have highlighted the therapeutic potential of small-molecule HDP-mimicking antibiotics, offering a promising avenue for the development of novel antibacterial agents [18,42–72].

In light of the aforementioned challenges, we proposed an effective strategy to develop host defense peptides-mimicking chimeric quinolone derivatives capable of mitigating antibiotic resistance. Specifically, we designed and synthesized a series of amphiphilic membrane-targeting ciprofloxacin derivatives by incorporating membrane-disrupting moieties of HDPs into the ciprofloxacin scaffold. Among these, compound **IPMCL-28b**, containing a rigid linker and three cationic amino acids along with a lipophilic acyl n-decanoyl tail, emerged as the most promising candidate, demonstrating impressive *in vitro* antibacterial activity and membrane selectivity against both Gram-positive and Gram-negative bacteria, including clinically relevant multidrug-resistant strains. Further investigations into the antibacterial mechanisms revealed that the quinolone derivative could kill the bacteria partly by mimicking the mechanisms of HDPs. Notably, the host defense peptides-mimicking chimeric derivative reversed the ciprofloxacin resistance successfully. Moreover, enhanced *in vivo* antibacterial efficacy and safety of **IPMCL-28b** were demonstrated in a murine subcutaneous abscess model infected with methicillin-resistant *Staphylococcus aureus* (MRSA). Taken together, this study provides valuable insights into the development of new antimicrobials using a host defense peptides-mimicking strategy by incorporating the HDP mimics into a quinolone scaffold, offering a promising and perhaps universal strategy for combating multidrug-resistant bacterial infections.

1.1. Design and synthesis of amphiphilic ciprofloxacin derivatives

Based on the structure-activity relationship of fluoroquinolone antibiotics [8,11], we conjugated an amphiphilic moiety to the nitrogen atom of the piperazine ring. As illustrated in **Scheme 1**, the synthesis began with commercially available ciprofloxacin. The carboxylic acid group on the quinolone core was protected as a methyl ester to furnish intermediate **1**, which was subsequently coupled with cationic amino acids (lysine, arginine, and histidine) under standard amidation conditions using 1-hydroxybenzotriazole (HOEt), 1-(3-dimethylaminopropyl)-3-ethylcarbodiimide (EDC), and N,N-diisopropylethylamine (DIPEA) in DMF. After deprotection, compounds **4a–c**, containing single cationic amino acids, were obtained in moderate yields.

^aReagents and conditions: (a) H₂SO₄, MeOH, reflux, 12 h. (b)

Boc-NH-amino acid, HOEt, EDC, DIPEA, DMF, room temperature (r.t.), 5 h. (c) LiOH, MeOH/H₂O, r.t., 2 h. (d) TFA/DCM, r.t., 2 h.

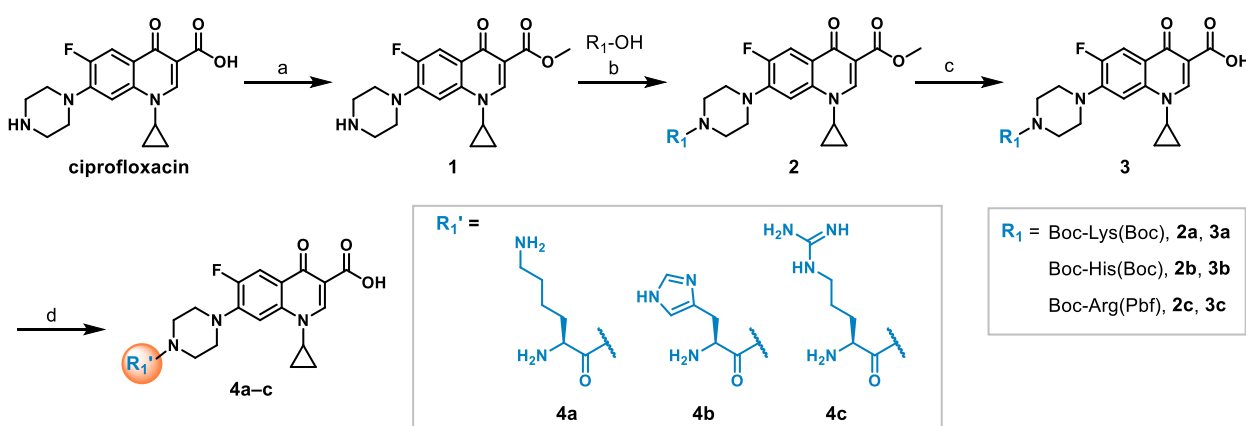
^bReagents and conditions: (a) Fmoc-NH amino acid, DIPEA, DCM, r.t., 2 h. (b) 20 % piperidine/DMF, r.t., 10 min (× 2). (c) HCTU, DIPEA, DMF, r.t., 4 h; then cleave from resin using 20 % HFIP/DCM, r.t., 2 h. (d) Ciprofloxacin, EDC, HOEt, DIPEA, DMF, r.t., 5 h. (e) TFA/DCM, r.t., 2 h.

Next, hydrophobic groups were introduced at the N-terminal of the amino acids. To streamline the synthesis, solid-phase peptide synthesis (SPPS) was employed. As shown in **Scheme 2**, the 2-chlorotriptyl chloride (CTC) resin was used as the solid support, onto which Fmoc-protected amino acids were sequentially added. Hydrophobic groups were then installed directly on the solid support. The resulting C-terminal free acid intermediate **7** was obtained with high crude purity and used directly without additional purification. In the final steps, ciprofloxacin was reacted with the pre-activated intermediate **7** to generate compound **8** in moderate yield (>60%). Deprotection of compound **8** furnished the final amphiphilic derivatives **9a–e** in a straightforward way.

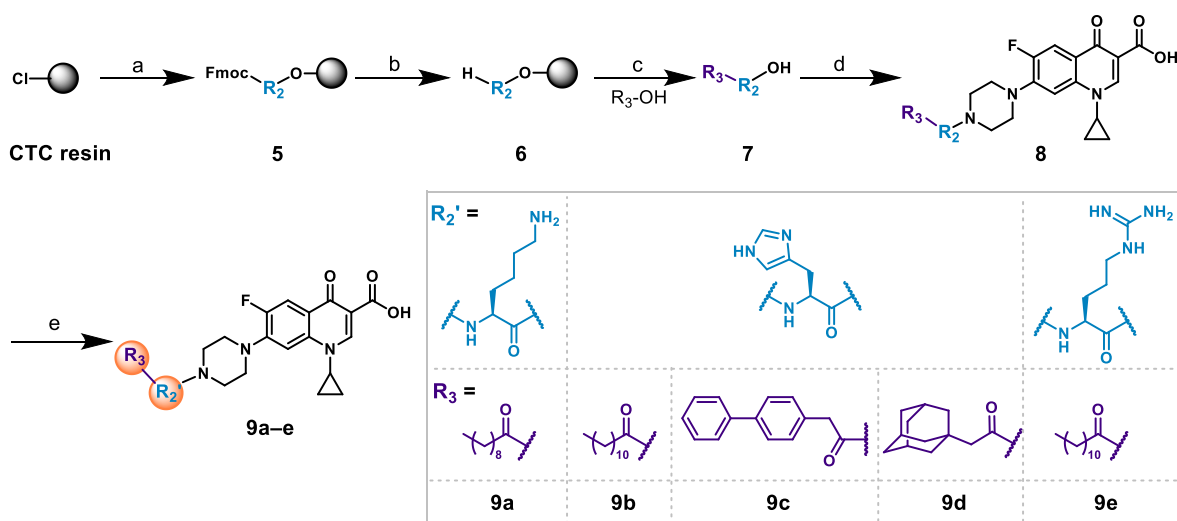
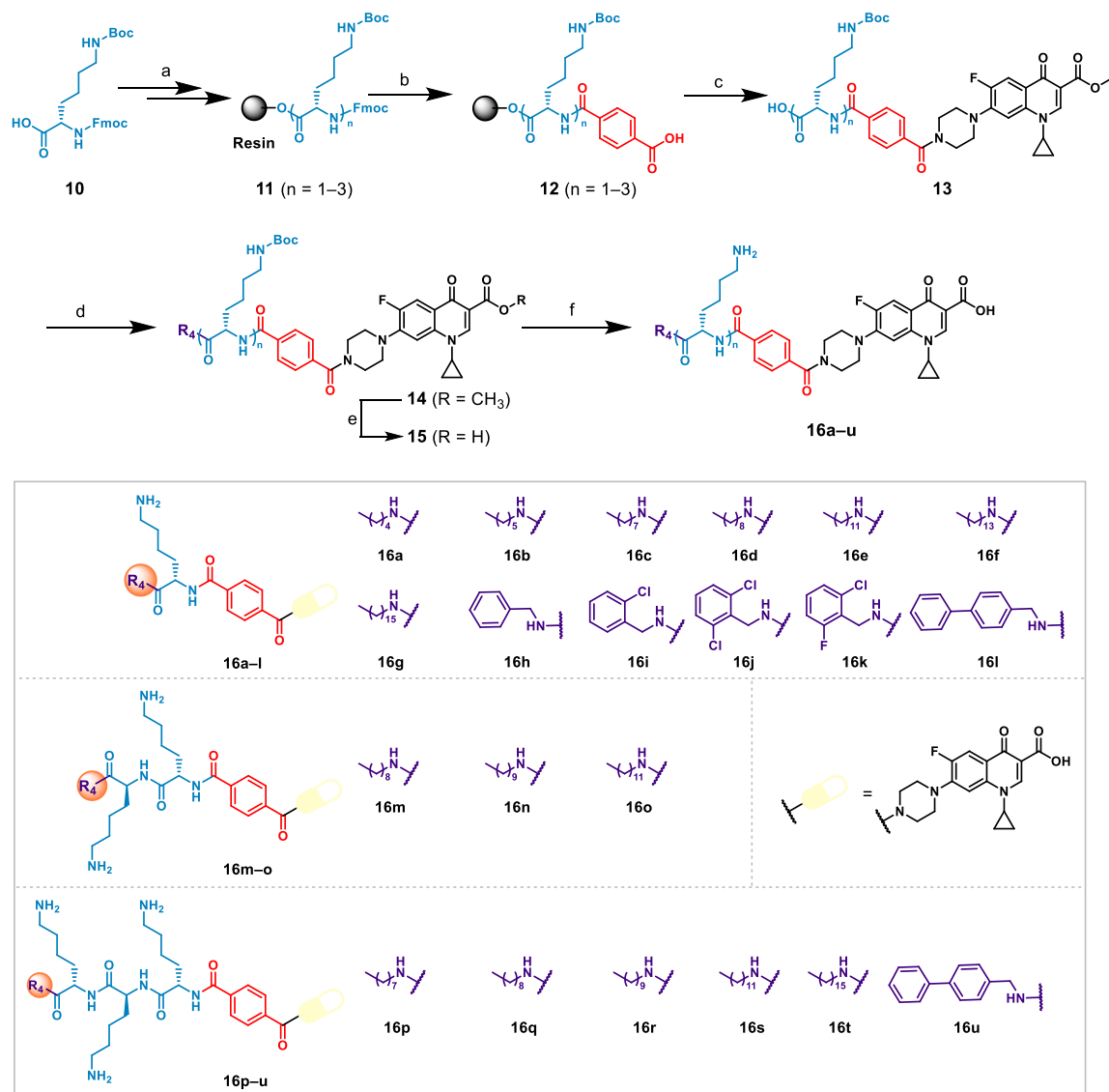
^cReagents and conditions: (a) 2-Chlorotriptylchloride resin, DIPEA, DCM, r.t., 1 h; then 20 % piperidine/DMF, r.t., 10 min (× 2); then Fmoc-Lys(Boc)-OH, EDC, HOEt, DIPEA, DMF, r.t., 2 h; repeat the procedure of de-Fmoc and amino acid coupling until the desired intermediate. (b) 20 % piperidine/DMF, r.t., 10 min (× 2); then Terephthalic acid, HCTU, DIPEA, DMF, r.t., 2 h. (c) Ciprofloxacin methyl ester **1**, HCTU/DIPEA, DMF, r.t., 5 h; then cleave from the resin using 20 % HFIP/DCM, r.t., 2 h. (d) EDC, HOEt, DIPEA, DMF, r.t., 2 h. (e) LiOH, MeOH/H₂O, r.t., 2 h. (f) TFA/DCM, r.t., 2 h.

^dReagents and conditions: (a) 20 % piperidine/DMF, r.t., 10 min (× 2). (b) Fmoc-NH-linker-COOH, EDC, HOEt, DIPEA, DMF, r.t., 2 h; then 20 % piperidine/DMF, r.t., 10 min (× 2); then Succinic anhydride, DIPEA, r.t., 2 h. (c) Ciprofloxacin methyl ester **1**, HCTU/DIPEA, DMF, r.t., 5 h; then cleave from the resin using 20 % HFIP/DCM, r.t., 2 h. (d) EDC, HOEt, DIPEA, DMF, r.t., 2 h. (e) LiOH, MeOH/H₂O, r.t., 2 h. (f) TFA/DCM, r.t., 2 h.

To better understand the structure–activity relationship, a series of amphiphilic ciprofloxacin derivatives with a rigid 1,4-dicarbonyl benzyl linker connecting the piperazine ring to N-terminal amino acids were further synthesized. This design was inspired by the potential of acylating cationic peptides with fatty acids to broaden their antibacterial spectrum and enhance resistance to proteolytic degradation. As illustrated in **Scheme 3**, we conjugated fatty acids of varying carbon chain lengths (e.g., C5–C16) and diverse lipophilic groups (e.g., aromatic groups and adamantanyl groups) to the positively charged electrostatic effector sequences. Compounds **16a–l** were made accordingly. We also investigated the impact of varying the number of lysine residues (*n* = 2–3) and incorporating different hydrophobic residues, including both aliphatic and aromatic moieties, to furnish compounds **16m–u**. To streamline the synthesis and simplify purification, we employed a



Scheme 1. Synthesis Route of Compounds **4a–c**^a.

Scheme 2. Synthesis Route of Compounds 9a–e^a.Scheme 3. Synthesis Route of Compounds 16a–u^a.

similar SPPS procedure as mentioned above. This approach minimized the need for extensive column chromatography, enabling efficient synthesis and easier isolation of compounds **16a–u**.

To further fine-tune amphipathicity and optimize activity, we explored various linkers beyond the rigid 1,4-dicarbonyl benzyl linker. Flexible and cleavable linkers were synthesized to assess their impact on biological activity (**22a–g**, **Scheme 4**). Given that HDPs are rich in lysine, arginine, and histidine, which act as dominant cationic moieties, we also introduced arginine and histidine residues to enhance the biocompatibility and hydrophilicity of ciprofloxacin derivatives. Using the same procedure depicted in **Scheme 5**, compounds bearing different amino acids in the cationic region (**28a–e**) were synthesized. For all final compounds **9a–e**, **16a–u**, **22a–g** and **28a–e**, the use of SPPS significantly streamlined preparation by simplifying intermediate purification. Furthermore, all reagents employed were common and inexpensive, enabling the production of these derivatives at a low cost. This efficient and cost-effective approach highlights the practicality of this synthetic strategy for developing novel antimicrobial agents.

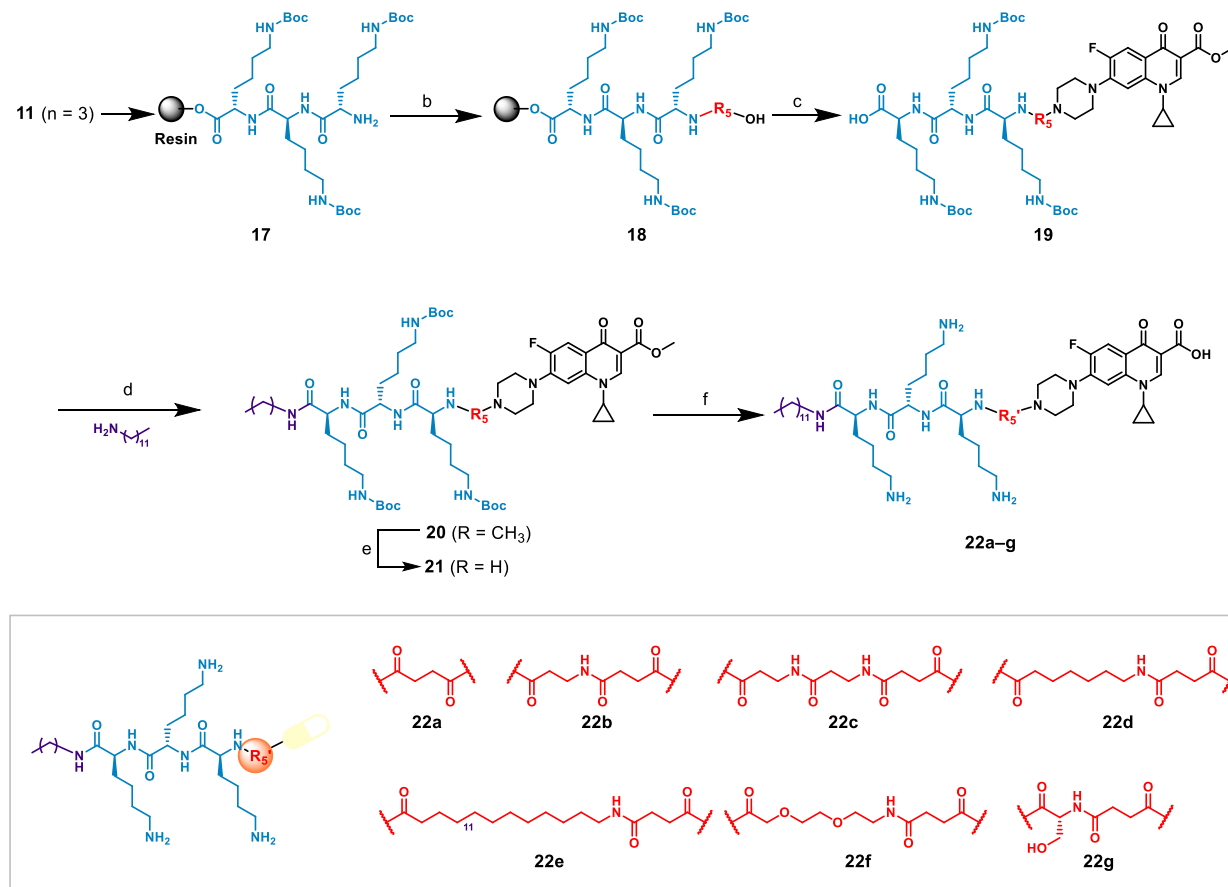
^aReagents and conditions: (a) 2-Chlorotriptylchloride resin, DIPEA, DCM, r.t., 1 h. (b) 20 % piperidine/DMF, r.t., 10 min (× 2); then Fmoc-amino acid-OH, EDC, HOEt, DIPEA, DMF, r.t., 2 h; repeat the procedure of de-Fmoc and amino acid coupling until the desired intermediate; then 20 % piperidine/DMF, r.t., 10 min (× 2); then Terephthalic acid, HCTU, DIPEA, DMF, r.t., 2 h. (c) Ciprofloxacin methyl ester **1**, HCTU, DIPEA, DMF, r.t., 5 h; then cleave from the resin using 20 % HFIP/DCM, r.t., 2 h. (d) EDC, HOEt, DIPEA, DMF, r.t., 2 h. (e) LiOH, MeOH/H₂O (5:1, v/v), r.t., 2 h. (f) TFA/DCM (19:1, v/v), r.t., 2 h.

1.2. In vitro antibacterial and Hemolytic Assays

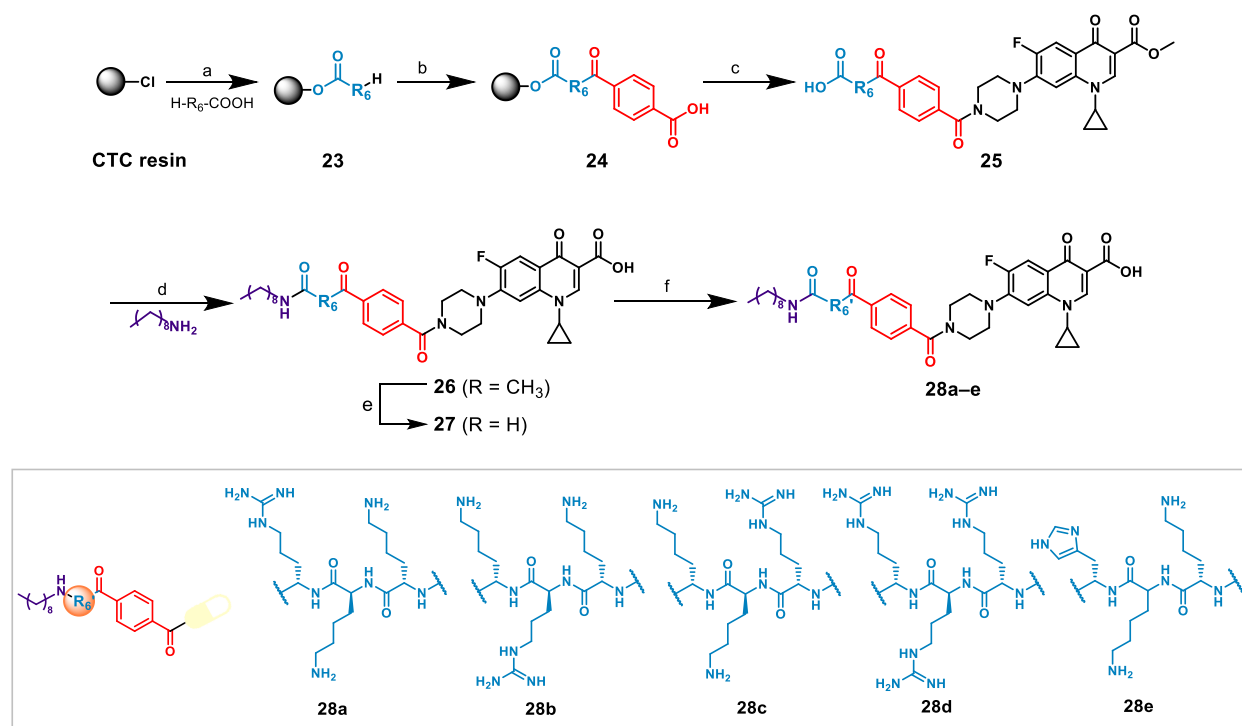
The *in vitro* antibacterial activities of the amphiphilic ciprofloxacin

derivatives against Gram-positive (G+) bacteria *S. aureus* ATCC 25923 were assessed by determining their minimal inhibitory concentrations (MICs) [73]. As summarized in **Table 1** and **S1**, ciprofloxacin, used as a positive control, exhibited an MIC of 0.78 µg/mL against *S. aureus* ATCC 25923. In the case of compounds **4a–c** featuring a single cationic amino acid (lysine, arginine, or histidine), a significant reduction in antibacterial activity was observed, with MIC values ≥ 12.5 µg/mL (see Supporting Information **Table S1**). However, when hydrophobic groups were introduced into the cationic template of **4a–c**, the corresponding compounds **9a–e** displayed enhanced antimicrobial activity (MIC = 6.25–12.5 µg/mL, see Supporting Information **Table S1**), highlighting the beneficial role of lipophilic elements in improving antibacterial effects. Conversely, ciprofloxacin derivatives **16a–g**, which incorporated varied alkyl tails, showed no significant improvement in activity. One exception was compound **16d**, which bears a nonyl group and exhibited moderate activity (MIC = 6.25 µg/mL). These findings underscore the critical importance of achieving a balance between hydrophobicity and hydrophilicity to optimize antibacterial efficacy.

We then investigated compounds with less bulky lipophilic groups, including various substituted benzyl groups containing fluoride and chloride atoms. However, none of these compounds (**16h–k**) demonstrated improved activity. Additionally, the introduction of a longer biphenyl group (**16l**) resulted in a complete loss of antibacterial activity, emphasizing the critical role of hydrophobic groups in maintaining antimicrobial potency. To enhance antimicrobial activity and provide greater flexibility for modifications, we increased the number of amino acids in the cationic moiety to two or three. This adjustment improved antibacterial efficacy by 1–3 times (compounds **16m–u**). Notably, compounds with octenyl, nonyl, or decanoyl groups (**16p**, **16q**, and **16r**, MIC_{S. aureus} = 3.12 µg/mL) and the biphenyl group (**16u**, MIC_{S. aureus} = 1.56 µg/mL) exhibited superior antibacterial activity (**Table 1**). We also



Scheme 4. Synthesis Route of Compounds **22a–g**^a.



Scheme 5. Synthesis Route of Compounds 28a–e^a.

systematically explored compounds with flexible (22a–f) and enzyme-cleavable (22g) linkers [20]. Of these, only compound 22e displayed acceptable activity ($MIC_{S. aureus} = 3.12 \mu\text{g/mL}$). When the terminal hydrophobic tail was fixed as a nonyl group, compounds 28a–e, incorporating different amino acids in the cationic region, were tested. Compounds 28a–c exhibited strong activity, with compound 28b (IPMCL-28b, MIC = 1.56 $\mu\text{g/mL}$) being the most potent, indicating that the position of arginine also affects antibacterial activity. Interestingly, compound 28d, containing three arginine residues, completely lost activity even at a concentration of 50 $\mu\text{g/mL}$. Replacing one arginine with histidine to create compound 28e slightly reduced activity.

To assess the therapeutic potential of ciprofloxacin derivatives, compounds 16u, 22e, 22g and IPMCL-28b, which exhibited strong antimicrobial activity against MRSA, were further screened against a broader range of Gram-positive (*S. aureus* ATCC 25923, *E. gallinarum* ATCC 49573, MRSA ATCC 43300 and *E. faecalis* ATCC 19433) and also Gram-negative bacteria (*E. coli* ATCC 25922, *P. aeruginosa* ATCC 27853 and *A. baumannii* ATCC 19606). As shown in Table 2, compounds 22e and IPMCL-28b were most active among these compounds with MIC values from 1.56 to 12.5 $\mu\text{g/mL}$. Notably, IPMCL-28b exhibited superior efficacy, with MIC values of 1.56 $\mu\text{g/mL}$ and 6.25 $\mu\text{g/mL}$ against *S. aureus* and MRSA respectively. Furthermore, IPMCL-28b also displayed superior activity against Gram-negative strains, including *E. coli*, *P. aeruginosa* and *A. baumannii* with MIC values below 6.25 $\mu\text{g/mL}$. These findings highlight IPMCL-28b as a promising candidate against both Gram-positive and Gram-negative bacteria.

To evaluate the safety of the chimeric compounds, we assessed their hemolytic activity, which represents the degree of red blood cells (RBCs) being lysed by candidate compounds, as recorded by HC_{50} values [74]. As shown in Fig. 2a, ciprofloxacin, 16u and IPMCL-28b did not exhibit any hemolytic activity against RBCs at 200 $\mu\text{g/mL}$, while compounds 22e and 22g displayed significant hemolytic activity even at 100 $\mu\text{g/mL}$. Further cytotoxicity testing was conducted on mouse fibroblast L929 cells using MTT assays (Fig. 2b). Compounds 22e and 22g exhibited substantial cytotoxicity at concentrations as low as 25 $\mu\text{g/mL}$, whereas ciprofloxacin and IPMCL-28b showed no significant toxicity at concentrations up to 100 $\mu\text{g/mL}$. Based on these results, IPMCL-28b was

identified as the most promising candidate among the chimeric ciprofloxacin derivatives and selected for further in-depth *in vitro* and *in vivo* studies.

1.2.1. Fast bacterial killing kinetics

Encouraged by the excellent *in vitro* antibacterial activity of IPMCL-28b, the bacterial killing kinetics were investigated to assess the bactericidal properties of IPMCL-28b against *S. aureus* ATCC 25923. It was found that IPMCL-28b achieved about 3.6-log reduction of MRSA within 4 h at a concentration of 4 \times MIC, and the bacteria were completely eradicated in 8 h (Fig. 3a). In contrast, MRSA was not efficiently killed by ciprofloxacin treatment at the same concentration. Compared with ciprofloxacin, the faster bacterial killing rate is one of the advantages of the HDP-mimicking amphiphilic ciprofloxacin derivative, which may be important in the treatment of bacterial infection in certain urgent situations and further proving that our chimeric ciprofloxacin derivative has the characteristics of HDP.

1.2.2. Insusceptibility to antibacterial resistance

With the rapid escalation of bacterial resistance, the effective lifespan of antibiotics is progressively diminishing. Therefore, it is particularly crucial to assess the potential for the development of resistance to novel antimicrobial agents intended for pre-clinical use. As shown in Fig. 3b, either MRSA or *E. coli* bacteria exposed to IPMCL-28b over successive generations did not develop noticeable resistance; in sharp contrast, exposure to ciprofloxacin at sub-MIC levels led to the development of bacterial resistance significantly, with a 32-fold increase in MIC values against MRSA and a 64-fold increase against *E. coli* after 25 generations of sequential exposure. These results suggest that the HDP-mimicking chimeric IPMCL-28b is less likely to induce or even reverse the drug resistance of ciprofloxacin.

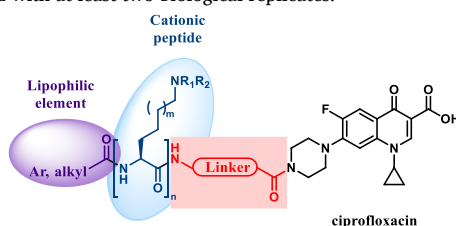
1.3. Antibacterial mechanistic studies

1.3.1. Membrane-targeting properties of IPMCL-28b

Based on the above results of low-frequency resistance observed in IPMCL-28b, we further investigated the antibacterial mechanism of this

Table 1

Structure-activity relationships of ciprofloxacin derivatives against *S. aureus* ATCC 25923. The minimum inhibitory concentration (MIC) is the lowest concentration that completely inhibits microbial growth after 20 h. All MIC determinations were performed with at least two biological replicates.



Cpd	Lipophilic element	Cationic peptide	Linker ciprofloxacin	MIC <i>S. aureus</i> (μ g/mL)
Lipophilic element variation				
16a	nC5NH-	-K-	-CO(1, 4-Ph)CO-C	25
16b	nC6NH-	-K-	-CO(1, 4-Ph)CO-C	25
16c	nC8NH-	-K-	-CO(1, 4-Ph)CO-C	12.5
16d	nC9NH-	-K-	-CO(1, 4-Ph)CO-C	6.25
16e	nC12NH-	-K-	-CO(1, 4-Ph)CO-C	50
16f	nC14NH-	-K-	-CO(1, 4-Ph)CO-C	25
16g	nC16NH-	-K-	-CO(1, 4-Ph)CO-C	>100
16h	4-Ph-CH2NH-	-K-	-CO(1, 4-Ph)CO-C	25
16i	(2-Cl-Ph)CH2NH-	-K-	-CO(1, 4-Ph)CO-C	25
16j	(2,6-Cl-Ph)CH2NH-	-K-	-CO(1, 4-Ph)CO-C	12.5
16k	(2-Cl-6-F-Ph)CH2NH-	-K-	-CO(1, 4-Ph)CO-C	25
16l	4-Ph-BnCH2NH-	-K-	-CO(1, 4-Ph)CO-C	50
16m	nC9NH-	-KK-	-CO(1, 4-Ph)CO-C	6.25
16n	nC10NH-	-KK-	-CO(1, 4-Ph)CO-C	6.25
16o	nC12NH-	-KK-	-CO(1, 4-Ph)CO-C	25
16p	nC8NH-	-KKK-	-CO(1, 4-Ph)CO-C	3.125
16q	nC9NH-	-KKK-	-CO(1, 4-Ph)CO-C	3.125
16r	nC10NH-	-KKK-	-CO(1, 4-Ph)CO-C	3.125
16s	nC12NH-	-KKK-	-CO(1, 4-Ph)CO-C	6.25
16t	nC16NH-	-KKK-	-CO(1, 4-Ph)CO-C	>50
16u	4-Ph-BnCH2NH-	-KKK-	-CO(1, 4-Ph)CO-C	1.56
Linker variation				
22a	nC12NH-	-KKK-	-COC2CO-C	>50
22b	nC12NH-	-KKK-	-COC2NH-COC2CO-C	>50
22c	nC12NH-	-KKK-	-(COC2NH) ₂ -COC2CO-C	6.25
22d	nC12NH-	-KKK-	-COC5CO-COC2CO-C	12.5
22e	nC12NH-	-KKK-	-COC11CO-COC2CO-C	3.125
22f	nC12NH-	-KKK-	-COC2CO-PEG2-NH-COC2CO-C	12.5
22g	nC12NH-	-KKK-	-Ser-COC2CO-C	6.25
Cationic peptide variation				
28a	nC9NH-	-RKK-	-CO(1, 4-Ph)CO-C	3.125
IPMCL-28b	nC9NH-	-KRK-	-CO(1, 4-Ph)CO-C	1.56
28c	nC9NH-	-KKR-	-CO(1, 4-Ph)CO-C	3.125
28d	nC12NH-	-RRR-	-CO(1, 4-Ph)CO-C	>50
28e	nC9NH-	-HKK-	-CO(1, 4-Ph)CO-C	6.25
Ciprofloxacin			-C	0.78

chimeric quinoline compound. Since these amphiphilic ciprofloxacin derivatives were designed to partly mimic the amphipathic structure of HDPs, we hypothesized they could replicate the membrane-disrupting mechanism of HDPs and exert bactericidal activity by compromising bacterial membranes. To prove this hypothesis, we performed flow cytometric analysis to assess the impact of **IPMCL-28b** on the membrane integrity of *S. aureus* [76]. Propidium iodide (PI) is a high-affinity nucleic acid-binding dye that can only penetrate bacterial cells with compromised membranes, resulting in increased fluorescence intensity. This allows us to monitor the membrane-disrupting effect of the drug by flow cytometry, quantifying the percentage of PI-positive bacteria after co-incubation with the drug. As shown in Fig. 3c, **IPMCL-28b** resulted in 26.75 % and 58.40 % PI-positive bacteria at concentrations of 4 × MIC

and 8 × MIC, respectively, compared to the PBS and ciprofloxacin controls (8 × MIC). These results demonstrate that **IPMCL-28b** effectively compromised the bacterial membranes. This result was also supported by the scanning electron microscopy (SEM) [77] characterization of MRSA treated with **IPMCL-28b** (Fig. 3d), where the MRSA cell membranes showed obvious damage when treated with both at 4 × MIC and 8 × MIC concentration of **IPMCL-28b**; nevertheless, ciprofloxacin (4 × MIC) did not induce noticeable change of bacterial membrane.

To further investigate the membrane-disrupting mechanistic of **IPMCL-28b**, we performed molecular dynamic (MD) simulation of ciprofloxacin and **IPMCL-28b** in the presence of a bacterial lipid membrane. As shown in Fig. 4, **IPMCL-28b** successfully embedded into the membrane during the 1000 ns MD simulation, regardless of its initial

Table 2

MIC values ($\mu\text{g/mL}$) of ciprofloxacin, **16u**, **22e**, **22g** and **IPMCL-28b** against a panel of Gram-Positive and Gram-Negative bacteria. All MIC determinations were performed with at least two biological replicates.

	MIC ($\mu\text{g/mL}$)				
	16u	22e	22g	IPMCL-28b	Ciprofloxacin
Gram-Positive Bacteria					
<i>S. aureus</i> ATCC 25923	1.56	3.125	6.25	1.56	0.78
<i>E. gallinarum</i> ATCC 49573	50	6.25	25	12.5	0.78
MRSA ATCC 43300	6.25	6.25	12.5	6.25	0.78
<i>E. faecalis</i> ATCC 19433	50	12.5	25	12.5	1.56
Gram-Negative Bacteria					
<i>E. coli</i> ATCC 25922	25	12.5	25	3.125	0.19
<i>P. aeruginosa</i> ATCC 27853	25	6.25	50	3.125	0.19
<i>A. baumannii</i> ATCC 19606	25	6.25	12.5	6.25	0.78

distance from the membrane (2 nm, 4 nm, or 6 nm, Fig. 4a, b, 4c, respectively). This embedding process was driven by its lipophilic non-decanoyl acyl tail and positively charged Lys/Arg side chains, demonstrating its strong membrane-interacting ability. In contrast,

ciprofloxacin, used as a reference control, did not embed into the membrane under the same conditions (Fig. S1). These results underscore the effectiveness of our design strategy for amphiphilic chimeric **IPMCL-28b**, which exhibits the ability to interact with and disrupt bacterial membranes.

Altogether, these findings indicate that the HDP-mimicking chimeric compound **IPMCL-28b** possesses a potent membrane-disrupting effect capability, effectively compromising the integrity of the bacterial cell membranes and consequently leading to bacterial death faster than the quinoline compound ciprofloxacin alone. Even excitingly, the naturally inspired HDP-mimicking strategy successfully reversed the antibiotic-resistance of ciprofloxacin, highlighting the potential of these chimeric quinolines to mitigate the development of antimicrobial resistance clinically.

1.3.2. *In vivo* antibacterial efficacy

Based on its superior *in vitro* antimicrobial efficacy and low-frequency resistance, we further evaluated the *in vivo* therapeutic potential of **IPMCL-28b** (single dose) using a murine subcutaneous abscess model infected with MRSA (Fig. 5a). Ciprofloxacin (25 mg/kg) was used as a positive control at an equivalent dosage. After 48 h of infection, the control group exhibited significant back swelling and subcutaneous pustules, indicative of severe abscess formation (Fig. 5b). In contrast, treatment with **IPMCL-28b** at the same dose of 25 mg/kg resulted in the absence of significant lesions, while visible abscesses persisted in the ciprofloxacin-treated group.

Histological analysis of skin tissues using H&E and Masson staining

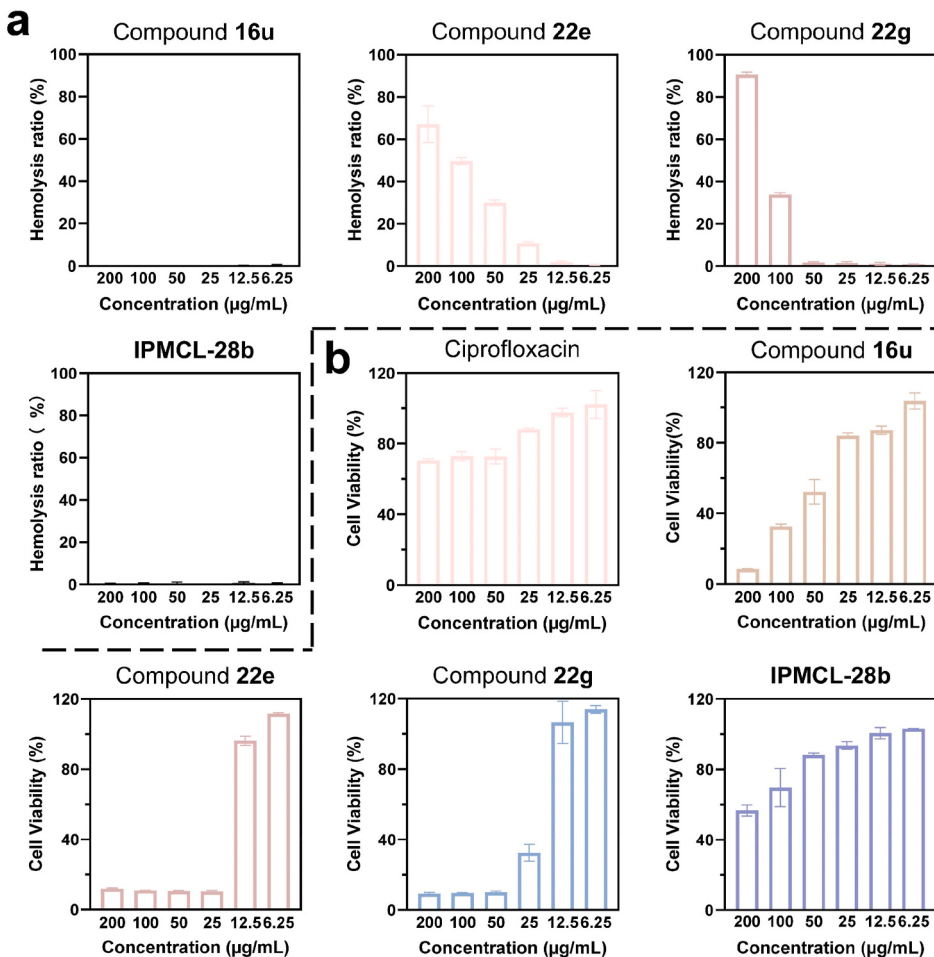


Fig. 2. Hemolysis and cytotoxicity of selected chimeric compounds. (a) Hemolytic toxicity of ciprofloxacin and its derivatives **16u**, **22e**, **22g** and **IPMCL-28b**. PBS and 2 % Triton X-100 were used as positive and negative controls, respectively. (b) Cytotoxicity results of ciprofloxacin and **16u**, **22e**, **22g**, and **IPMCL-28b** at different concentrations on mouse fibroblast L929 cells. The incubation time was 24 h.

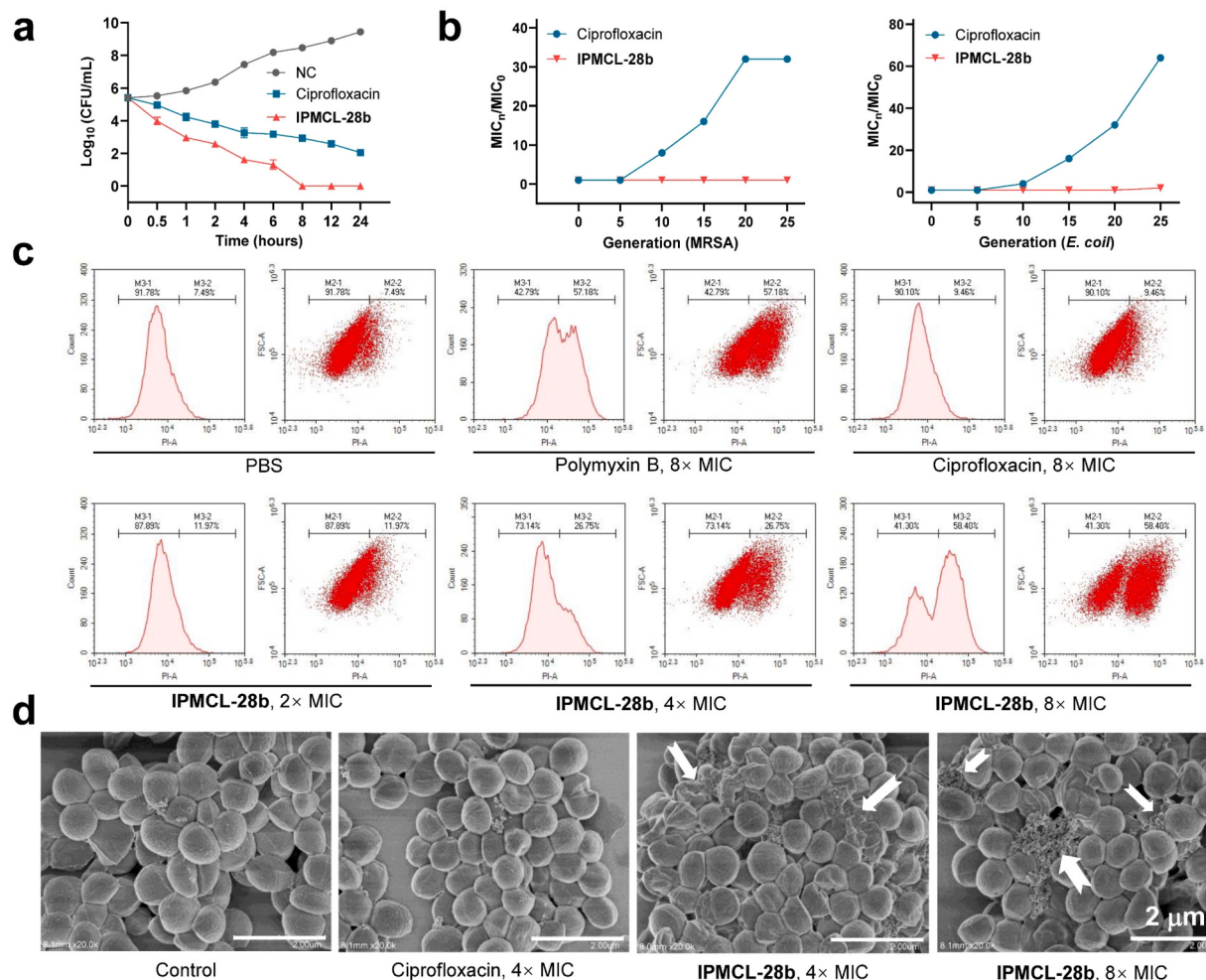


Fig. 3. Antibacterial kinetics, insusceptibility to resistance, and mechanism study of IPMCL-28b. (a) Bacterial killing kinetics of ciprofloxacin and IPMCL-28b against *S. aureus* ATCC 25923 at 4 × MIC concentration. (b) Resistance acquisition of MRSA (ATCC 33591) and *E. coli* (ATCC 25922) during consecutive passaging in the presence of sub-MIC levels of ciprofloxacin and IPMCL-28b. (c) Flow cytometric analysis of *S. aureus* cells stained by PI after co-incubation of IPMCL-28b with *S. aureus* ATCC 25923 at different concentrations for 30 min. Cells treated with PBS were used as blank control. Cells treated with polymyxin-B [75] (8 × MIC) and ciprofloxacin (8 × MIC) were used as positive and negative controls respectively. (d) SEM characterization of the cell morphology of *S. aureus* ATCC 25923 treated with PBS (control), ciprofloxacin (4 × MIC) IPMCL-28b (4 × MIC and 8 × MIC) respectively.

further revealed extensive infiltration of inflammatory cells in the control group (Fig. 5c). Ciprofloxacin treatment partially reduced inflammation, whereas the skin of mice treated with IPMCL-28b exhibited histological features closely resembling those of healthy skin. Additionally, Giemsa staining confirmed a substantial bacterial presence at the infection sites in the control group. A reduced bacterial load was also observed in mice treated with ciprofloxacin, while the bacterial burden was even lower in the IPMCL-28b-treated group (Fig. 5d). These findings highlight the superior therapeutic efficacy of IPMCL-28b in mitigating infection and inflammation in this *in vivo* model.

To further evaluate the therapeutic potential of IPMCL-28b, we homogenized the skin tissue to quantify bacterial load and assess levels of inflammatory biomarkers. Enzyme-linked immunosorbent assay (ELISA) results showed that treatment with IPMCL-28b significantly reduced tumor necrosis factor-alpha (TNF- α) ($p < 0.001$) and interleukin-6 (IL-6) ($p < 0.01$) levels in the infected skin compared to the control group. Moreover, the anti-inflammatory effect of IPMCL-28b was significantly greater than that of ciprofloxacin ($p < 0.01$) (Fig. 5e and f). Quantitative analysis of bacterial burden in the skin revealed that IPMCL-28b eliminated up to 99.99 % (4.4 log) of MRSA from the infected site, demonstrating superior efficacy compared to ciprofloxacin-treated mice ($p < 0.05$) (Fig. 5d–g, h). These findings indicate that the amphiphilic chimeric quinoline IPMCL-28b has

significant potential for the treatment of bacterial infections. It not only effectively reduced the inflammatory response associated with infection but also eradicated the bacteria at the infection site with remarkable efficiency.

1.3.3. In vivo safety and toxicity analysis

In order to further evaluate the clinical potential of IPMCL-28b, we conducted a comprehensive pathological analysis of the skin, heart, liver, spleen, lungs, and kidneys in mice to evaluate both local and systemic toxicity. As shown in Fig. 6a, subcutaneous injection of IPMCL-28b (25 mg/kg, single dose) demonstrated favorable skin compatibility. Additionally, histological examination of these organs using H&E staining revealed no significant pathological alterations (Fig. 6b). These findings suggest that the amphiphilic chimeric quinoline IPMCL-28b does not induce local or systemic toxic reactions during treatment, highlighting its safety profile and significant clinical promise for further development and investigation.

2. Conclusions

In our pursuit of developing novel ciprofloxacin-based antimicrobials to combat bacterial resistance, we proposed a host defense peptides-mimicking design strategy. A series of amphiphilic

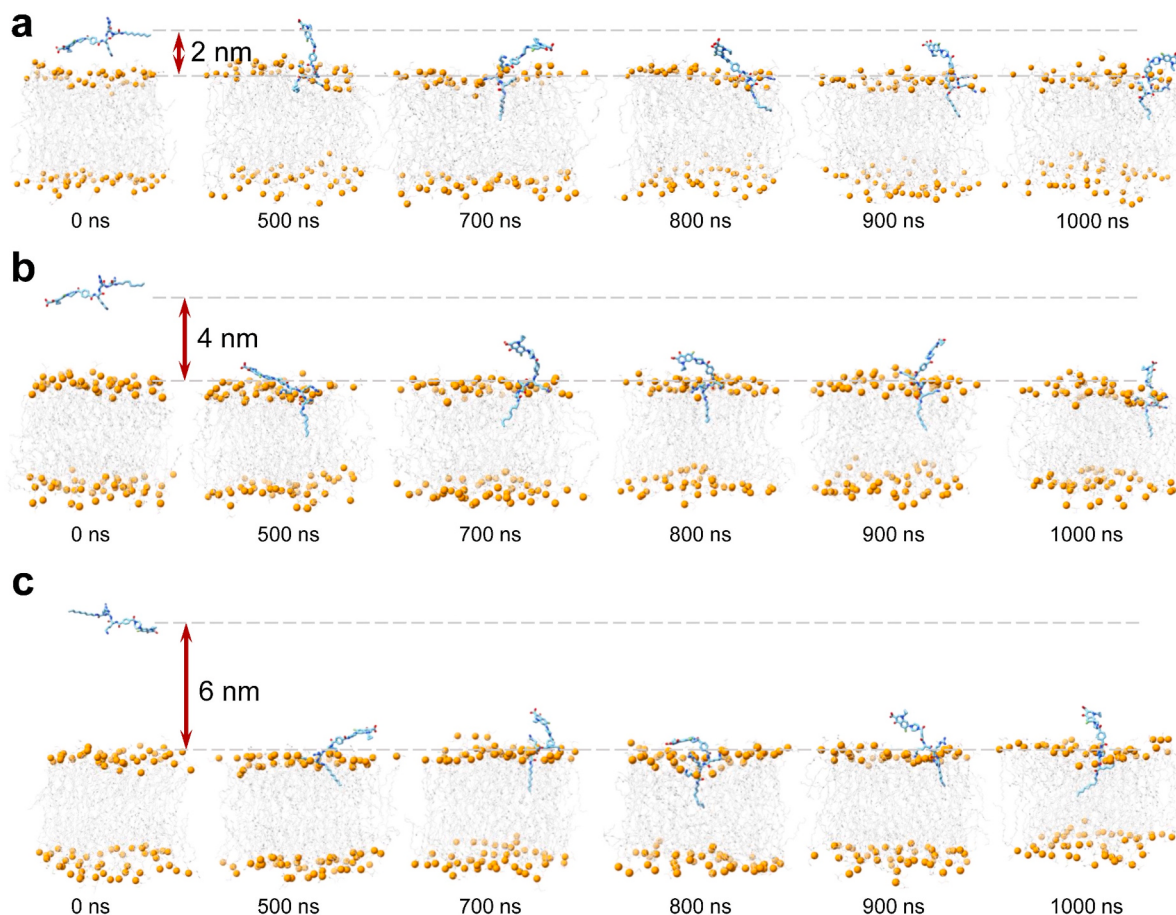


Fig. 4. Mechanistic details of IPMCL-28b insertion into the bacterial membrane were revealed by 1000 ns MD simulations. Lipid head groups were shown as orange spheres, tails were shown as gray lines, and IPMCL-28b were shown as cyanine stick format. (For interpretation of the references to colour in this figure legend, the reader is referred to the Web version of this article.)

ciprofloxacin derivatives containing positively charged amino acid side chains and hydrophobic residues were synthesized and evaluated. These compounds were systematically assessed for their *in vitro* antibacterial activity, hemolytic activity, cytotoxicity, mechanisms of action, time-kill dynamics, resistance development, and *in vivo* antibacterial efficacy and safety. Among the derivatives, **IPMCL-28b** emerged as a promising candidate, demonstrating potent and broad-spectrum antibacterial activity against both Gram-positive and Gram-negative bacteria. Notably, **IPMCL-28b** exhibited excellent specificity toward bacterial cells and no hemolytic activity was detected. Mechanistic studies revealed that it mimics the mechanism of action of HDPs, exerting bactericidal effects by disrupting bacterial membranes. Molecular dynamics simulations showed that **IPMCL-28b** demonstrates significantly stronger disruptive interactions with cell membranes than ciprofloxacin. Interestingly, unlike ciprofloxacin, **IPMCL-28b** showed no evidence of resistance development in MRSA and *E. coli* even after 25 generations of sequential exposure. Moreover, *in vivo* studies, **IPMCL-28b** exhibited remarkable anti-infective efficacy in a murine subcutaneous abscess model, alongside excellent biocompatibility and safety. This class of chimeric quinolone derivatives, which integrates the characteristics of HDPs with traditional small-molecule antibiotics, represents a significant advancement in developing potent, high-therapeutic-index agents against drug-resistant bacterial pathogens.

3. Experimental section

General Information. All solvents and reagents were purchased from commercial sources and were used without further purification. All

final compounds were purified by reverse-phase HPLC with acetonitrile and water (both including 0.1 % v/v trifluoroacetic acid) as a gradient eluent, using the C18 column (Waters, 19 mm × 250 mm, 5 µm, 120 Å) with a flow rate of 16 mL/min. All final compounds were more than 95 % pure by HPLC analysis. NMR spectra were recorded using a Bruker AVANCE III 500 MHz NMR spectrometer, with chemical shift values (δ) reported in parts per million (ppm) relative to tetramethylsilane (TMS) as the internal standard. Peak shapes are described using the following abbreviations: s (singlet), d (doublet), t (triplet), q (quartet), m (multiplet), brs (broad singlet) with coupling constants (J) reported in hertz (Hz). The HRMS of tested ciprofloxacin derivatives **4a–b**, **16a–u**, **22a–g** and **28a–e** were identified by an Agilent 6224 Accurate-Mass TOF LC/MS using electrospray ionization (ESI) in positive mode. The LC-MS data of the intermediates were obtained using a Shimadzu LCMS-2020 with ESI in positive mode. Melting points (mp) were measured in open capillary tubes, using a M – 560 melting point apparatus (0–300 °C). For the preparative HPLC gradient system, 0.1 % TFA in water was used as solvent A, 0.1 % TFA in acetonitrile was used as solvent B.

7-(4-(*L*-lysyl)piperazin-1-yl)-1-cyclopropyl-6-fluoro-4-oxo-1,4-dihydroquinoline-3-carboxylic acid (4a**).** To a solution of ciprofloxacin (3 g, 9.1 mmol) in MeOH (150 mL) was added concentrated H₂SO₄ (9.8 mL, 182 mmol) dropwise over 10 min under ice bath. The mixture was then heated to reflux overnight. After completion, MeOH was evaporated under high vacuum before quenching with saturated solution of NaHCO₃. The mixture was extracted with DCM (× 3) and the organic phase was washed with brine, separated, dried over anhydrous Na₂SO₄, and concentrated under vacuum. the desired compound **1** was obtained (2.9 g, yield 93 %) as white powder, which was used directly without

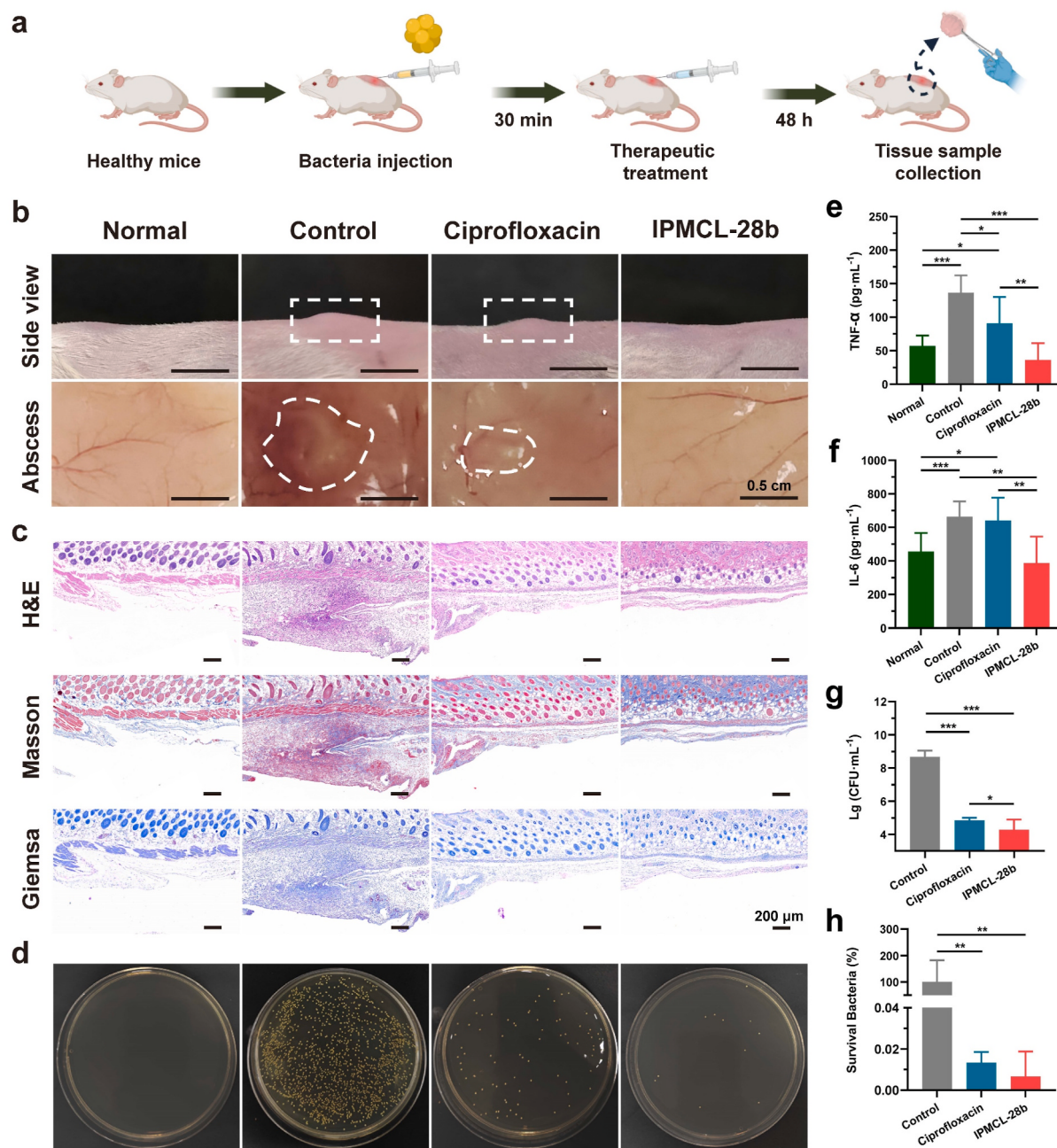


Fig. 5. *In vivo* antimicrobial activity of IPMCL-28b. (a) Schematic representation of the protocol for MRSA-induced murine subcutaneous infection model. (b) Skin photographs from the mice after different treatments captured 48 h post-infection. (c) Images of H&E staining, Masson staining and Giemsa staining of the different skin samples. (d) Representative photographs of MRSA colonies grown from the skin homogenates of each group. The levels of TNF- α (e) and IL-6 (f) in the skin homogenates of each group. Bacterial burden (g) and bacterial survival (h) in the skin of mice after different treatments. Images are representative of three independent experiments, data are presented as the mean \pm SD ($n = 6$, each group). * $p < 0.05$, ** $p < 0.01$, *** $p < 0.001$.

further purification. Next, to a solution of Boc-Lys(Boc)-OH (300 mg, 0.87 mmol), EDC (250 mg, 1.31 mmol) and HOBT (177 mg, 1.31 mmol) in anhydrous DMF (8 mL) was added DIPEA (303 μL , 1.74 mmol) at 0 °C, the solution was stirred for 5 min, followed by adding a pre-mixed solution of compound 1 (452 mg, 1.31 mmol) and DIPEA (303 μL , 1.74 mmol) in anhydrous DMF (4 mL) dropwise. The reaction was stirred for 5 h at room temperature before quenching with HCl (1 M). The mixture was extracted with DCM ($\times 2$) and the organic phase was washed with brine, separated, dried over anhydrous Na_2SO_4 , and concentrated under vacuum to give the crude residue 2a, which was used directly without further purification. Then, to a solution of compound 2a (882 mg, 1.31 mmol) in 10 mL of MeOH/H₂O (5:1, v/v) was added LiOH (550 mg,

13.1 mmol) partwise. The reaction mixture was stirred for 2 h at room temperature. Upon completion, the reaction was quenched with HCl (1 M), and then extracted with DCM ($\times 2$). The combined organic layer was washed with brine, dried over Na_2SO_4 , and concentrated under reduced pressure. The crude residue 3a (863 mg, 1.31 mmol) was dissolved in 6 mL of TFA/DCM (19/1, v/v). The reaction mixture was stirred for 2 h at room temperature. Upon completion, the solvents were concentrated in vacuo. Crude compound of 4a was dissolved in water/methanol (1:1) solution (10 mL) and purified by preparative HPLC to give pure 4a as white powder (173 mg, 28.7 %) after preparative HPLC ($R_t = 7.5$ min) and lyophilization. White solid, m.p. 155–157 °C, yield 28.7 %; ^1H NMR (500 MHz, CD_3OD) δ 8.75 (s, 1H), 7.86 (d, $J = 13.1$ Hz,

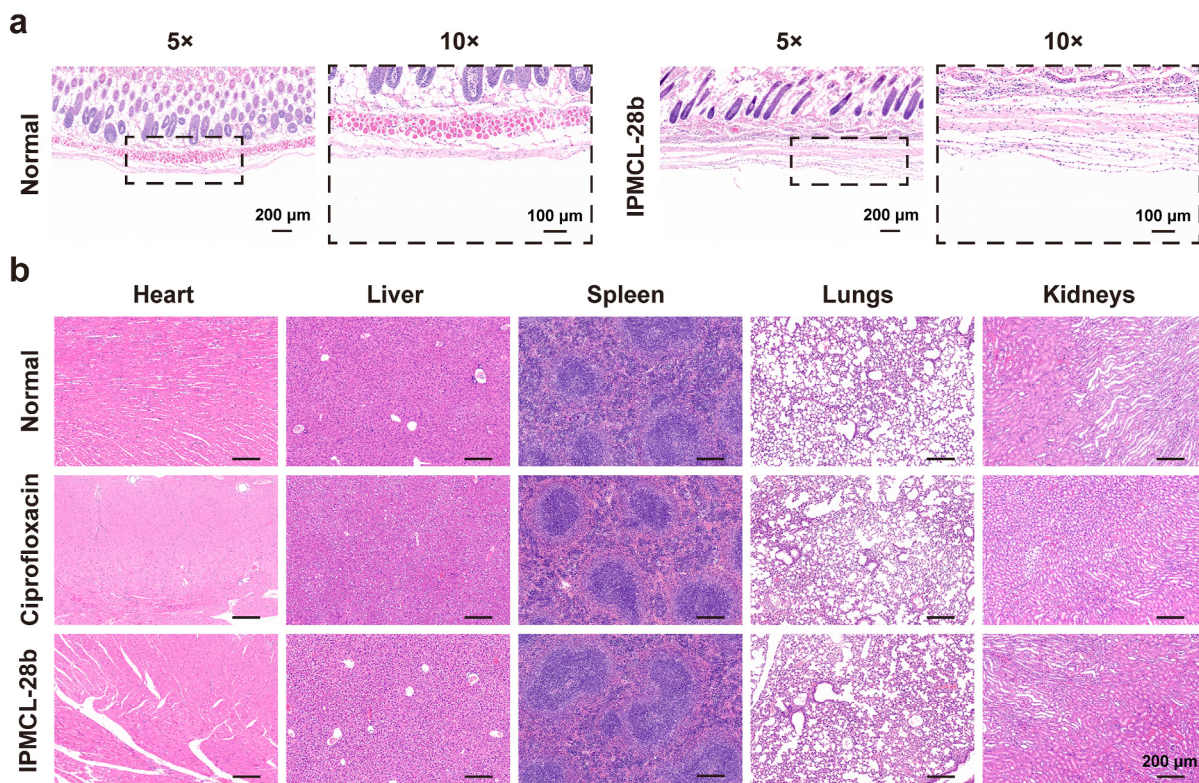


Fig. 6. *In vivo* safety and toxicity analysis. (a) H&E staining of skin sections from the normal and IPMCL-28b treated mice. (b) Representative H&E-stained sections of various organs isolated from each group.

1H), 7.57 (s, 1H), 4.56 (t, $J = 6.1$ Hz, 1H), 4.05 (d, $J = 13.0$ Hz, 1H), 3.87 (s, 1H), 3.77 (s, 3H), 3.52 (s, 2H), 3.42 (d, $J = 9.7$ Hz, 1H), 3.34 (s, 1H), 2.98 (t, $J = 7.5$ Hz, 2H), 1.99–1.85 (m, 2H), 1.75 (m, 2H), 1.55 (s, 2H), 1.46–1.37 (m, 2H), 1.23 (s, 2H). ^{13}C NMR (126 MHz, CD₃OD) δ 177.98, 169.23, 168.70, 154.83 (d, $J = 250.2$ Hz, C-6), 149.17, 146.53 (d, $J = 10.2$ Hz, C-7), 140.58, 120.55 (d, $J = 7.7$ Hz, C-4a), 112.31 (d, $J = 23.5$ Hz, 5-C), 107.93, 107.31 (d, $J = 3.2$ Hz, 8-C), 51.50, 50.87 (d, $J = 5.2$ Hz), 50.30 (d, $J = 4.1$ Hz), 46.40, 43.18, 40.25, 36.94, 31.49, 28.21, 22.61, 8.53 (2C). ESI-HRMS calcd for C₂₃H₃₀FN₅O₄ [M+H]⁺: 460.2282; found 460.2361.

The compounds **4b–c** were synthesized following the similar procedure of **4a**.

7-(4-(L-lysyl)piperazin-1-yl)-1-cyclopropyl-6-fluoro-4-oxo-1,4-dihydroquinoline-3-carboxylic acid (4b). Light yellow solid, m.p. 211–213 °C, yield 24.6 %; ^1H NMR (500 MHz, CD₃OD) δ 8.94 (s, 1H), 8.74 (s, 1H), 7.86 (d, $J = 12.9$ Hz, 1H), 7.53 (brs, 2H), 4.04 (s, 1H), 3.93 (s, 1H), 3.77 (s, 3H), 3.44 (m, 4H), 3.37 (m, 3H), 1.43 (t, 2H), 1.24 (s, 2H). ^{13}C NMR (126 MHz, CD₃OD) δ 178.06, 169.28, 167.45, 154.88 (d, $J = 250.2$ Hz, C-6), 149.25, 146.50 (d, $J = 10.4$ Hz, C-7), 140.61, 136.26, 127.94, 120.66 (C-4a), 120.11, 112.40 (d, $J = 23.6$ Hz, C-5), 107.98, 107.35 (d, $J = 3.0$ Hz, C-8), 50.77, 50.42, 50.34, 46.39, 43.36, 36.94, 27.11, 8.53 (2C). ESI-HRMS calcd for C₂₃H₂₅FN₆O₄ [M+H]⁺: 469.1921; found 469.2000.

7-(4-(L-arginy)piperazin-1-yl)-1-cyclopropyl-6-fluoro-4-oxo-1,4-dihydroquinoline-3-carboxylic acid (4c). White solid, m.p. 168–170 °C, yield 27.4 %; ^1H NMR (500 MHz, CD₃OD) δ 8.79–8.65 (m, 1H), 7.91–7.72 (m, 1H), 7.55 (s, 1H), 4.59 (t, $J = 5.8$ Hz, 1H), 4.00 (d, $J = 6.3$ Hz, 1H), 3.92–3.71 (m, 4H), 3.56–3.34 (m, 4H), 3.27 (m, 2H), 1.95 (m, 2H), 1.76 (m, 2H), 1.41 (d, $J = 6.3$ Hz, 2H), 1.23 (m, 2H). ^{13}C NMR (126 MHz, CD₃OD) δ 178.04, 169.32, 168.58, 158.79, 154.88 (d, $J = 250.1$ Hz, C-6), 149.24, 146.54 (d, $J = 10.3$ Hz, C-7), 140.62, 120.64 (C-4a), 112.38 (d, $J = 24.2$ Hz, C-5), 107.97, 107.39 (C-8), 51.38, 50.91, 50.33, 46.41, 43.21, 41.75, 36.95, 29.03, 24.98, 8.53 (2C). ESI-HRMS calcd for C₂₃H₃₀FN₇O₄ [M+H]⁺: 488.2343; found 488.2428.

1-cyclopropyl-7-(4-(decanoyl-L-lysyl)piperazin-1-yl)-6-fluoro-4-oxo-1,4-dihydroquinoline-3-carboxylic acid (9a). 2-Chlorotriptylchloride (CTC) resin (500 mg, 0.37 mmol) was swelled in 6 mL of DCM for 15 min. The attachment of the first amino acid to the resin was achieved by adding Fmoc-Lys(Boc)-OH (347 mg, 0.74 mmol) and DIPEA (233 μ L, 1.34 mmol) to the beads in the reaction vessel, which was allowed to shake at room temperature for 2 h. After that, the reaction solution was drained, followed by washing with DMF (4 mL \times 3) and DCM (4 mL \times 3). The unreacted 2-chlorotriptylchloride moieties were capped with 6 mL of DIPEA/MeOH/DCM (1/2/17, v/v/v) for 30 min to afford **5a**. The beads were washed with DCM (4 mL \times 3) and DMF (4 mL \times 3). The Fmoc group was removed by treating beads with 20 % piperidine/DMF (v/v) solution for 10 min (\times 2) at room temperature to afford **6a**. Next, decanoic acid (143 μ L, 0.74 mmol), HCTU (278 mg, 0.67 mmol), and DIPEA (232 μ L, 1.34 mmol) were premixed in 2 mL DMF for 5 min before getting transferred to the reaction vessel. The reaction was shaken at room temperature for 2 h, and the solution was removed. After DMF (4 mL \times 3) and DCM (4 mL \times 3) wash, the intermediate was cleaved from resin with 8 mL of the cleavage cocktail (HFIP/DCM 1:4, v/v) for 2 h. The solution was collected, and the remaining beads were washed with 4 mL of the cleavage cocktail solution three times. All the solution was combined and concentrated in vacuo with coevaporation with hexane multiple times. The crude compound of **7a** was purified by silica gel column chromatography to give pure **7a** as white powder (130 mg, 87 %). *N*⁶-(tert-butoxycarbonyl)-*N*²-decanoyl-L-lysine (**7a**). White solid, yield 87 %; ^1H NMR (500 MHz, CDCl₃) δ 6.60 (d, $J = 6.7$ Hz, 1H), 4.69–4.50 (m, 1H), 3.15–3.00 (t, 2H), 2.28–2.19 (t, 2H), 1.92–1.71 (m, 2H), 1.61 (m, 2H), 1.51–1.34 (m, 13H), 1.32–1.22 (m, 12H), 0.87 (t, 3H).

To a solution of **7a** (130 mg, 0.32 mmol), EDC (92 mg, 0.48 mmol) and HOBr (65 mg, 0.48 mmol) in anhydrous DMF (10 mL) was added DIPEA (112 μ L, 0.64 mmol) at 0 °C, the solution was stirred for 5 min, followed by adding a pre-mixed solution of ciprofloxacin (158 mg, 0.48 mmol) and DIPEA (112 μ L, 0.64 mmol) in anhydrous DMF (5 mL)

dropwise. The reaction was stirred for 5 h at room temperature before quenching with HCl (1 M). The mixture was diluted with DCM ($\times 2$) and the organic phase was washed with brine, separated, dried over anhydrous Na_2SO_4 , and concentrated under vacuum. The crude residue **8a** was used directly without further purification. Compound **8a** (232 mg, 0.32 mmol) was dissolved in 6 mL of TFA/DCM (19/1, v/v). The reaction mixture was stirred for 2 h at room temperature. Upon completion, the solvents were concentrated in vacuo to give crude compound of **9a**, which was dissolved in water/methanol (1:1) solution (10 mL) and purified by preparative HPLC (R_t = 6.8 min) and lyophilization. White solid, m.p. 113–115 °C, yield 41.8 %; ¹H NMR (500 MHz, CD_3OD) δ 8.74–8.65 (s, 1H), 7.81–7.73 (m, 1H), 7.52 (d, J = 7.1 Hz, 1H), 4.06–3.93 (m, 2H), 3.83–3.70 (m, 2H), 3.66 (m, 1H), 3.46 (m, 2H), 3.41–3.32 (m, 1H), 3.30 (m, 1H), 3.27 (m, 1H), 2.93 (t, 2H), 2.24 (m, 2H), 1.86–1.78 (m, 1H), 1.70 (m, 3H), 1.59 (m, 2H), 1.51–1.36 (m, 4H), 1.32–1.18 (m, 14H), 0.85 (t, 3H). ¹³C NMR (126 MHz, CD_3OD) δ 178.33, 176.19, 172.41, 169.53, 155.10 (d, J = 250.2 Hz, C-6), 149.45, 146.89 (d, J = 10.4 Hz, C-7), 140.85, 120.86 (d, J = 7.6 Hz, C-4a), 112.60 (d, J = 23.2 Hz, C-5), 108.20, 107.54 (C-8), 51.32, 50.66, 50.11, 46.79, 43.27, 40.67, 37.14, 36.90, 33.19, 32.61, 30.79, 30.65, 30.58, 30.53, 28.45, 27.13, 23.90, 23.88, 14.60, 8.73 (2C). ESI-HRMS calcd for $\text{C}_{33}\text{H}_{48}\text{FN}_5\text{O}_5$ [M+H]⁺: 614.3639; found 614.3709.

The compounds **7b–e** were synthesized following the similar procedure of **7a**.

N^a-dodecanoyl-*N*^t-trityl-*L*-histidine (**7b**). White solid, yield 79.1 %; ¹H NMR (500 MHz, CDCl_3) δ 8.09 (d, J = 1.6 Hz, 1H), 7.41 (d, J = 1.7 Hz, 5H), 7.40 (m, 3H), 7.11–7.07 (m, 6H), 7.04 (d, J = 6.8 Hz, 1H), 6.83 (d, J = 1.4 Hz, 1H), 4.71 (dd, J = 6.6 Hz, 1H), 3.35 (dd, J = 15.0, 5.3 Hz, 1H), 3.20 (dd, J = 15.0, 6.8 Hz, 1H), 2.11 (m, 2H), 1.56–1.43 (m, 2H), 1.32–1.17 (m, 17H), 0.87 (t, 3H).

N^a-(2-([1,1'-biphenyl]-4-yl)acetyl)-*N*^t-trityl-*L*-histidine (**7c**). Light yellow solid, yield 85.3 %; ¹H NMR (500 MHz, CDCl_3) δ 7.82 (d, J = 1.6 Hz, 1H), 7.69 (d, J = 8.2 Hz, 1H), 7.33–7.32 (m, 2H), 7.30 (d, J = 1.7 Hz, 1H), 7.30–7.28 (m, 1H), 7.27 (d, J = 1.7 Hz, 2H), 7.26–7.25 (m, 2H), 7.22 (d, J = 3.9 Hz, 2H), 7.20 (s, 3H), 7.19 (s, 1H), 7.18 (s, 2H), 7.16 (s, 1H), 6.86 (s, 3H), 6.84 (d, J = 1.3 Hz, 3H), 6.72 (d, J = 1.4 Hz, 1H), 4.75 (m, 1H), 3.50–3.40 (m, 2H), 3.26 (dd, J = 15.0, 4.6 Hz, 1H), 3.05 (dd, J = 15.0, 9.6 Hz, 1H).

The compounds **9b–e** were synthesized following the similar procedure of **9a**.

*1-cyclopropyl-7-(4-(dodecanoyl-*L*-histidyl)piperazin-1-yl)-6-fluoro-4-oxo-1,4-dihydroquinoline-3-carboxylic acid (**9b**)*. White solid, m.p. 182–184 °C, yield 38.4 %; ¹H NMR (500 MHz, CD_3OD) δ 8.82 (d, J = 1.4 Hz, 1H), 8.74 (m, 1H), 7.91–7.80 (m, 1H), 7.55 (m, 1H), 7.37 (s, 1H), 5.27 (m, 1H), 4.02–3.85 (m, 2H), 3.79–3.69 (m, 3H), 3.52–3.32 (m, 4H), 3.22 (m, 1H), 3.08 (m, 1H), 2.26–2.12 (m, 2H), 1.54 (m, 2H), 1.40 (m, 2H), 1.25 (m, 18H), 0.86 (t, 3H). ¹³C NMR (126 MHz, CD_3OD) δ 178.12, 175.65, 170.29, 169.28, 154.91 (d, J = 250.2 Hz, C-6), 149.25, 146.63 (d, J = 10.0 Hz, C-7), 140.65, 134.93, 131.28, 120.71 (d, J = 7.7 Hz, C-4a), 118.69, 112.45 (d, J = 23.9 Hz, C-5), 108.05, 107.34 (C-8), 51.12, 50.42, 49.29, 46.51, 43.20, 36.94, 36.65, 33.04, 30.76, 30.72, 30.64, 30.46, 30.43, 30.31, 28.21, 26.86, 23.71, 14.42, 8.56 (2C). ESI-HRMS calcd for $\text{C}_{35}\text{H}_{47}\text{FN}_6\text{O}_5$ [M+H]⁺: 651.3592; found 651.3672.

*7-(4-((2-([1,1'-biphenyl]-4-yl)acetyl)-*L*-histidyl)piperazin-1-yl)-1-cyclopropyl-6-fluoro-4-oxo-1,4-dihydroquinoline-3-carboxylic acid (**9c**)*. White solid, m.p. 112–114 °C, yield 29 %; ¹H NMR (500 MHz, CD_3OD) δ 8.83 (s, 1H), 8.66 (s, 1H), 7.90 (m, 2H), 7.79 (d, J = 13.0 Hz, 1H), 7.72 (d, J = 7.4 Hz, 2H), 7.64 (d, J = 7.6 Hz, 2H), 7.51–7.34 (m, 5H), 5.50 (s, 1H), 4.08 (d, J = 12.9 Hz, 1H), 3.99 (s, 1H), 3.81 (s, 2H), 3.73 (s, 1H), 3.64 (s, 1H), 3.44 (m, 4H), 3.32–3.21 (m, 4H), 1.27 (m, 2H), 1.14 (s, 2H). ¹³C NMR (126 MHz, CD_3OD) δ 177.94, 170.24, 169.16, 169.07, 154.81 (d, J = 250.2 Hz, C-6), 149.09, 146.59 (d, J = 10.1 Hz, C-7), 146.04, 140.81, 140.47, 134.96, 133.18, 131.38, 130.06 (2C), 129.28, 129.14, 128.06 (2C), 128.02 (2C), 120.57 (C-4a), 118.76, 112.31 (d, J = 23.2 Hz, C-5), 107.93, 107.25 (C-8), 50.87, 50.57, 50.28, 46.51, 44.58, 43.38, 36.85, 28.16, 8.46 (2C). ESI-HRMS calcd for $\text{C}_{37}\text{H}_{53}\text{FN}_6\text{O}_5$

[M+H]⁺: 663.2653; found 663.2627.

*7-(4-((2-(adamantan-1-yl)acetyl)-*L*-histidyl)piperazin-1-yl)-1-cyclopropyl-6-fluoro-4-oxo-1,4-dihydroquinoline-3-carboxylic acid (**9d**)*. White solid, m.p. 201–203 °C, yield 32 %; ¹H NMR (500 MHz, $\text{DMSO}-d_6$) δ 15.17 (s, 1H), 14.28 (s, 1H), 9.00 (d, J = 1.4 Hz, 1H), 8.68 (s, 1H), 8.29 (d, J = 8.8 Hz, 1H), 7.94 (d, J = 13.1 Hz, 1H), 7.57 (d, J = 7.4 Hz, 1H), 7.41 (s, 1H), 5.22 (m, 1H), 3.83 (m, 3H), 3.79–3.72 (m, 1H), 3.64 (m, 1H), 3.43 (m, 4H), 3.30–3.24 (m, 2H), 3.03 (dd, J = 15.1, 5.3 Hz, 1H), 2.95 (dd, J = 15.2, 9.4 Hz, 1H), 1.89–1.80 (m, 5H), 1.62 (d, J = 12.1 Hz, 3H), 1.51 (s, 2H), 1.49–1.46 (m, 2H), 1.45 (t, 1H), 1.34–1.29 (m, 4H), 1.23–1.16 (m, 2H). ¹³C NMR (126 MHz, $\text{DMSO}-d_6$) δ 176.55, 169.82, 168.91, 166.07, 153.12 (d, J = 249.1 Hz, C-6), 148.31, 144.91 (d, J = 11.0 Hz, C-7), 139.30, 133.87, 129.77, 119.08 (d, J = 7.7 Hz, C-4a), 117.64, 111.26 (d, J = 22.9 Hz, C-5), 106.97, 106.77 (C-8), 49.70 (2C), 49.50, 47.17, 44.84, 42.02 (3C), 41.57, 36.53 (3C), 36.07, 32.28, 28.12 (3C), 27.13, 7.76 (2C). ESI-HRMS calcd for $\text{C}_{35}\text{H}_{41}\text{FN}_6\text{O}_5$ [M+H]⁺: 645.3122; found 645.3202.

*1-cyclopropyl-7-(4-(dodecanoyl-*L*-arginyl)piperazin-1-yl)-6-fluoro-4-oxo-1,4-dihydroquinoline-3-carboxylic acid (**9e**)*. Light yellow solid, m.p. 139–141 °C, yield 35 %; ¹H NMR (500 MHz, CD_3OD) δ 8.76 (s, 1H), 7.87 (d, J = 13.1 Hz, 1H), 7.58 (s, 1H), 4.94 (dd, J = 8.3, 5.4 Hz, 1H), 4.06–3.94 (m, 2H), 3.85–3.65 (m, 3H), 3.50 (m, 2H), 3.38 (m, 2H), 3.23 (m, 2H), 2.27 (t, J = 7.5 Hz, 2H), 1.84 (m, 1H), 1.77–1.66 (m, 2H), 1.62 (m, 3H), 1.42 (m, 2H), 1.35–1.31 (m, 4H), 1.26 (m, 14H), 0.88 (t, 3H). ¹³C NMR (126 MHz, CD_3OD) δ 178.19, 176.06, 172.02, 169.36, 158.67, 154.95 (d, J = 250.4 Hz, C-6), 149.29, 146.71 (d, J = 10.1 Hz, C-7), 140.69, 120.74 (d, J = 7.7 Hz, C-4a), 112.47 (d, J = 23.4 Hz, C-5), 108.06, 107.39 (C-8), 51.15, 50.51, 49.70, 46.61, 43.12, 42.06, 36.97, 36.74, 33.05, 30.75, 30.73, 30.65, 30.47, 30.46, 30.36, 30.08, 26.96, 26.16, 23.71, 14.42, 8.56 (2C). ESI-HRMS calcd for $\text{C}_{35}\text{H}_{52}\text{FN}_7\text{O}_5$ [M+H]⁺: 670.4014; found 670.4096.

(S)-7-(4-((4-((6-amino-1-oxo-1-pentylamino)hexan-2-yl)carbamoyl)benzoyl)piperazin-1-yl)-1-cyclopropyl-6-fluoro-4-oxo-1,4-dihydroquinoline-3-carboxylic acid (**16a**). CTC-resin (300 mg, 0.22 mmol) was swelled in 6 mL of DCM for 15 min. The attachment of the first amino acid to the resin was achieved by adding Fmoc-Lys(Boc)-OH (208 mg, 0.44 mmol) and DIPEA (140 μ L, 0.79 mmol) to the beads in the reaction vessel, which was allowed to shake at room temperature for 2 h. After that, the reaction solution was drained, followed by washing with DMF (4 mL \times 3) and DCM (4 mL \times 3). The unreacted 2-chlorotriptylchloride moieties were capped with 5 mL of DIPEA/MeOH/DCM (1/2/17, v/v/v) for 30 min. The beads were washed with DCM (4 mL \times 3) and DMF (4 mL \times 3). The Fmoc group was removed by treating beads with 20 % piperidine/DMF (v/v) solution for 10 min (\times 2) at room temperature to afford **11a** (n = 1). Then Terephthalic acid (185 mg, 1.1 mmol), HCTU (415 mg, 0.99 mmol), and DIPEA (349 μ L, 1.98 mmol) were premixed in 3 mL DMF for 5 min before getting transferred to the reaction vessel. The reaction was shaken at room temperature for 2 h, and the solution was removed to afford **12a** (n = 1). After DMF (3 mL \times 3) and DCM (3 mL \times 3) wash, to a solution of HCTU (166 mg, 0.40 mmol) and DIPEA (140 μ L, 0.79 mmol) in 3 mL DMF were added to the beads in the reaction vessel for 5 min, followed by adding a pre-mixed solution of ciprofloxacin methyl ester (154 mg, 0.44 mmol) and DIPEA (78 μ L, 0.44 mmol) in 3 mL DMF for 5 h at room temperature, and the solution was removed. After DMF (3 mL \times 3) and DCM (3 mL \times 3) wash, the intermediate was cleaved from resin with 5 mL of the cleavage cocktail (HFIP/DCM 1:4, v/v) for 2 h. The solution was collected, and the remaining beads were washed with 3 mL of the cleavage cocktail solution three times. All the solution was combined and concentrated in vacuo with coevaporation with hexane multiple times to afford **13a** (n = 1). Crude compound of **13a** (n = 1) was dissolved in water/methanol (1:1) solution (10 mL), filtered through a Whatman filter unit (0.22 μ m), and checked by analytic HPLC. Pure **13a** (n = 1) was obtained as white powder (122 mg, 81 %) after preparative HPLC and lyophilization. The preparative HPLC gradient system employed a program of 30 %–100 % linear gradient of solvent B (0.1 % TFA in acetonitrile) in A (0.1 % TFA in water) over the

duration of 15 min at a flow rate of 16 mL/min, Rt = 8.9 min. *N*⁶-(*tert*-butoxycarbonyl)-*N*²-(4-(4-(1-cyclopropyl-6-fluoro-3-(methoxycarbonyl)-4-oxo-1,4-dihydroquinolin-7-yl)piperazine-1-carbonyl)benzoyl)-*L*-lysine (**13a**). White solid, yield 77 %; ¹H NMR (500 MHz, CD₃OD) δ 8.62 (s, 1H), 7.98 (d, J = 8.4 Hz, 2H), 7.82–7.76 (m, 1H), 7.59 (d, J = 8.4 Hz, 2H), 7.49 (d, J = 7.2 Hz, 1H), 4.59 (m, 1H), 4.06–3.93 (m, 2H), 3.85 (s, 3H), 3.65 (m, 3H), 3.48–3.40 (m, 2H), 3.34–3.31 (m, 2H), 3.05 (m, 2H), 2.00 (m, 1H), 1.87 (m, 1H), 1.57–1.46 (m, 4H), 1.41 (s, 9H), 1.36 (m, 2H), 1.17 (m, 2H). ¹³C NMR (126 MHz, CD₃OD) δ 175.43, 174.61, 171.57, 169.38, 166.61, 158.54, 154.75 (d, J = 248.6 Hz, C-6), 150.07, 145.92 (d, J = 10.5 Hz, C-7), 139.84, 139.59, 136.88, 129.03 (2C), 128.34 (2C), 122.95 (d, J = 11.5 Hz, C-4a), 112.90 (d, J = 23.2 Hz, C-5), 109.67, 107.46 (d, J = 1.6 Hz, C-8), 79.83, 54.33, 52.28, 51.16, 50.68, 43.21, 41.08 (2C), 36.52, 32.11, 30.58, 28.79 (3C), 24.52, 8.55 (2C). LC-MS calcd for C₃₇H₄₄FN₅O₉ [M+H]⁺: 722.31; found 722.42.

To a solution of **13a** (n = 1) (122 mg, 0.17 mmol), EDC (50 mg, 0.26 mmol) and HOBr (36 mg, 0.26 mmol) in anhydrous DMF (8 mL) was added DIPEA (60 μL, 0.34 mmol) at 0 °C, the solution was stirred for 5 min, and followed by adding a pre-mixed solution of butan-1-amine (34 μL, 0.34 mmol) and DIPEA (60 μL, 0.34 mmol) in anhydrous DMF (5 mL) dropwise. The reaction was stirred for 5 h at room temperature before quenching with HCl (1 M). The mixture was diluted with DCM (× 2) and the organic phase was washed with brine, separated, dried over anhydrous Na₂SO₄, and concentrated under vacuum. The crude residue **14a** was used directly without further purification. Then, to a solution of compound **14a** (132 mg, 0.17 mmol) in 6 mL of MeOH/H₂O (5:1, v/v) was added LiOH (73 mg, 1.7 mmol) partwise. The reaction mixture was stirred for 2 h at room temperature. Upon completion, the reaction was quenched with HCl (1 M), and then extracted with DCM (× 2). The combined organic layer was washed with brine, dried over Na₂SO₄, and concentrated under reduced pressure. The crude residue **15a** was used directly without further purification. Finally, the compound **15a** (130 mg, 0.17 mmol) was dissolved in 5 mL of TFA/DCM (19/1, v/v/v). The reaction mixture was stirred for 2 h at room temperature. Upon completion, the solvents were concentrated in vacuo to give crude compound of **16a**, which was purified by preparative HPLC (Rt = 7.5 min) and lyophilization. Light yellow solid, m.p. 114–116 °C, yield 48.8 %; ¹H NMR (500 MHz, CD₃OD) δ 8.73 (s, 1H), 7.99 (d, J = 7.5 Hz, 2H), 7.84 (d, J = 13.0 Hz, 1H), 7.59 (d, J = 7.6 Hz, 3H), 4.55 (dd, J = 8.9, 5.5 Hz, 1H), 4.02 (m, 2H), 3.68 (m, 3H), 3.50 (m, 2H), 3.38 (m, 2H), 3.21 (t, 2H), 2.94 (s, 2H), 1.93 (m, 1H), 1.84 (m, 1H), 1.72 (m, 2H), 1.53 (m, 4H), 1.40 (m, 2H), 1.33 (m, 4H), 1.22 (m, 2H), 0.90 (t, J = 6.9 Hz, 3H). ¹³C NMR (126 MHz, CD₃OD) δ 178.06, 173.98, 171.57, 169.25, 169.19, 154.93 (d, J = 250.2 Hz, C-6), 149.22, 146.71 (d, J = 10.2 Hz, C-7), 140.62, 139.70, 136.72, 129.05 (2C), 128.35 (2C), 120.70 (d, J = 8.1 Hz, C-4a), 112.36 (d, J = 23.6 Hz, C-5), 107.99, 107.55 (d, J = 2.8 Hz, C-8), 55.31, 51.09, 50.48, 43.16, 40.61, 40.51, 40.50, 36.97, 32.62, 30.16, 30.05, 28.16, 24.10, 23.39, 14.35, 8.54 (2C). ESI-HRMS calcd for C₃₆H₄₅FN₆O₆ [M+H]⁺: 677.3385; found 677.3475.

The compounds **13m** (n = 2) and **13p** (n = 3) were synthesized following the similar procedure of **13a**.

*N*⁶-(*tert*-butoxycarbonyl)-*N*²-(*N*⁶-(*tert*-butoxycarbonyl)-*N*²-(4-(4-(1-cyclopropyl-6-fluoro-3-(methoxycarbonyl)-4-oxo-1,4-dihydroquinolin-7-yl)piperazine-1-carbonyl)benzoyl)-*L*-lysyl)-*L*-lysine (**13m**). Light yellow solid, yield 83 %; ¹H NMR (500 MHz, CD₃OD) δ 8.67 (d, J = 22.1 Hz, 1H), 8.00 (m, 2H), 7.91–7.78 (m, 1H), 7.60 (dd, J = 21.7, 8.0 Hz, 2H), 7.51 (m, 1H), 4.71–4.56 (m, 1H), 4.41 (d, J = 4.0 Hz, 1H), 4.01 (m, 2H), 3.88 (d, J = 21.8 Hz, 3H), 3.68 (d, J = 1.4 Hz, 3H), 3.50 (d, J = 48.7 Hz, 2H), 3.35 (m, 2H), 3.05 (m, 4H), 2.01–1.83 (m, 3H), 1.75 (m, 1H), 1.62–1.49 (m, 9H), 1.43 (m, 18H), 1.37 (m, 2H), 1.24–1.16 (m, 2H). ¹³C NMR (126 MHz, CD₃OD) δ 175.19, 174.58, 174.51, 171.54, 169.15, 166.59, 158.53, 158.47, 154.74 (d, J = 248.7 Hz, C-6), 150.06, 145.92 (d, J = 10.5 Hz, C-7), 139.82, 139.58, 136.82, 129.07 (2C), 128.33 (2C), 122.90 (d, J = 7.2 Hz, C-4a), 112.91 (d, J = 23.5 Hz, C-5), 109.68, 107.44 (d, J = 2.6 Hz, C-8), 79.84 (2C), 55.35, 53.60, 52.27, 51.23, 50.66, 43.21, 41.14 (3C), 36.52, 32.75, 32.28, 30.64, 30.47, 28.81 (3C),

28.80 (3C), 24.30, 24.17, 8.55 (2C). LC-MS calcd for C₄₈H₆₄FN₇O₁₂ [M+H]⁺: 950.46; found 950.35.

*N*⁶-(*tert*-butoxycarbonyl)-*N*²-(*N*⁶-(*tert*-butoxycarbonyl)-*N*²-(4-(4-(1-cyclopropyl-6-fluoro-3-(methoxycarbonyl)-4-oxo-1,4-dihydroquinolin-7-yl)piperazine-1-carbonyl)benzoyl)-*L*-lysyl)-*L*-lysyl (**13p**). Light yellow solid, yield 85 %; ¹H NMR (500 MHz, CD₃OD) δ 8.65 (d, J = 3.5 Hz, 1H), 8.06–7.97 (m, 2H), 7.83 (d, J = 13.2 Hz, 1H), 7.59 (d, J = 8.0 Hz, 2H), 7.51 (d, J = 7.2 Hz, 1H), 4.59 (d, J = 5.5 Hz, 1H), 4.47–4.33 (m, 2H), 4.01 (m, 2H), 3.86 (s, 3H), 3.76–3.62 (m, 3H), 3.51–3.41 (m, 2H), 3.35 (m, 3H), 3.08–3.00 (m, 5H), 1.95–1.81 (m, 4H), 1.77–1.66 (m, 3H), 1.58–1.46 (m, 11H), 1.42 (m, 27H), 1.37 (d, J = 7.0 Hz, 2H), 1.21–1.15 (m, 2H). ¹³C NMR (126 MHz, CD₃OD) δ 175.11, 174.54, 174.52, 174.15, 171.54, 169.22, 166.65, 158.50, 158.45 (2C), 154.80 (d, J = 249.1 Hz, C-6), 150.09, 146.02 (d, J = 10.4 Hz, C-7), 139.91, 139.60, 136.80, 129.13 (2C), 128.33 (2C), 122.80 (d, J = 7.3 Hz, C-4a), 112.93 (d, J = 23.2 Hz, C-5), 109.65, 107.45 (C-8), 79.81 (3C), 55.49, 54.57, 53.49, 52.32, 51.23, 50.66, 43.21, 41.31, 41.19 (2C), 41.08, 36.58, 32.74, 32.72, 32.31, 30.63, 30.53, 30.44, 28.83 (9C), 24.41, 24.12, 24.06, 8.57 (2C). LC-MS calcd for C₅₉H₈₄FN₉O₁₅ [M+2H]²⁺: 590.31; found 590.16.

The compounds **16b–u** were synthesized following the similar procedure of **16a**.

(*S*)-7-(4-(4-((6-amino-1-(hexylamino)-1-oxohexan-2-yl)carbamoyl)benzoyl)piperazin-1-yl)-1-cyclopropyl-6-fluoro-4-oxo-1,4-dihydroquinoline-3-carboxylic acid (**16b**). Light yellow solid, m.p. 139–131 °C, yield 46 %; ¹H NMR (500 MHz, CD₃OD) δ 8.72 (s, 1H), 7.99 (d, J = 7.5 Hz, 2H), 7.81 (d, J = 13.0 Hz, 1H), 7.60 (d, J = 7.4 Hz, 3H), 4.56 (dd, J = 8.8, 5.6 Hz, 1H), 4.08–3.91 (m, 2H), 3.69 (m, 3H), 3.45 (m, 4H), 3.22 (t, 2H), 2.94 (t, 2H), 1.95 (m, 1H), 1.89–1.80 (m, 1H), 1.73 (m, 2H), 1.52 (m, 4H), 1.41 (m, 2H), 1.37–1.29 (m, 6H), 1.23 (m, 2H), 0.94–0.87 (t, 3H). ¹³C NMR (126 MHz, CD₃OD) δ 178.04, 173.98, 171.55, 169.21, 169.17, 154.90 (d, J = 250.0 Hz, C-6), 149.19, 146.69 (d, J = 9.8 Hz, C-7), 140.60, 139.69, 136.70, 129.05 (2C), 128.35 (2C), 120.65 (d, J = 7.7 Hz, C-4a), 112.33 (d, J = 23.8 Hz, C-5), 107.97, 107.53 (C-8), 55.32, 51.06, 50.54, 43.17, 40.60, 40.51 (2C), 36.99, 32.63, 30.32 (2C), 28.16, 27.63, 24.10, 23.63, 14.36, 8.54 (2C). ESI-HRMS calcd for C₃₇H₄₇FN₆O₆ [M+H]⁺: 691.3541; found 691.3637.

(*S*)-7-(4-(4-((6-amino-1-(octylamino)-1-oxohexan-2-yl)carbamoyl)benzoyl)piperazin-1-yl)-1-cyclopropyl-6-fluoro-4-oxo-1,4-dihydroquinoline-3-carboxylic acid (**16c**). Light yellow solid, m.p. 136–138 °C, yield 52 %; ¹H NMR (500 MHz, CD₃OD) δ 8.74 (s, 1H), 8.00 (s, 2H), 7.84 (d, J = 12.6 Hz, 1H), 7.61 (brs, 3H), 4.55 (t, 1H), 4.04 (m, 2H), 3.70 (m, 3H), 3.61–3.33 (m, 4H), 3.22 (t, J = 7.0 Hz, 2H), 2.96 (m, 2H), 1.95 (m, 1H), 1.86 (m, 1H), 1.74 (m, 2H), 1.58–1.49 (m, 4H), 1.42 (m, 1H), 1.37–1.24 (m, 13H), 0.92–0.88 (t, 3H). ¹³C NMR (126 MHz, CD₃OD) δ 178.06, 173.97, 171.56, 169.24, 169.17, 154.93 (d, J = 250.2 Hz, C-6), 149.22, 146.71 (d, J = 10.3 Hz, C-7), 140.62, 139.70, 136.71, 129.05 (2C), 128.35 (2C), 120.70 (d, J = 8.0 Hz, C-4a), 112.36 (d, J = 23.5 Hz, C-5), 107.99, 107.55 (d, J = 2.8 Hz, C-8), 55.31, 51.09, 50.51, 43.16, 40.60, 40.51 (2C), 36.97, 32.95, 32.62, 30.36 (3C), 28.16, 27.95, 24.10, 23.69, 14.43, 8.54 (2C). ESI-HRMS calcd for C₃₉H₅₁FN₆O₆ [M+H]⁺: 719.3854; found 719.3944.

(*S*)-7-(4-(4-((6-amino-1-(nonylamino)-1-oxohexan-2-yl)carbamoyl)benzoyl)piperazin-1-yl)-1-cyclopropyl-6-fluoro-4-oxo-1,4-dihydroquinoline-3-carboxylic acid (**16d**). Light yellow solid, m.p. 133–135 °C, yield 50 %; ¹H NMR (500 MHz, CD₃OD) δ 8.72 (s, 1H), 7.97 (d, J = 7.7 Hz, 2H), 7.82 (d, J = 13.0 Hz, 1H), 7.58 (d, J = 8.0 Hz, 3H), 4.53 (dd, J = 8.9, 5.6 Hz, 1H), 4.01 (m, 2H), 3.67 (m, 3H), 3.43 (m, 4H), 3.19 (t, 2H), 2.92 (m, 2H), 1.96–1.88 (m, 1H), 1.84 (m, 1H), 1.71 (m, 2H), 1.50 (m, 4H), 1.39 (m, 2H), 1.33–1.24 (m, 13H), 1.20 (m, 2H), 0.88 (t, 2H). ¹³C NMR (126 MHz, CD₃OD) δ 178.26, 173.97, 171.59, 169.42, 169.22, 155.04 (d, J = 249.9 Hz, C-6), 149.36, 146.78 (d, J = 10.5 Hz, C-7), 140.71, 139.71, 136.71, 129.06 (2C), 128.37 (2C), 120.90 (d, J = 8.3 Hz, C-4a), 112.48 (d, J = 23.6 Hz, C-5), 108.07, 107.67 (C-8), 55.26, 49.46, 49.29, 43.16, 40.51 (3C), 37.00, 33.04, 32.61, 30.66, 30.42, 30.39, 30.37, 28.16, 27.95, 24.10, 23.72, 14.45, 8.56 (2C). ESI-HRMS

calcd for $C_{40}H_{53}FN_6O_6$ [M+H]⁺: 733.4011; found 733.4087.

(S)-7-(4-((6-amino-1-(dodecylamino)-1-oxohexan-2-yl)carbamoyl)benzoylpiperazin-1-yl)-1-cyclopropyl-6-fluoro-4-oxo-1,4-dihydroquinoline-3-carboxylic acid (**16e**). Light yellow solid, m.p. 139–141 °C, yield 38 %; ¹H NMR (500 MHz, CD₃OD) δ 8.76 (s, 1H), 8.00 (d, *J* = 7.8 Hz, 2H), 7.95 (d, *J* = 8.1 Hz, 1H), 7.87 (d, *J* = 13.1 Hz, 1H), 7.61 (d, *J* = 7.8 Hz, 3H), 4.55 (d, *J* = 10.1, 5.1 Hz, 1H), 4.03 (m, 2H), 3.76 (m, 1H), 3.69 (m, 2H), 3.51 (m, 2H), 3.39 (m, 2H), 3.22 (m, 2H), 2.97–2.91 (m, 2H), 1.99–1.92 (m, 1H), 1.86 (m, 1H), 1.73 (m, 2H), 1.57–1.48 (m, 4H), 1.42 (m, 2H), 1.29 (m, 18H), 1.23 (m, 2H), 0.91–0.88 (t, 3H). ¹³C NMR (126 MHz, CD₃OD) δ 178.18, 173.97, 171.57, 169.34, 169.19, 154.99 (d, *J* = 249.9 Hz, C-6), 149.29, 146.74 (d, *J* = 10.2 Hz, C-7), 140.66, 139.69, 136.72, 130.78, 129.06, 128.65, 128.36, 120.86 (C-4a), 112.44 (d, *J* = 23.3 Hz, C-5), 108.06, 107.61 (C-8), 55.30, 51.13, 50.50, 43.13, 40.51 (3C), 36.98, 33.05, 32.60, 30.78, 30.74, 30.72, 30.70, 30.46, 30.42, 30.37, 28.15, 27.97, 24.10, 23.72, 14.44, 8.55 (2C). ESI-HRMS calcd for $C_{43}H_{59}FN_6O_6$ [M+H]⁺: 775.4480; found 775.4573.

(S)-7-(4-((6-amino-1-oxo-1-(tetradecylamino)hexan-2-yl)carbamoyl)benzoylpiperazin-1-yl)-1-cyclopropyl-6-fluoro-4-oxo-1,4-dihydroquinoline-3-carboxylic acid (**16f**). Light yellow solid, m.p. 167–169 °C, yield 45 %; ¹H NMR (500 MHz, CD₃OD) δ 8.74 (s, 1H), 7.99 (d, *J* = 7.8 Hz, 2H), 7.85 (d, *J* = 13.0 Hz, 1H), 7.60 (d, *J* = 7.8 Hz, 3H), 4.55 (dd, *J* = 8.9, 5.6 Hz, 1H), 4.02 (m, 2H), 3.72 (m, 3H), 3.50 (m, 2H), 3.38 (m, 2H), 3.21 (m, 2H), 2.94 (t, 2H), 1.94 (m, 1H), 1.85 (m, 1H), 1.72 (m, 2H), 1.59–1.46 (m, 4H), 1.41 (m, 2H), 1.34–1.26 (m, 22H), 1.22 (m, 2H), 0.89 (t, 3H). ¹³C NMR (126 MHz, CD₃OD) δ 178.35, 174.14, 171.74, 169.49, 169.35, 155.16 (d, *J* = 250.2 Hz, C-6), 149.46, 146.91 (d, *J* = 10.2 Hz, C-7), 140.84, 139.87, 136.89, 129.23 (2C), 128.53 (2C), 121.03 (C-4a), 112.61 (d, *J* = 23.5 Hz, C-5), 108.23, 107.78 (C-8), 55.45, 49.63, 49.45, 43.33, 40.69 (3C), 37.16, 33.23, 32.77, 30.97, 30.95 (2C), 30.93, 30.90, 30.88, 30.64, 30.59, 30.54, 28.33, 28.14, 24.27, 23.89, 14.61, 8.72 (2C). ESI-HRMS calcd for $C_{45}H_{63}FN_6O_6$ [M+H]⁺: 803.4793; found 803.4876.

(S)-7-(4-((6-amino-1-(hexadecylamino)-1-oxohexan-2-yl)carbamoyl)benzoylpiperazin-1-yl)-1-cyclopropyl-6-fluoro-4-oxo-1,4-dihydroquinoline-3-carboxylic acid (**16g**). Light yellow solid, m.p. 181–183 °C, yield 54 %; ¹H NMR (500 MHz, CD₃OD) δ 8.76 (s, 1H), 8.00 (s, 2H), 7.87 (d, *J* = 12.8 Hz, 1H), 7.72–7.48 (m, 3H), 4.56 (dd, *J* = 8.8, 5.5 Hz, 1H), 4.04 (m, 2H), 3.70 (m, 2H), 3.52 (m, 2H), 3.40 (m, 2H), 3.32 (m, 1H), 3.23 (t, 2H), 2.96 (s, 2H), 1.91 (m, 2H), 1.74 (m, 2H), 1.53 (m, 4H), 1.42 (m, 2H), 1.28 (m, 26H), 1.23 (m, 2H), 0.90 (t, *J* = 6.9 Hz, 3H). ¹³C NMR (126 MHz, DMSO-*d*₆) δ 176.37, 171.40, 168.53, 165.89, 165.71, 152.97 (d, *J* = 249.9 Hz, C-6), 148.05, 144.85 (d, *J* = 10.0 Hz, C-7), 139.12, 138.22, 135.12, 127.78 (2C), 126.89 (2C), 118.94 (d, *J* = 7.7 Hz, C-4a), 111.03 (d, *J* = 23.0 Hz, C-5), 106.81, 106.77 (C-8), 53.38, 49.56, 49.14, 46.74, 41.25, 38.72, 38.54, 35.90, 31.31, 31.17, 29.08 (8C), 29.03, 28.77, 28.72, 26.68, 26.35, 22.75, 22.11, 13.94, 7.61 (2C). ESI-HRMS calcd for $C_{47}H_{67}FN_6O_6$ [M+H]⁺: 831.5106; found 831.5189.

(S)-7-(4-((6-amino-1-(benzylamino)-1-oxohexan-2-yl)carbamoyl)benzoylpiperazin-1-yl)-1-cyclopropyl-6-fluoro-4-oxo-1,4-dihydroquinoline-3-carboxylic acid (**16h**). Light yellow solid, m.p. 155–157 °C, yield 40 %; ¹H NMR (500 MHz, CD₃OD) δ 8.70 (s, 1H), 7.99 (s, 2H), 7.80 (d, *J* = 12.7 Hz, 1H), 7.58 (brs, 3H), 7.29 (m, 4H), 7.22 (m, 1H), 4.61 (dd, *J* = 8.8, 5.4 Hz, 1H), 4.41 (s, 2H), 3.99 (m, 2H), 3.67 (m, 3H), 3.58–3.33 (m, 4H), 2.92 (m, 2H), 1.98 (m, 1H), 1.88 (m, 1H), 1.71 (m, 2H), 1.51 (m, *J* = 30.3 Hz, 2H), 1.40 (m, 2H), 1.26–1.15 (m, 2H). ¹³C NMR (126 MHz, CD₃OD) δ 178.01, 174.12, 171.55, 169.30, 169.21, 154.89 (d, *J* = 249.8 Hz, C-6), 149.18, 146.68 (d, *J* = 10.7 Hz, C-7), 140.58, 139.84, 139.68, 136.68, 129.53 (2C), 129.08 (2C), 128.49 (2C), 128.34 (2C), 128.22, 120.64 (d, *J* = 7.3 Hz, C-4a), 112.33 (d, *J* = 23.2 Hz, C-5), 107.96, 107.53 (C-8), 55.40, 51.03, 50.42, 44.10, 43.18, 40.57, 40.50, 37.01, 32.51, 28.12, 24.11, 8.55 (2C). ESI-HRMS calcd for $C_{38}H_{41}FN_6O_6$ [M+H]⁺: 697.3072; found 697.3159.

(S)-7-(4-((6-amino-1-((2-chlorobenzyl)amino)-1-oxohexan-2-yl)carbamoyl)benzoylpiperazin-1-yl)-1-cyclopropyl-6-fluoro-4-oxo-1,4-dihydroquinoline-3-carboxylic acid (**16i**). Light yellow solid, m.p. 165–167 °C,

yield 34 %; ¹H NMR (500 MHz, CD₃OD) δ 8.74 (s, 1H), 8.01 (s, 2H), 7.85 (d, *J* = 12.7 Hz, 1H), 7.60 (brs, 3H), 7.44–7.36 (m, 2H), 7.31–7.23 (m, 2H), 4.64 (t, 1H), 4.51 (s, 2H), 4.03 (m, 2H), 3.69 (m, 3H), 3.45 (m, 4H), 2.94 (m, 2H), 1.99 (m, 1H), 1.90 (m, 1H), 1.74 (m, 2H), 1.55 (m, 2H), 1.41 (m, 2H), 1.24 (m, 2H). ¹³C NMR (126 MHz, CD₃OD) δ 178.06, 174.31, 171.57, 169.40, 169.27, 154.93 (d, *J* = 250.4 Hz, C-6), 149.22, 146.71 (d, *J* = 10.5 Hz, C-7), 140.62, 139.70, 136.80, 136.68, 134.22, 130.43, 130.27, 129.86, 129.09 (2C), 128.35 (2C), 128.16, 120.69 (d, *J* = 8.0 Hz, C-4a), 112.37 (d, *J* = 23.0 Hz, C-5), 107.99, 107.53 (C-8), 55.40, 51.03, 50.46, 43.16, 42.12, 40.61, 40.51, 36.98, 32.44, 28.14, 24.12, 8.55 (2C). ESI-HRMS calcd for $C_{38}H_{40}ClFN_6O_6$ [M+H]⁺: 731.2682; found 731.2763.

(S)-7-(4-((6-amino-1-((2,6-dichlorobenzyl)amino)-1-oxohexan-2-yl)carbamoyl)benzoylpiperazin-1-yl)-1-cyclopropyl-6-fluoro-4-oxo-1,4-dihydroquinoline-3-carboxylic acid (**16j**). Light yellow solid, m.p. 201–203 °C, yield 36 %; ¹H NMR (500 MHz, CD₃OD) δ 8.72 (s, 1H), 7.96 (d, *J* = 7.5 Hz, 2H), 7.81 (d, *J* = 12.9 Hz, 1H), 7.68–7.49 (m, 3H), 7.41 (d, *J* = 8.0 Hz, 2H), 7.32–7.27 (m, 1H), 4.76 (m, 1H), 4.66 (m, 1H), 4.61 (m, 1H), 4.02 (m, 2H), 3.68 (m, 3H), 3.51 (m, 2H), 3.37 (m, 2H), 2.92 (m, 2H), 1.97–1.81 (m, 2H), 1.71 (m, 2H), 1.51 (m, 2H), 1.45–1.36 (m, 2H), 1.22 (m, 2H). ¹³C NMR (126 MHz, CD₃OD) δ 177.97, 173.79, 171.53, 169.17, 169.11, 154.87 (d, *J* = 250.7 Hz, C-6), 149.15, 146.67 (d, *J* = 9.9 Hz, C-7), 140.57, 139.66, 137.44 (2C), 136.68, 134.14, 131.21, 129.70 (2C), 129.03 (2C), 128.35 (2C), 120.57 (C-4a), 112.33 (d, *J* = 23.6 Hz, C-5), 107.96, 107.50 (C-8), 55.02, 51.04, 50.47, 43.14, 40.63, 40.53, 40.38, 37.00, 32.73, 28.16, 24.03, 8.56 (2C). ESI-HRMS calcd for $C_{38}H_{39}Cl_2FN_6O_6$ [M+H]⁺: 765.2292; found 765.2374.

(S)-7-(4-((6-amino-1-((2-chloro-6-fluorobenzyl)amino)-1-oxohexan-2-yl)carbamoyl)benzoylpiperazin-1-yl)-1-cyclopropyl-6-fluoro-4-oxo-1,4-dihydroquinoline-3-carboxylic acid (**16k**). Light yellow solid, m.p. 196–198 °C, yield 47 %; ¹H NMR (500 MHz, CD₃OD) δ 8.74 (s, 1H), 7.96 (d, *J* = 7.2 Hz, 2H), 7.84 (d, *J* = 12.8 Hz, 1H), 7.59 (brs, 3H), 7.33 (m, 1H), 7.27 (d, *J* = 8.1 Hz, 1H), 7.11 (m, 1H), 4.64 (dd, *J* = 14.0, 1.6 Hz, 1H), 4.59 (dd, *J* = 8.5, 5.7 Hz, 1H), 4.54 (dd, *J* = 14.1, 1.5 Hz, 1H), 4.01 (m, 2H), 3.69 (m, 3H), 3.45 (m, 4H), 2.91 (m, 2H), 1.92 (m, 1H), 1.84 (m, 1H), 1.70 (m, 2H), 1.44 (m, 4H), 1.27–1.17 (m, 2H). ¹³C NMR (151 MHz, CD₃OD) δ 178.21, 173.72, 171.58, 169.38, 169.20, 163.20 (d, *J* = 249.5 Hz), 155.01 (d, *J* = 250.2 Hz, C-6), 149.32, 146.77 (d, *J* = 10.3 Hz, C-7), 140.68, 139.70, 136.76, 136.71, 131.30 (d, *J* = 9.8 Hz), 129.03 (2C), 128.36 (2C), 126.63 (d, *J* = 3.3 Hz), 124.59 (d, *J* = 17.7 Hz), 120.86 (d, *J* = 7.7 Hz, C-4a), 115.39 (d, *J* = 23.0 Hz), 112.45 (d, *J* = 23.6 Hz, C-5), 108.05, 107.63 (d, *J* = 2.1 Hz, C-8), 54.96, 51.14, 50.51, 43.16, 40.60, 40.51, 36.99, 35.88 (d, *J* = 4.3 Hz), 32.63, 28.15, 23.97, 8.55 (2C). ESI-HRMS calcd for $C_{38}H_{39}Cl_2N_6O_6$ [M+H]⁺: 749.2588; found 749.2674.

(S)-7-(4-((1-((1'-biphenyl)-4-ylmethyl)amino)-6-amino-1-oxohexan-2-yl)carbamoyl)benzoylpiperazin-1-yl)-1-cyclopropyl-6-fluoro-4-oxo-1,4-dihydroquinoline-3-carboxylic acid (**16l**). Light yellow solid, m.p. 174–176 °C, yield 28 %; ¹H NMR (500 MHz, CD₃OD) δ 8.73 (s, 1H), 8.00 (s, 2H), 7.85 (d, *J* = 12.9 Hz, 1H), 7.56 (dd, *J* = 7.7, 4.5 Hz, 7H), 7.39 (m, 4H), 7.30 (t, 1H), 4.64 (dd, *J* = 8.0 Hz, 1H), 4.46 (s, 2H), 4.01 (m, 2H), 3.66 (m, 3H), 3.48 (m, 2H), 3.42–3.31 (m, 2H), 2.94 (m, 2H), 2.05–1.97 (m, 1H), 1.91 (m, 1H), 1.73 (m, 2H), 1.61–1.47 (m, 2H), 1.39 (m, 2H), 1.20 (m, 2H). ¹³C NMR (126 MHz, CD₃OD) δ 177.91, 174.19, 171.49, 169.28, 169.15, 154.81 (d, *J* = 250.5 Hz, C-6), 149.08, 146.60 (d, *J* = 10.3 Hz, C-7), 141.81, 141.20, 140.49, 139.64, 138.98, 136.65, 129.86 (2C), 129.10 (2C), 129.02 (3C), 128.34 (2C), 127.99 (2C), 127.76 (2C), 120.55 (d, *J* = 7.8 Hz, C-4a), 112.32 (d, *J* = 23.6 Hz, C-5), 107.93, 107.41 (C-8), 55.50, 51.05, 50.42, 43.80, 43.12, 40.60, 40.51, 36.93, 32.49, 28.14, 24.15, 8.54 (2C). ESI-HRMS calcd for $C_{44}H_{45}FN_6O_6$ [M+H]⁺: 773.3385; found 773.3446.

7-(4-((*((S)*-6-amino-1-(((*S*)-6-amino-1-nonylamino)-1-oxohexan-2-yl)amino)-1-oxohexan-2-yl)carbamoyl)benzoylpiperazin-1-yl)-1-cyclopropyl-6-fluoro-4-oxo-1,4-dihydroquinoline-3-carboxylic acid (**16m**). Light yellow solid, m.p. 138–140 °C, yield 33 %; ¹H NMR (500 MHz, CD₃OD) δ 8.67 (s, 1H), 8.00 (d, *J* = 8.3 Hz, 2H), 7.77–7.68 (m, 1H), 7.60 (d, *J* =

8.2 Hz, 2H), 7.54 (d, J = 6.2 Hz, 1H), 4.52 (dd, J = 8.4, 6.2 Hz, 1H), 4.36 (dd, J = 9.4, 5.0 Hz, 1H), 4.02 (s, 2H), 3.71 (m, 3H), 3.48 (m, 2H), 3.38 (m, 2H), 3.18 (m, 2H), 2.95 (m, 4H), 1.99–1.82 (m, 3H), 1.78–1.67 (m, 5H), 1.58–1.48 (m, 5H), 1.41 (m, 2H), 1.34–1.25 (m, 13H), 1.21 (m, 2H), 0.92–0.87 (t, 3H). ^{13}C NMR (126 MHz, CD₃OD) δ 178.16, 174.31, 173.86, 171.56, 169.56, 169.33, 154.98 (d, J = 250.1 Hz, C-6), 149.27, 146.74 (d, J = 10.3 Hz, C-7), 140.66, 139.75, 136.62, 129.09 (2C), 128.36 (2C), 120.79 (d, J = 8.1 Hz, C-4a), 112.41 (d, J = 23.5 Hz, C-5), 108.03, 107.60 (d, J = 2.4 Hz, C-8), 55.68, 54.44, 51.11, 50.51, 43.12, 40.61, 40.50, 40.46, 40.40, 36.98, 33.02, 32.63, 32.08, 30.65, 30.42, 30.40, 30.34, 28.12, 27.98, 27.96, 24.02, 23.80, 23.71, 14.43, 8.55 (2C). ESI-HRMS calcd for C₄₆H₆₅FN₈O₇ [M+H]⁺: 861.4960; found 861.5061.

7-(4-(4-(((S)-6-amino-1-(((S)-6-amino-1-(decylamino)-1-oxohexan-2-yl)amino)-1-oxohexan-2-yl)carbamoyl)benzoyl)piperazin-1-yl)-1-cyclopropyl-6-fluoro-4-oxo-1,4-dihydroquinoline-3-carboxylic acid (16n). Light yellow solid, m.p. 135–137 °C, yield 36 %; ^1H NMR (500 MHz, CD₃OD) δ 8.63 (d, J = 2.4 Hz, 1H), 8.07–7.97 (m, 2H), 7.69–7.65 (m, 1H), 7.59 (d, J = 5.7 Hz, 2H), 7.55–7.49 (m, 1H), 4.52 (m, 1H), 4.41–4.33 (m, 1H), 4.01 (m, 2H), 3.70 (m, 3H), 3.49 (m, 2H), 3.37 (m, 2H), 3.23–3.14 (m, 2H), 3.02–2.91 (m, 4H), 2.01–1.88 (m, 3H), 1.85 (m, 1H), 1.78–1.73 (m, 3H), 1.71–1.66 (m, 2H), 1.59 (m, 2H), 1.51 (m, 4H), 1.43–1.38 (m, 3H), 1.28 (m, 10H), 1.24 (m, 2H), 1.21 (m, 2H), 0.88 (t, 3H). ^{13}C NMR (126 MHz, CD₃OD) δ 177.92, 174.32, 173.85, 171.52, 169.52, 169.18, 154.83 (d, J = 250.6 Hz, C-6), 149.11, 146.69 (C-7), 140.54, 139.68, 136.56, 129.10 (2C), 128.34 (2C), 120.52 (d, J = 8.1 Hz, C-4a), 112.27 (d, J = 24.3 Hz, C-5), 107.91, 107.47 (C-8), 55.72, 54.48, 49.45, 48.49, 43.17, 40.56, 40.47 (3C), 36.97, 33.00, 32.55, 32.04, 30.66, 30.40, 30.31, 28.07 (2C), 27.96, 27.91 (2C), 24.01, 23.78, 23.68, 14.43, 8.54 (2C). ESI-HRMS calcd for C₄₇H₆₇FN₈O₇ [M+H]⁺: 875.5117; found 875.5189.

7-(4-(4-(((S)-6-amino-1-(((S)-6-amino-1-(dodecylamino)-1-oxohexan-2-yl)amino)-1-oxohexan-2-yl)carbamoyl)benzoyl)piperazin-1-yl)-1-cyclopropyl-6-fluoro-4-oxo-1,4-dihydroquinoline-3-carboxylic acid (16o). Light yellow solid, m.p. 135–137 °C, yield 42 %; ^1H NMR (500 MHz, CD₃OD) δ 8.76 (s, 1H), 8.00 (s, 2H), 7.86 (d, J = 12.7 Hz, 1H), 7.61 (brs, 3H), 4.52 (m, 1H), 4.37 (dd, J = 9.4, 4.9 Hz, 1H), 4.04 (m, 2H), 3.70 (m, 3H), 3.53 (m, 1H), 3.41 (m, 3H), 3.19 (m, 2H), 2.95 (m, 4H), 1.98–1.83 (m, 3H), 1.72 (m, 5H), 1.60–1.48 (m, 6H), 1.42 (m, 2H), 1.31 (m, 18H), 1.26 (m, 2H), 0.90 (t, 3H). ^{13}C NMR (151 MHz, CD₃OD) δ 178.13, 174.33, 173.87, 171.55, 169.57, 169.35, 154.97 (d, J = 250.3 Hz, C-6), 149.27, 146.74 (d, J = 10.2 Hz, C-7), 140.65, 139.73, 136.60, 129.10 (2C), 128.36 (2C), 120.77 (d, J = 7.8 Hz, C-4a), 112.40 (d, J = 23.5 Hz, C-5), 108.00, 107.60 (d, J = 2.2 Hz, C-8), 55.69, 54.43, 51.10, 50.48, 43.16, 40.58, 40.50 (2C), 40.48, 36.99, 33.05, 32.60, 32.06, 30.78, 30.75 (2C), 30.71, 30.46, 30.43, 30.34, 28.11, 27.99, 27.94, 24.03, 23.80, 23.72, 14.44, 8.55 (2C). ESI-HRMS calcd for C₄₉H₇₁FN₈O₇ [M+H]⁺: 903.5430; found 903.5499.

7-(4-(4-(((S)-6-amino-1-(((S)-6-amino-1-((octylamino)-1-oxohexan-2-yl)amino)-1-oxohexan-2-yl)amino)-1-oxohexan-2-yl)carbamoyl)benzoyl)piperazin-1-yl)-1-cyclopropyl-6-fluoro-4-oxo-1,4-dihydroquinoline-3-carboxylic acid (16p). Light yellow solid, m.p. 133–135 °C, yield 48 %; ^1H NMR (500 MHz, CD₃OD) δ 8.77 (s, 1H), 8.00 (d, J = 8.2 Hz, 2H), 7.89 (d, J = 13.0 Hz, 1H), 7.60 (d, J = 8.1 Hz, 3H), 4.50 (dd, J = 8.8, 5.9 Hz, 1H), 4.36 (dd, J = 9.0, 5.3 Hz, 1H), 4.29 (dd, J = 9.1, 5.3 Hz, 1H), 4.03 (m, 2H), 3.76 (m, 1H), 3.68 (m, 2H), 3.51 (m, 2H), 3.38 (m, 2H), 3.26–3.10 (m, 2H), 2.94 (m, 6H), 1.92 (m, 3H), 1.71 (m, 10H), 1.56–1.47 (m, 5H), 1.45–1.38 (m, 3H), 1.38–1.25 (m, 11H), 1.23 (m, 2H), 0.92–0.86 (m, 3H). ^{13}C NMR (126 MHz, CD₃OD) δ 178.17, 174.80, 174.05, 173.80, 171.58, 169.68, 169.38, 154.99 (d, J = 250.3 Hz, C-6), 149.29, 146.75 (d, J = 10.3 Hz, C-7), 140.67, 139.78, 136.57, 129.15 (2C), 128.34 (2C), 120.79 (d, J = 7.8 Hz, C-4a), 112.42 (d, J = 23.5 Hz, C-5), 108.02, 107.60 (d, J = 2.7 Hz, C-8), 56.04, 54.77, 54.60, 51.10, 50.49, 43.17, 40.55, 40.50, 40.47, 40.46 (2C), 36.98, 32.96, 32.64, 32.04, 31.99, 30.36, 30.36, 30.31, 28.12, 28.00, 27.97, 27.92, 24.12, 23.85, 23.76, 23.68, 14.41, 8.54 (2C). ESI-HRMS calcd for C₅₁H₇₅FN₁₀O₈ [M+H]⁺: 975.5753; found 975.5850.

7-(4-(4-(((S)-6-amino-1-(((S)-6-amino-1-((nonylamino)-1-oxohexan-2-yl)amino)-1-oxohexan-2-yl)amino)-1-oxohexan-2-yl)carbamoyl)benzoyl)piperazin-1-yl)-1-cyclopropyl-6-fluoro-4-oxo-1,4-dihydroquinoline-3-carboxylic acid (16q). Light yellow solid, m.p. 134–136 °C, yield 43 %; ^1H NMR (500 MHz, CD₃OD) δ 8.89–8.62 (m, 1H), 7.95 (brs, 3H), 7.78 (s, 1H), 7.61 (brs, 2H), 4.49 (m, 1H), 4.32 (m, 2H), 4.19–3.90 (m, 2H), 3.76 (m, 2H), 3.57–3.37 (m, 3H), 3.17 (m, 3H), 3.07–2.83 (m, 7H), 1.92 (m, 2H), 1.73 (m, 10H), 1.51 (m, 8H), 1.29 (m, 16H), 0.89 (t, J = 6.8 Hz, 3H). ^{13}C NMR (126 MHz, CD₃OD) δ 178.15, 174.85, 174.07, 173.81, 171.55, 169.67, 169.37, 154.98 (d, J = 249.8 Hz, C-6), 149.30, 146.74 (d, J = 8.4 Hz, C-7), 140.65, 139.75, 136.55, 129.17 (2C), 128.34 (2C), 120.77 (d, J = 8.0 Hz, C-4a), 112.39 (d, J = 25.3 Hz, C-5), 108.00, 107.63 (C-8), 56.09, 54.79, 54.59, 51.10, 50.54, 43.17, 40.53, 40.48 (2C), 40.44 (2C), 37.08, 33.02, 32.62, 31.97, 30.66, 30.42 (2C), 30.40, 30.31, 28.11, 27.97 (2C), 27.91, 24.12, 23.85, 23.77, 23.71, 14.44, 8.56 (2C). ESI-HRMS calcd for C₅₂H₇₇FN₁₀O₈ [M+H]⁺: 989.5910; found 989.5965.

7-(4-(4-(((S)-6-amino-1-(((S)-6-amino-1-(decylamino)-1-oxohexan-2-yl)amino)-1-oxohexan-2-yl)amino)-1-oxohexan-2-yl)carbamoyl)benzoyl)piperazin-1-yl)-1-cyclopropyl-6-fluoro-4-oxo-1,4-dihydroquinoline-3-carboxylic acid (16r). Light yellow solid, m.p. 135–137 °C, yield 47 %; ^1H NMR (500 MHz, CD₃OD) δ 8.79 (s, 1H), 7.96 (m, 4H), 7.61 (m, 2H), 4.49 (m, 1H), 4.35 (m, 1H), 4.29 (m, 1H), 4.04 (m, 2H), 3.64 (m, 3H), 3.44 (m, 2H), 3.28–3.11 (m, 3H), 2.94 (m, 7H), 1.90 (m, 4H), 1.69 (m, 10H), 1.51 (m, 6H), 1.28 (m, 18H), 0.88 (t, 3H). ^{13}C NMR (126 MHz, DMSO-d₆) δ 176.78, 172.37, 171.76, 171.64, 169.03, 166.64, 166.43, 153.41 (d, J = 249.3 Hz, C-6), 148.44, 145.30 (d, J = 10.8 Hz, C-7), 139.55, 138.78, 135.41, 128.22 (2C), 127.39 (2C), 119.34 (d, J = 7.8 Hz, C-4a), 111.44 (d, J = 23.0 Hz, C-5), 107.22, 107.15 (C-8), 54.18, 52.93, 52.90, 49.62, 47.12, 41.73, 40.75, 39.36, 39.16, 39.13, 38.97, 36.33, 31.98, 31.73, 31.57, 31.23, 29.45, 29.40, 29.37, 29.16, 29.14, 27.11, 27.06, 26.99, 26.75, 23.21, 22.73, 22.61, 22.53, 14.36, 8.03 (2C). ESI-HRMS calcd for C₅₃H₇₉FN₁₀O₈ [M+H]⁺: 1003.6066; found 1003.6124.

7-(4-(4-(((S)-6-amino-1-(((S)-6-amino-1-(dodecylamino)-1-oxohexan-2-yl)amino)-1-oxohexan-2-yl)amino)-1-oxohexan-2-yl)carbamoyl)benzoyl)piperazin-1-yl)-1-cyclopropyl-6-fluoro-4-oxo-1,4-dihydroquinoline-3-carboxylic acid (16s). Light yellow solid, m.p. 141–143 °C, yield 55 %; ^1H NMR (500 MHz, CD₃OD) δ 8.75 (s, 1H), 8.01 (d, J = 7.8 Hz, 2H), 7.90–7.82 (m, 1H), 7.60 (d, J = 7.8 Hz, 3H), 4.50 (dd, J = 8.7, 6.0 Hz, 1H), 4.35 (dd, J = 9.1, 5.2 Hz, 1H), 4.29 (dd, J = 9.2, 5.2 Hz, 1H), 4.03 (m, 2H), 3.72 (m, 3H), 3.51 (m, 2H), 3.39 (m, 2H), 3.24–3.10 (m, 2H), 3.01–2.89 (m, 6H), 2.00–1.86 (m, 3H), 1.79–1.61 (m, 9H), 1.52 (m, 6H), 1.4–1.38 (m, 3H), 1.34–1.25 (m, 19H), 1.22 (m, 2H), 0.91–0.88 (t, 3H). ^{13}C NMR (126 MHz, CD₃OD) δ 177.95, 174.65, 173.89, 173.62, 171.38, 169.46, 169.15, 154.78 (d, J = 249.5 Hz, C-6), 149.07, 146.55 (d, J = 10.3 Hz, C-7), 140.47, 139.59, 136.37, 129.00 (2C), 128.17 (2C), 117.85 (d, J = 292.4 Hz, C-4a), 112.21 (d, J = 23.5 Hz, C-5), 107.83, 107.42 (C-8), 55.89, 54.63, 54.42, 50.95, 50.30, 43.00, 40.37, 40.33, 40.28 (3C), 36.82, 32.87, 32.44, 31.80, 30.60, 30.56 (2C), 30.53, 30.27 (2C), 30.25, 30.15, 27.92, 27.81 (2C), 27.73, 23.92, 23.66, 23.58, 23.53, 14.26, 8.38 (2C). ESI-HRMS calcd for C₅₅H₈₃FN₁₀O₈ [M+H]⁺: 1031.6379; found 1031.6473.

7-(4-(4-(((S)-6-amino-1-(((S)-6-amino-1-(hexadecylamino)-1-oxohexan-2-yl)amino)-1-oxohexan-2-yl)amino)-1-oxohexan-2-yl)carbamoyl)benzoyl)piperazin-1-yl)-1-cyclopropyl-6-fluoro-4-oxo-1,4-dihydroquinoline-3-carboxylic acid (16t). Light yellow solid, m.p. 146–148 °C, yield 38 %; ^1H NMR (500 MHz, CD₃OD) δ 8.77 (s, 1H), 8.01 (s, 2H), 7.88 (d, J = 12.6 Hz, 1H), 7.61 (brs, 3H), 4.50 (t, 1H), 4.37 (t, 1H), 4.30 (dd, J = 9.0, 5.1 Hz, 1H), 4.04 (m, 2H), 3.85–3.62 (m, 3H), 3.49 (m, 2H), 3.35 (m, 2H), 3.18 (m, 2H), 2.97 (m, 6H), 1.91 (m, 3H), 1.73 (m, 9H), 1.56–1.48 (m, 5H), 1.41 (m, 3H), 1.33–1.24 (m, 30H), 0.90 (t, 3H). ^{13}C NMR (126 MHz, CD₃OD) δ 178.18, 174.81, 174.05, 173.79, 171.56, 169.66, 169.36, 154.99 (d, J = 251.2 Hz, C-6), 149.29, 146.75 (d, J = 10.2 Hz, C-7), 140.68, 139.77, 136.56, 129.16 (2C), 128.35 (2C), 120.82 (d, J = 7.7 Hz, C-4a), 112.55 (d, J = 3.8 Hz, C-5),

108.04, 107.70 (C-8), 56.04, 54.78, 54.59, 49.46, 49.28, 43.23, 41.41, 40.51, 40.46 (3C), 37.07, 33.04, 32.63, 32.02, 31.98, 30.77 (3C), 30.75, 30.74, 30.73 (2C), 30.72 (2C), 30.44, 30.33, 28.11, 27.99, 27.92 (2C), 24.11, 23.84, 23.75, 23.70, 14.44, 8.56 (2C). ESI-HRMS calcd for C₅₉H₉₁FN₁₀O₈ [M+H]⁺: 1087.7005; found 1087.7079.

7-(4-(4-((S)-1-(((S)-1-((1,1'-biphenyl)-4-ylmethyl)amino)-6-amino-1-oxohexan-2-yl)amino)-6-amino-1-oxohexan-2-yl)amino)-6-amino-1-oxohexan-2-yl)carbamoylbenzoylpiperazin-1-yl)-1-cyclopropyl-6-fluoro-4-oxo-1,4-dihydroquinoline-3-carboxylic acid (16u). Light yellow solid, m.p. 188–190 °C, yield 43 %; ¹H NMR (500 MHz, CD₃OD) δ 8.77 (s, 1H), 8.00 (d, J = 8.2 Hz, 2H), 7.89 (dd, J = 13.0, 4.3 Hz, 1H), 7.58 (m, 7H), 7.41 (t, J = 7.7 Hz, 2H), 7.37 (d, J = 8.2 Hz, 2H), 7.32 (t, J = 7.4 Hz, 1H), 4.49 (dd, J = 8.8, 5.9 Hz, 1H), 4.44 (s, 2H), 4.38 (m, 2H), 4.02 (m, 2H), 3.74 (m, 1H), 3.66 (m, 2H), 3.50 (m, 2H), 3.36 (m, 2H), 2.99–2.93 (m, 2H), 2.89 (m, 4H), 1.96–1.84 (m, 4H), 1.77 (m, 4H), 1.70–1.64 (m, 4H), 1.51 (m, 6H), 1.40 (m, 2H), 1.21 (m, 2H). ¹³C NMR (126 MHz, DMSO-*d*₆) δ 176.78, 172.36, 171.99, 171.93, 169.00, 166.58, 166.38, 153.41 (d, J = 249.2 Hz, C-6), 148.41, 145.29 (d, J = 10.2 Hz, C-7), 140.38, 139.54, 139.22, 138.99, 138.80, 135.46, 129.38 (2C), 128.22 (2C), 127.79 (2C), 127.40 (2C), 127.01 (5C), 119.35 (d, J = 4.4 Hz, C-4a), 111.47 (d, J = 26.7 Hz, C-5), 107.25, 107.15 (C-8), 54.14, 53.00, 52.86, 49.63, 47.15, 42.27, 40.97, 39.41, 39.18 (2C), 39.14, 36.32, 31.90, 31.66, 31.29, 27.14, 27.08, 27.04, 23.25, 22.79, 22.64, 8.04 (2C). ESI-HRMS calcd for C₅₆H₆₉FN₁₀O₈ [M+H]⁺: 1029.5284; found 1029.5335.

The compounds 22a–g were synthesized following the similar procedure of 16s except using different linker as shown in Scheme 4.

1-cyclopropyl-6-fluoro-4-oxo-7-(4-((6S,9S,12S)-6,9,12-tris(4-amino-butyl)-4,7,10,13-tetraoxo-5,8,11,14-tetraazahexacosanoyl)piperazin-1-yl)-1,4-dihydroquinoline-3-carboxylic acid (22a). Light yellow solid, m.p. 134–136 °C, yield 47 %; ¹H NMR (500 MHz, DMSO-*d*₆) δ 8.64 (s, 1H), 8.29 (d, J = 7.1 Hz, 1H), 7.97 (m, 7H), 7.87 (d, J = 13.1 Hz, 1H), 7.78–7.72 (m, 2H), 7.56 (d, J = 5.8 Hz, 1H), 4.17–4.10 (m, 3H), 3.82 (m, 2H), 3.74–3.67 (m, 3H), 3.64 (m, 1H), 3.38 (m, 4H), 3.00 (m, 2H), 2.80–2.74 (m, 6H), 2.69–2.62 (m, 2H), 2.44 (m, 1H), 1.77–1.68 (m, 3H), 1.58–1.50 (m, 9H), 1.39–1.31 (m, 10H), 1.20 (m, 18H), 1.12 (m, 2H), 0.83 (t, J = 6.8 Hz, 3H). ¹³C NMR (126 MHz, DMSO-*d*₆) δ 176.38, 172.55, 172.24, 171.39, 171.17, 170.45, 165.97, 152.99 (d, J = 249.6 Hz, C-6), 148.02, 144.96 (d, J = 10.3 Hz, C-7), 139.17, 118.84 (d, J = 7.8 Hz, C-4a), 111.04 (d, J = 23.9 Hz, C-5), 106.83, 106.57 (C-8), 53.07, 52.74, 52.56, 49.54, 49.20, 44.50, 40.91, 38.70, 38.67 (2C), 38.56, 35.91, 31.43, 31.35, 30.87, 30.69, 30.31, 29.12, 29.08, 28.97, 28.79, 28.77, 27.97, 26.70, 26.65, 26.59, 26.36, 22.49, 22.45, 22.29, 22.14, 13.96, 7.64 (2C). ESI-HRMS calcd for C₅₁H₈₃FN₁₀O₈ [M+H]⁺: 983.6379; found 983.6461.

1-cyclopropyl-6-fluoro-4-oxo-7-(4-((10S,13S,16S)-10,13,16-tris(4-aminobutyl)-4,8,11,14,17-pentaoxo-5,9,12,15,18-pentaazatriacontanoyl)piperazin-1-yl)-1,4-dihydroquinoline-3-carboxylic acid (22b). Light yellow solid, m.p. 92–94 °C, yield 55 %; ¹H NMR (500 MHz, CD₃OD) δ 8.83–8.64 (m, 1H), 8.00–7.80 (m, 1H), 7.64–7.42 (m, 1H), 4.24 (dd, J = 9.0, 4.7 Hz, 2H), 4.20–4.16 (m, 1H), 3.77 (m, 4H), 3.49–3.35 (m, 5H), 3.16 (m, 3H), 2.93 (m, 7H), 2.68 (m, 2H), 2.54 (dd, J = 30.5, 11.6 Hz, 3H), 2.43 (m, 1H), 1.88 (d, J = 15.3 Hz, 4H), 1.70 (m, 8H), 1.56 (m, 2H), 1.51–1.46 (m, 4H), 1.44–1.41 (m, 2H), 1.32–1.26 (m, 20H), 1.23 (d, J = 1.1 Hz, 2H), 0.89 (t, 3H). ¹³C NMR (126 MHz, CD₃OD) δ 178.09, 176.20, 175.35, 174.50, 174.39, 173.81, 171.85, 169.33, 154.89 (d, J = 250.2 Hz, C-6), 149.19, 146.75 (d, J = 10.2 Hz, C-7), 140.65, 120.55 (d, J = 7.8 Hz, C-4a), 112.35 (d, J = 23.9 Hz, C-5), 107.97, 107.33 (d, J = 2.6 Hz, C-8), 55.81, 55.41, 54.73, 50.84, 50.50, 46.33, 42.52, 40.49 (2C), 40.46, 40.42, 36.96, 36.73, 33.53, 33.03, 32.34, 32.02, 31.87, 31.71, 31.42, 30.77, 30.73, 30.72, 30.69, 30.44, 30.41, 30.25, 28.05, 28.01, 27.94, 27.92, 24.11, 24.07, 23.92, 23.70, 14.43, 8.56 (2C). ESI-HRMS calcd for C₅₄H₈₈FN₁₁O₉ [M+H]⁺: 1054.6751; found 1054.6823.

1-cyclopropyl-6-fluoro-4-oxo-7-(4-((14S,17S,20S)-14,17,20-tris(4-aminobutyl)-4,8,12,15,18,21-hexaoxo-5,9,13,16,19,22-hexaaazatetra-triacontanoyl)piperazin-1-yl)-1,4-dihydroquinoline-3-carboxylic acid

(22c). Light yellow solid, m.p. 150–152 °C, yield 38 %; ¹H NMR (500 MHz, CD₃OD) δ 8.52 (s, 1H), 7.85 (s, 1H), 7.53 (d, J = 13.1 Hz, 1H), 7.39 (d, J = 6.3 Hz, 1H), 4.15 (m, 2H), 4.08 (dd, J = 9.2, 4.8 Hz, 1H), 3.75–3.67 (m, 4H), 3.63 (m, 1H), 3.41–3.26 (m, 8H), 3.06 (m, 2H), 2.86 (d, J = 7.6 Hz, 6H), 2.61 (t, 2H), 2.54–2.42 (m, 3H), 2.35–2.25 (m, 3H), 1.84–1.75 (m, 4H), 1.62 (m, 8H), 1.43–1.36 (m, 5H), 1.34–1.29 (m, 3H), 1.17 (d, J = 12.9 Hz, 20H), 1.12 (m, 2H), 0.78 (t, 3H). ¹³C NMR (126 MHz, CD₃OD) δ 177.84, 176.14, 175.29, 174.48, 174.42, 173.78, 173.56, 171.91, 169.17, 154.73 (d, J = 250.4 Hz, C-6), 149.02, 146.66 (d, J = 10.1 Hz, C-7), 140.52, 120.26 (d, J = 7.8 Hz, C-4a), 112.19 (d, J = 23.0 Hz, C-5), 107.85, 107.18 (C-8), 55.79, 55.47, 54.64, 50.76, 50.42, 46.31, 42.48, 40.47, 40.43, 37.09, 36.94, 36.61, 36.57, 33.61, 32.98, 32.29, 32.05, 31.87, 31.66, 31.37, 30.72, 30.68 (2C), 30.65, 30.39, 30.36, 30.20, 28.05, 28.00, 27.97, 27.88 (2C), 24.10, 24.01, 23.83, 23.65, 14.43, 8.53 (2C). ESI-HRMS calcd for C₅₇H₉₂FN₁₂O₁₀ [M+H]⁺: 1125.7122; found 1125.7215.

1-cyclopropyl-6-fluoro-4-oxo-7-(4-((14S,17S,20S)-14,17,20-tris(4-aminobutyl)-4,12,15,18,21-pentaoxo-5,13,16,19,22-pentaazatetra-triacontanoyl)piperazin-1-yl)-1,4-dihydroquinoline-3-carboxylic acid (22d).

Light yellow solid, m.p. 118–120 °C, yield 32 %; ¹H NMR (500 MHz, DMSO-*d*₆) δ 8.66 (s, 1H), 8.32 (d, J = 6.6 Hz, 1H), 8.09 (d, J = 7.6 Hz, 1H), 8.04–8.01 (m, 1H), 7.91 (m, 7H), 7.67–7.62 (m, 2H), 7.58 (brs, 1H), 4.14–4.07 (m, 3H), 3.69 (m, 4H), 3.44 (m, 4H), 3.33 (d, J = 25.5 Hz, 2H), 3.01 (m, 4H), 2.77 (m, 5H), 2.39–2.35 (m, 4H), 1.75–1.64 (m, 4H), 1.60–1.47 (m, 12H), 1.36 (d, J = 13.7 Hz, 9H), 1.30–1.27 (m, 5H), 1.23 (m, 18H), 1.19 (m, 2H), 0.85 (t, J = 6.8 Hz, 3H). ¹³C NMR (126 MHz, DMSO-*d*₆) δ 176.81, 173.35, 172.87, 172.04, 171.92, 171.52, 171.32, 166.38, 153.41 (d, J = 249.4 Hz, C-6), 148.47, 145.40 (d, J = 10.1 Hz, C-7), 139.59, 119.24 (d, J = 7.6 Hz, C-4a), 111.44 (d, J = 23.1 Hz, C-5), 107.22, 107.04 (C-8), 53.82, 53.45, 52.97, 50.13, 49.71, 45.05, 41.09, 39.13, 39.09 (3C), 38.98, 36.35, 32.64, 31.77, 31.19, 31.16, 30.97, 30.89, 29.54, 29.49 (3C), 29.46, 29.35, 29.21, 29.19 (2C), 29.02, 27.12, 27.07, 27.01, 26.81, 26.74, 25.16, 23.01, 22.97, 22.79, 22.56, 14.40, 8.05 (2C). ESI-HRMS calcd for C₅₈H₉₆FN₁₁O₉ [M+H]⁺: 1110.7377; found 1110.7430.

1-cyclopropyl-6-fluoro-4-oxo-7-(4-((19S,22S,25S)-19,22,25-tris(4-aminobutyl)-4,17,20,23,26-pentaoxo-5,18,21,24,27-pentaazanona-triacontanoyl)piperazin-1-yl)-1,4-dihydroquinoline-3-carboxylic acid (22e).

Light yellow solid, m.p. 119–121 °C, yield 41 %; ¹H NMR (500 MHz, CD₃OD) δ 8.76 (s, 1H), 7.86 (d, J = 13.1 Hz, 1H), 7.59 (d, J = 7.3 Hz, 1H), 4.35–4.21 (m, 3H), 3.83 (s, 4H), 3.79–3.74 (m, 1H), 3.50–3.43 (m, 2H), 3.41–3.36 (m, 2H), 3.23–3.13 (m, 4H), 2.98–2.92 (m, 6H), 2.76 (t, 2H), 2.54 (t, 2H), 2.30–2.21 (m, 2H), 1.84 (m, 3H), 1.72 (m, 9H), 1.62–1.56 (m, 2H), 1.54–1.47 (m, 8H), 1.45–1.41 (m, 3H), 1.30 (d, J = 10.4 Hz, 33H), 1.23 (m, 2H), 0.90 (t, 3H). ¹³C NMR (126 MHz, CD₃OD) δ 176.68, 175.31, 173.46, 173.23, 172.66, 172.41, 171.47, 167.95, 153.52 (d, J = 250.2 Hz, C-6), 147.82, 145.46 (d, J = 10.6 Hz, C-7), 139.29, 119.14 (d, J = 7.6 Hz, C-4a), 110.99 (d, J = 23.7 Hz, C-5), 106.62, 105.92 (C-8), 53.72, 53.34, 53.17, 49.53, 49.22, 45.00, 41.32, 39.15, 39.13, 39.10, 39.08, 35.63, 35.34, 31.67, 31.24, 30.69 (2C), 30.53, 29.40, 29.37 (2C), 29.34, 29.31 (2C), 29.26, 29.08 (3C), 29.06 (2C), 29.00, 28.95, 27.90, 26.70, 26.65, 26.61, 26.53, 25.51 (3C), 22.50, 22.44, 22.34 (2C), 13.10, 7.22 (2C). ESI-HRMS calcd for C₆₃H₁₀₆FN₁₁O₉ [M+H]⁺: 1180.8159; found 1180.8235.

1-cyclopropyl-6-fluoro-4-oxo-7-(4-((16S,19S,22S)-16,19,22-tris(4-aminobutyl)-4,14,17,20,23-pentaoxo-8,11-dioxa-5,15,18,21,24-pentaaza-hexatriacontanoyl)piperazin-1-yl)-1,4-dihydroquinoline-3-carboxylic acid (22f).

Light yellow solid, m.p. 131–133 °C, yield 32 %; ¹H NMR (500 MHz, CD₃OD) δ 8.68 (s, 1H), 7.73 (d, J = 13.0 Hz, 1H), 7.53 (d, J = 7.0 Hz, 1H), 4.39 (d, J = 4.9 Hz, 2H), 4.25 (m, 2H), 4.17 (m, 1H), 3.84 (m, 2H), 3.78–3.71 (m, 5H), 3.70–3.66 (m, 2H), 3.56 (m, 2H), 3.46–3.39 (m, 4H), 3.37 (d, J = 5.6 Hz, 1H), 3.15 (m, 2H), 3.01–2.91 (m, 7H), 2.70–2.61 (m, 1H), 2.59–2.53 (m, 2H), 2.44 (m, 1H), 1.94–1.85 (m, 4H), 1.78–1.68 (m, 8H), 1.62–1.53 (m, 3H), 1.52–1.46 (m, 4H), 1.44–1.41 (m, 3H), 1.26 (m, 18H), 1.23 (d, J = 6.4 Hz, 2H), 0.88 (t, 3H). ¹³C NMR (126 MHz, CD₃OD) δ 176.69, 175.05, 174.12, 173.34, 173.14, 172.45,

168.98, 167.94, 153.52 (d, $J = 250.3$ Hz, C-6), 147.82, 145.38 (d, $J = 10.4$ Hz, C-7), 139.28, 119.18 (d, $J = 7.6$ Hz, C-4a), 110.99 (d, $J = 22.8$ Hz, C-5), 106.61, 106.00 (C-8), 70.35, 69.66, 69.11, 68.75, 54.63, 54.20, 53.38, 49.43, 49.13, 44.02, 41.28, 39.14 (2C), 39.08, 39.06 (2C), 35.63, 31.67, 30.94, 30.61, 30.36, 30.27, 29.94, 29.40, 29.36, 29.32, 29.07, 29.04, 28.86, 26.67, 26.63, 26.59 (2C), 26.54, 22.81, 22.72, 22.64, 22.51, 22.33, 13.08, 7.21 (2C). ESI-HRMS calcd for $C_{57}H_{94}FN_{11}O_{11}$ [M+H]⁺: 1128.7118; found 1128.7206.

1-cyclopropyl-6-fluoro-4-oxo-7-(4-((6S,9S,12S)-9,12,15-tris(4-aminobutyl)-6-(hydroxymethyl)-4,7,10,13,16-pentaaoxo-5,8,11,14,17-pentaazanonacosanoyl)piperazin-1-yl)-1,4-dihydroquinoline-3-carboxylic acid (22g). Light yellow solid, m.p. 138–140 °C, yield 41 %; ¹H NMR (500 MHz, CD₃OD) δ 8.72 (s, 1H), 7.79 (d, $J = 13.1$ Hz, 1H), 7.55 (d, $J = 6.1$ Hz, 1H), 4.28 (m, 4H), 3.96 (dd, $J = 11.0, 5.0$ Hz, 1H), 3.91–3.71 (m, 6H), 3.49–3.38 (m, 3H), 3.23–3.12 (m, 2H), 2.95 (d, $J = 6.6$ Hz, 7H), 2.88–2.80 (m, 2H), 2.68 (dd, $J = 15.1, 6.7$ Hz, 1H), 2.54 (m, 1H), 1.96 (m, 1H), 1.91–1.81 (m, 3H), 1.73 (m, 9H), 1.54–1.46 (m, 6H), 1.45–1.40 (m, 3H), 1.28 (d, $J = 10.5$ Hz, 18H), 1.23 (m, 2H), 0.89 (t, 3H). ¹³C NMR (126 MHz, CD₃OD) δ 176.64, 174.81, 173.37, 172.58, 172.40, 172.34, 171.54, 167.96, 153.47 (d, $J = 250.0$ Hz, C-6), 147.80, 145.36 (d, $J = 10.0$ Hz, C-7), 139.26, 119.07 (d, $J = 7.9$ Hz, C-4a), 110.93 (d, $J = 22.7$ Hz, C-5), 106.58, 105.90 (C-8), 61.17, 56.44, 53.96, 53.71, 53.16, 49.37, 49.17, 44.89, 41.41, 39.25, 39.14 (2C), 39.08, 35.61, 31.66, 31.12, 30.38, 30.24, 30.19, 29.79, 29.39, 29.36, 29.32, 29.07, 29.04, 28.91, 28.00, 26.58 (2C), 26.52 (2C), 22.68, 22.49, 22.43, 22.33, 13.07, 7.21 (2C). ESI-HRMS calcd for $C_{54}H_{88}FN_{11}O_{10}$ [M+H]⁺: 1070.6700; found 1070.6757.

The compounds **28a–e** were synthesized following the similar procedure of **16q** except using different amino acids as shown in Scheme 4.

7-(4-(4-((S)-6-amino-1-(((S)-6-amino-1-((S)-5-guanidino-1-(nonylamino)-1-oxopentan-2-yl)amino)-1-oxohexan-2-yl)amino)-1-oxohexan-2-yl)carbamoyl)benzoylpiperazin-1-yl)-1-cyclopropyl-6-fluoro-4-oxo-1,4-dihydroquinoline-3-carboxylic acid (28a). Light yellow solid, m.p. 213–215 °C, yield 32 %; ¹H NMR (500 MHz, CD₃OD) δ 8.66 (s, 1H), 7.91 (dd, $J = 7.8, 4.1$ Hz, 2H), 7.79 (m, 1H), 7.49 (d, $J = 7.7$ Hz, 3H), 4.46–4.36 (m, 1H), 4.23 (m, 2H), 3.92 (m, 2H), 3.65 (m, 1H), 3.58 (m, 2H), 3.40 (m, 2H), 3.26 (d, $J = 12.2$ Hz, 2H), 3.17–3.07 (m, 3H), 3.06–3.03 (m, 1H), 2.87 (m, 4H), 1.91–1.74 (m, 4H), 1.63 (m, 7H), 1.55–1.49 (m, 2H), 1.42 (m, 5H), 1.31 (m, 2H), 1.19 (m, 12H), 1.09 (d, $J = 14.5$ Hz, 2H), 0.78 (q, $J = 7.0$ Hz, 3H). ¹³C NMR (126 MHz, CD₃OD) δ 178.17, 174.74, 174.08, 173.55, 171.57, 169.67, 169.37, 158.67, 154.99 (d, $J = 250.1$ Hz, C-6), 149.30, 146.78 (C-7), 140.67, 139.77, 136.56, 129.12 (2C), 128.34 (2C), 118.20 (d, $J = 292.7$ Hz, C-4a), 112.54 (C-5), 108.08, 107.58 (C-8), 55.95, 54.80, 54.32, 51.07, 50.49, 43.16, 42.25, 41.92, 40.52, 40.48, 40.46, 36.98, 33.00, 32.05, 32.00, 30.62, 30.47, 30.40, 30.37, 30.31, 28.12, 27.97, 27.91, 26.33, 24.10, 23.73, 23.68, 14.41, 8.54 (2C). ESI-HRMS calcd for $C_{52}H_{77}FN_{12}O_8$ [M+H]⁺: 1017.5971; found 1017.6033.

7-(4-(4-((S)-6-amino-1-(((S)-1-((S)-6-amino-1-(nonylamino)-1-oxohexan-2-yl)amino)-5-guanidino-1-oxopentan-2-yl)amino)-1-oxohexan-2-yl)carbamoyl)benzoylpiperazin-1-yl)-1-cyclopropyl-6-fluoro-4-oxo-1,4-dihydroquinoline-3-carboxylic acid (28b, IPMCL-28b). Light yellow solid, m.p. 150–152 °C, yield 37 %; ¹H NMR (500 MHz, CD₃OD) δ 8.69 (s, 1H), 8.01 (d, $J = 7.4$ Hz, 2H), 7.76 (d, $J = 13.0$ Hz, 1H), 7.60 (m, 3H), 4.51 (dd, $J = 7.7$ Hz, 1H), 4.38 (dd, $J = 8.3, 5.2$ Hz, 1H), 4.30 (dd, $J = 9.1, 5.2$ Hz, 1H), 4.02 (m, 2H), 3.68 (m, 3H), 3.51 (m, 2H), 3.37 (d, $J = 16.7$ Hz, 2H), 3.24–3.15 (m, 4H), 2.98 (m, 2H), 2.90 (t, 2H), 2.00–1.90 (m, 3H), 1.73 (m, 12H), 1.54–1.48 (m, 3H), 1.41 (m, 2H), 1.29 (m, 12H), 1.22 (m, 2H), 0.89 (t, 3H). ¹³C NMR (126 MHz, CD₃OD) δ 178.14, 174.83, 173.79 (2C), 171.58, 169.70, 169.34, 158.66, 154.95 (d, $J = 249.7$ Hz, C-6), 149.24, 146.72 (d, $J = 11.0$ Hz, C-7), 140.64, 139.76, 136.54, 129.15, 128.32, 120.74 (d, $J = 9.0$ Hz, C-4a), 112.40 (d, $J = 21.2$ Hz, C-5), 108.01, 107.58 (d, $J = 2.9$ Hz, C-8), 56.08, 54.64, 54.56, 49.46, 49.28, 41.94, 40.50 (2C), 40.44 (3C), 36.98, 32.99, 32.59, 31.94, 30.62, 30.39, 30.36, 30.30, 29.79, 28.10, 27.98, 27.94, 26.28, 24.09, 23.84, 23.67, 14.41, 8.54 (2C). ESI-HRMS calcd for $C_{52}H_{77}FN_{12}O_8$ [M+H]⁺:

1017.5971; found 1017.6047.

7-(4-(4-((6S,9S,12S)-1-amino-9,12-bis(4-aminobutyl)-1-imino-7,10,13-trioxo-2,8,11,14-tetraazatricosan-6-yl)carbamoyl)benzoylpiperazin-1-yl)-1-cyclopropyl-6-fluoro-4-oxo-1,4-dihydroquinoline-3-carboxylic acid (28c). Light yellow solid, m.p. 151–153 °C, yield 30 %; ¹H NMR (500 MHz, CD₃OD) δ 8.70 (s, 1H), 8.01 (d, $J = 8.1$ Hz, 2H), 7.76 (d, $J = 13.0$ Hz, 1H), 7.60 (d, $J = 7.9$ Hz, 2H), 7.56 (d, $J = 6.2$ Hz, 1H), 4.51 (dd, $J = 13.6, 8.1$ Hz, 1H), 4.36 (dd, $J = 9.1, 5.3$ Hz, 1H), 4.30 (dd, $J = 9.2, 4.4$ Hz, 1H), 4.02 (m, 2H), 3.74 (m, 1H), 3.68 (m, 2H), 3.50 (m, 2H), 3.38 (m, 2H), 3.27 (t, 2H), 3.22–3.12 (m, 2H), 2.92 (m, 4H), 2.04–1.89 (m, 3H), 1.79 (m, 4H), 1.73–1.63 (m, 5H), 1.56–1.46 (m, 5H), 1.42 (m, 3H), 1.30 (m, 12H), 1.22 (m, 2H), 0.89 (t, 3H). ¹³C NMR (126 MHz, CD₃OD) δ 178.14, 174.83, 173.79 (2C), 171.58, 169.70, 169.34, 158.66, 154.95 (d, $J = 249.7$ Hz, C-6), 149.24, 146.72 (d, $J = 11.0$ Hz, C-7), 140.64, 139.76, 136.54, 129.15 (2C), 128.32 (2C), 120.74 (d, $J = 9.0$ Hz, C-4a), 112.40 (d, $J = 21.2$ Hz, C-5), 108.01, 107.58 (d, $J = 2.9$ Hz, C-8), 56.08, 54.64, 54.56, 49.46, 49.28, 41.94, 40.50 (3C), 40.44 (2C), 36.98, 32.99, 32.59, 31.94, 30.62, 30.39, 30.36, 30.30, 29.79, 28.10, 27.98, 27.94, 26.28, 24.09, 23.84, 23.67, 14.41, 8.54 (2C). ESI-HRMS calcd for $C_{52}H_{77}FN_{12}O_8$ [M+H]⁺: 1017.5971; found 1017.6041.

7-(4-(4-((6S,9S,12S)-1-amino-9,12-bis(3-guanidinopropyl)-1-imino-7,10,13-trioxo-2,8,11,14-tetraazatricosan-6-yl)carbamoyl)benzoylpiperazin-1-yl)-1-cyclopropyl-6-fluoro-4-oxo-1,4-dihydroquinoline-3-carboxylic acid (28d). Light yellow solid, m.p. 159–161 °C, yield 31 %; ¹H NMR (500 MHz, CD₃OD) δ 8.78 (s, 1H), 7.99 (d, $J = 7.7$ Hz, 2H), 7.90 (d, $J = 13.0$ Hz, 1H), 7.60 (d, $J = 7.6$ Hz, 3H), 4.57–4.51 (m, 1H), 4.39 (dd, $J = 8.5, 5.2$ Hz, 1H), 4.32 (dd, $J = 8.7, 5.4$ Hz, 1H), 4.03 (m, 2H), 3.76 (m, 1H), 3.68 (m, 2H), 3.51 (m, 2H), 3.38 (m, 2H), 3.26 (m, 2H), 3.23–3.14 (m, 6H), 2.05–1.96 (m, 1H), 1.96–1.87 (m, 2H), 1.86–1.75 (m, 4H), 1.67 (m, 4H), 1.55–1.47 (m, 2H), 1.41 (m, 2H), 1.33–1.26 (m, 13H), 1.22 (s, 2H), 0.92–0.87 (m, 3H). ¹³C NMR (126 MHz, CD₃OD) δ 178.22, 174.54, 173.82, 173.59, 171.58, 169.72, 169.42, 158.75, 158.70, 158.65, 155.02 (d, $J = 250.1$ Hz, C-6), 149.32, 146.77 (d, $J = 10.3$ Hz, C-7), 140.69, 139.79, 136.49, 129.13 (2C), 128.36 (2C), 120.91 (d, $J = 24.9$ Hz, C-4a), 112.46 (d, $J = 23.4$ Hz, C-5), 108.05, 107.61 (C-8), 55.62, 54.55, 54.37, 51.08 (d, $J = 2.3$ Hz), 50.51, 43.16, 41.99, 41.94, 41.93, 41.16, 40.54, 36.99, 33.02, 30.64, 30.46, 30.41, 30.40, 30.32, 29.90, 29.71, 27.97, 26.54, 26.34, 26.26, 23.70, 14.42, 8.55 (2C). ESI-HRMS calcd for $C_{52}H_{77}FN_{16}O_8$ [M+H]⁺: 1073.6094; found 1073.6094.

7-(4-(4-((2S)-1-((1-((S)-3-(1H-imidazole-4-yl)-1-(nonylamino)-1-oxopropan-2-yl)amino)-6-amino-1-oxohexan-2-yl)amino)-6-amino-1-oxohexan-2-yl)carbamoyl)benzoylpiperazin-1-yl)-1-cyclopropyl-6-fluoro-4-oxo-1,4-dihydroquinoline-3-carboxylic acid (28e). Light yellow solid, m.p. 148–150 °C, yield 38 %; ¹H NMR (500 MHz, CD₃OD) δ 8.81 (s, 1H), 8.66 (s, 1H), 8.02 (d, $J = 8.2$ Hz, 2H), 7.69 (d, $J = 13.0$ Hz, 1H), 7.61 (d, $J = 8.2$ Hz, 2H), 7.54 (d, $J = 7.0$ Hz, 1H), 7.36 (s, 1H), 4.69 (dd, $J = 8.7, 5.4$ Hz, 1H), 4.53 (dd, $J = 8.5, 6.0$ Hz, 1H), 4.33 (dd, $J = 9.2, 5.2$ Hz, 1H), 4.03 (m, 2H), 3.72 (m, 3H), 3.51 (m, 2H), 3.39 (m, 2H), 3.32–3.26 (m, 1H), 3.23–3.13 (m, 3H), 3.02 (t, 2H), 2.96 (t, 2H), 1.97 (m, 2H), 1.86 (m, 1H), 1.81–1.75 (m, 3H), 1.73–1.68 (m, 2H), 1.62 (m, 2H), 1.53–1.48 (m, 3H), 1.43 (m, 2H), 1.34–1.27 (m, 13H), 1.23 (m, 2H), 0.90 (t, 3H). ¹³C NMR (126 MHz, CD₃OD) δ 177.92, 174.81, 174.13, 171.65, 171.54, 169.61, 169.24, 154.84 (d, $J = 250.0$ Hz, C-6), 149.12, 146.66 (d, $J = 10.1$ Hz, C-7), 140.55, 139.68, 136.49, 134.85, 130.99, 129.11 (2C), 128.33 (2C), 120.50 (d, $J = 8.1$ Hz, C-4a), 118.44, 112.26 (d, $J = 23.6$ Hz, C-5), 107.89, 107.46 (C-8), 55.84, 54.97, 53.68, 50.98, 50.44, 43.15, 40.75, 40.62, 40.44, 40.41, 36.97, 32.96, 31.98, 31.79, 30.59, 30.36, 30.34, 30.22, 28.26, 28.05, 27.91, 27.84, 24.03, 23.80, 23.65, 14.41, 8.53 (2C). ESI-HRMS calcd for $C_{52}H_{72}FN_{11}O_8$ [M+H]⁺: 998.5549; found 998.5614.

Minimum Inhibitory Concentrations (MICs) against Bacteria. The bacterial strains used in the experiment were *S. aureus* (ATCC 25923), *E. gallinarum* ATCC 49573, MRSA ATCC 43300, *E. faecalis* ATCC 19433, *E. coli* ATCC 25922, *P. aeruginosa* ATCC 27853 and *A. baumannii* ATCC 19606. The antimicrobial activities of ciprofloxacin derivatives **4a–b**, **16a–u**, **22a–g** and **28a–e** were evaluated by the microbroth

dilution method according to the Clinical and Laboratory Standards Institute (CLSI) guidelines. Bacterial strains were placed in Mueller–Hinton broth (MHB) and incubated on a shaker (37°C , 200 rpm) for 3–5 h, followed by dilution to a final concentration of 1×10^5 CFU/mL. The concentration of the compound's stock solution was set at 256 $\mu\text{g}/\text{mL}$ and serial dilutions were performed using the 2-fold dilution method. Dilutions of compounds and bacterial suspensions were then added sequentially to a 96-well plate. The positive control group was ciprofloxacin, the negative control group was MHB culture solution (200 μL), and the blank group was bacterial solution (1×10^5 CFU/mL, 200 μL). At last, the 96-well plates were incubated for 16–18 h at 37°C to observe and record the results. The MICs of the compound were identified as the lowest concentration at which no bacterial growth could be observed visually. The experiments were repeated at least three times with duplicates each time.

Hemolytic Assays. Freshly drawn SD rats with additive sodium heparin anticoagulant were washed with PBS buffer several times and centrifuged at 800 g for 5 min until a clear supernatant was observed. The supernatant was removed and the red blood cells were diluted into 8 % (v/v) suspension with 1 \times PBS. Two-fold serial dilutions of compounds dissolved in 1 \times PBS from 200 $\mu\text{g}/\text{mL}$ through 6.25 $\mu\text{g}/\text{mL}$ were added to a sterile 96-well plate to make up a total volume of 100 μL in each well. The plate was then incubated at 37°C for 1 h and centrifuged at 3500 rpm for 15 min. Subsequently, the supernatant (80 μL) was aspirated into a fresh plate and the absorbance of the mixture at 490 nm was read on a Biotek Synergy HT plate reader. The positive control was 2 % Triton X-100, and the negative control was 1 \times PBS alone. The percent hemolysis was determined by the following equation: % hemolysis = $[(\text{Abs}_{\text{sample}} - \text{Abs}_{\text{PBS}})/(\text{Abs}_{\text{Triton}} - \text{Abs}_{\text{PBS}})] \times 100$. The experiment was repeated at least three times with duplicates each time.

MTT Assays. L929 cells were used to assess the cell viability with treatment of compounds **16u**, **22e**, **22g** and **IPMCL-28b** using standard procedure [78]. Cells were seeded in 96-well plate in 200 μL of media per well. Control and blank wells were prepared accordingly. Serial dilutions of compounds at concentrations of 200, 100, 50, 25, 12.5 and 6.25 $\mu\text{g}/\text{mL}$ were prepared by diluting stock solution with media. After incubation for 24 h, 20 μL of 3-(4,5-dimethylthiazol-2-yl)-2,5-diphenyltetrazolium bromide (MTT) reagent at a concentration of 5 mg/mL was added and then incubation for another 4 h at 37°C . The media in cells were then removed and washed with 150 μL of dimethyl sulfoxide (DMSO). Then the absorbance of the mixture at 570 nm was read on a multifunctional microplate reader. The data were calculated based on the following equation: cell viability % = $[(\text{Abs}_{\text{sample}} - \text{Abs}_{\text{blank}})/(\text{Abs}_{\text{control}} - \text{Abs}_{\text{blank}})] \times 100$. The measurements were repeated at least three times.

Time-Kill Kinetics Study. The kinetics of bacterial killing of the *S. aureus* 25923 strain by **IPMCL-28b** at the $8 \times \text{MIC}$ was determined. Briefly, the bacteria *S. aureus* 25923 grew to mid-logarithmic phase in Mueller-Hinton (MH) liquid medium, from which the suspension (1.0×10^6 CFU/mL) was made. The suspension was incubated with different concentrations of **IPMCL-28b** for 0 min, 30 min, 1 h, 2 h, 4 h, 6 h, 8 h, 12 h and 24 h. Aliquots of the bacterial suspension were taken and appropriately diluted in MH medium. The diluted samples were then spread evenly on MH agar plates using a spreader. The plates were incubated overnight at 37°C , and the number of colonies grown on each plate was recorded. The experiment was repeated three times, and the colony counts were statistically analyzed and used to plot a growth curve.

Drug Resistance Study. The first-generation MIC data of **IPMCL-28b** and ciprofloxacin against MRSA (ATCC 33591) were obtained as described in the MIC study mentioned above. Then, MRSA in the well next to the last clear well was diluted to 10^6 CFU/mL to determine the MICs again at 37°C incubation for 12 h. The step was repeated until 25 passages. Drug resistance of **IPMCL-28b** and ciprofloxacin against *E. coli* (ATCC 25922) was conducted with the same method.

Flow Cytometry Analysis. Evaluation of loss of membrane integrity of *S. aureus* 25923 after treatment with **IPMCL-28b** by using flow

cytometry to detect the fluorescence signal of PI [76]. The cultured *S. aureus* (10^6 – 10^7 CFU/mL) was suspended in PBS, and **IPMCL-28b** solution was diluted in PBS to $8 \times \text{MIC}$, $4 \times \text{MIC}$, and $2 \times \text{MIC}$. The positive control group was polymyxin B and ciprofloxacin ($8 \times \text{MIC}$), and the negative control group was PBS, followed by incubation for 1 h at 37°C . Afterward, the mixture was centrifuged for 5 min (35,000 rpm, 4°C) to remove the supernatant, washed twice using PBS, and finally resuspended in 1.0 mL of PBS. To the resuspended *S. aureus* solution, 3 μL PI dye was added, incubated for 10 min under light-proof conditions, and finally analyzed by flow cytometry.

Scanning Electron Microscopy. The bacteria *S. aureus* 25923 were incubated in MH medium in a shaker at 37°C for 6 h to achieve a bacterial suspension concentration of 1.0×10^8 CFU/mL, and then PBS (control), ciprofloxacin ($4 \times \text{MIC}$) and **IPMCL-28b** ($4 \times \text{MIC}$) were added and incubated at 37°C for 4 h on a shaking incubator. After that, the mixture was centrifuged for 10 min (35,000 rpm, 4°C) to remove the supernatant, then the pellet washed with PBS. The bacteria are then fixed overnight at 4°C using 2.5 % glutaraldehyde in PBS. Afterward, the samples were first eluted by dehydration through a graded ethanol series (30 %, 50 %, 70 %, 80 %, 90 %, 100 %). The sample is resuspended in absolute ethanol, carefully applied to silicon wafers, and air-dried for 12 h. Finally, the samples are gold-coated and observed under a scanning electron microscope.

Molecular Dynamics Simulations. The force field parameters for **IPMCL-28b** and ciprofloxacin were generated using SwissParam [79], which provides MMFF-based parameters. The Gram-positive bacterial membrane, consisting of a POPE/POPG (1:3) lipid bilayer, was constructed using the CHARMM-GUI web server [80]. After a 100 ns equilibration under NPT conditions, the final snapshot of the equilibrated membrane was used to assemble the simulation systems. System assembly was performed using PyMOL, with **IPMCL-28b** and ciprofloxacin individually placed at distances of 2 nm, 4 nm, and 6 nm above the membrane surface to evaluate the influence of starting positions on interaction dynamics. The systems were solvated with TIP3P water molecules, and NaCl was added to neutralize the system and ensure a final concentration of 150 mM, mimicking physiological conditions. The CHARMM36 force field [81] was used to describe the membrane and solvent, while SwissParam [79] provided the parameters for the two molecules. MD simulations were performed using GROMACS 2023.2 [82]. The systems underwent energy minimization using the steepest descent algorithm until the maximum force was less than $1000 \text{ kJ mol}^{-1} \text{ nm}^{-1}$. Simulations were conducted in the NPT ensemble at a temperature of 310.15 K and a pressure of 1 bar. The temperature was regulated separately for **IPMCL-28b**, ciprofloxacin, the membrane, and the solvent using the V-rescale thermostat, while the pressure was controlled with the Parrinello–Rahman barostat. Key simulation parameters included a 2-fs time-step and the Leap-Frog integrator. Bond lengths involving hydrogen atoms were constrained using the LINCS algorithm. Long-range electrostatic interactions were treated with the particle-mesh Ewald (PME) algorithm, with a cutoff of 1.2 nm for both van der Waals and short-range electrostatic interactions. Initial velocities were assigned based on a Maxwell distribution at 310.15 K. Each system was simulated for 1000 ns, and trajectory analyses were performed to investigate the structural and dynamic properties of **IPMCL-28b** and ciprofloxacin interactions with the membrane.

In Vivo Antibacterial Assessment and Biocompatibility Evaluation. All animal experiments were performed with the approval of the Institutional Animal Care and Use Committee (IACUC) of Jinan University (Approval number: 20240306-0026). The healthy male ICR mice (20 ± 2 g) were procured from the Guangdong Medical Laboratory Animal Centre. Subsequently, the mice were randomly divided into five groups, including control group, normal group, ciprofloxacin group and **IPMCL-28b** group. The concentrations of ciprofloxacin and **IPMCL-28b** utilized were both set at 5 mg mL^{-1} . After the back-hair removal, the mice were injected subcutaneously with MRSA (50 μL , 2×10^8 CFU mL^{-1}). At 30 min post-injection, 100 μL of sterile PBS, ciprofloxacin

hydrochloride solution, or **IPMCL-28b** solution was administered to the infected site. The infected skins were collected 48h post-injection, fixed with 4 % paraformaldehyde, embedded with paraffin, and stained with hematoxylin and eosin (H&E), Masson and Giemsa for assessing the antibacterial performance of various groups. Bacteria in the infected skin were quantified by plate counting and the bacterial colonies grown on MHA plates also imaged. Levels of IL-6 and TNF- α in the skin homogenate solutions were assessed by ELISA kits (Dakewe, Shenzhen, China). The major organs, including heart, liver, spleen, lung, and kidney, were also harvested for H&E analysis to investigate the systemic toxicity. In the local toxicity study, sterile PBS and **IPMCL-28b** (100 μ L, 5 mg mL $^{-1}$) was subcutaneously injected into the shaved backs of mice. At 2 h post-injection, the local skin tissues of mice were collected for H&E staining.

CRediT authorship contribution statement

Qi Wen: Writing – original draft, Methodology, Data curation. **Yuhang He:** Validation, Methodology, Data curation. **Jiaying Chi:** Methodology, Formal analysis, Data curation. **Luyao Wang:** Validation, Formal analysis. **Yixuan Ren:** Validation, Formal analysis. **Xiaoke Niu:** Resources, Formal analysis. **Yanqing Yang:** Software, Resources. **Kang Chen:** Formal analysis. **Qi Zhu:** Investigation, Data curation. **Juncheng Lin:** Validation, Formal analysis. **Yanghui Xiang:** Formal analysis, Data curation. **Junqiu Xie:** Validation, Resources. **Wenteng Chen:** Writing – review & editing. **Yongping Yu:** Writing – review & editing, Formal analysis. **Baohong Wang:** Resources, Formal analysis. **Bo Wang:** Writing – review & editing, Validation, Conceptualization. **Ying Zhang:** Writing – review & editing, Validation, Supervision, Methodology, Conceptualization. **Chao Lu:** Writing – review & editing, Supervision, Methodology, Conceptualization. **Kairong Wang:** Writing – review & editing, Supervision, Methodology, Conceptualization. **Peng Teng:** Writing – review & editing, Writing – original draft, Visualization, Validation, Supervision, Resources, Project administration, Investigation, Funding acquisition, Conceptualization. **Ruhong Zhou:** Writing – review & editing, Resources, Funding acquisition, Conceptualization.

Declaration of competing interest

The authors declare the following financial interests/personal relationships which may be considered as potential competing interests: Peng Teng reports financial support was provided by Zhejiang Provincial Natural Science Foundation of China. Ruhong Zhou reports financial support was provided by National Key R&D Program of China. Ruhong Zhou reports financial support was provided by National Center of Technology Innovation for Biopharmaceuticals. Ruhong Zhou reports financial support was provided by Shanghai Artificial Intelligence Lab. Ruhong Zhou reports financial support was provided by National Independent Innovation Demonstration Zone Shanghai Zhangjiang Major Projects. If there are other authors, they declare that they have no known competing financial interests or personal relationships that could have appeared to influence the work reported in this paper.

Acknowledgments

We thank the financial support from Zhejiang Provincial Natural Science Foundation of China (No. LMS25B020003), the National Key R&D Program of China (2021YFF1200404 and 2021YFA1201200), the National Center of Technology Innovation for Biopharmaceuticals (NCTIB2022HS02010), Shanghai Artificial Intelligence Lab (P22KN00272), the National Independent Innovation Demonstration Zone Shanghai Zhangjiang Major Projects (ZJZX2020014), the Starry Night Science Fund of Zhejiang University Shanghai Institute for Advanced Study (SN-ZJU-SIAS-003), Startup Funding of Zhejiang University, and Huahai Young Scholars Scientific Research Innovation Foundation at School of Pharmacy, Zhejiang University. We thank

Jianyang Pan (Research and Service Center, College of Pharmaceutical Sciences, Zhejiang University) for performing NMR spectrometry for structure elucidation. The authors also appreciate the support from Hanbon Sci & Tech of China for their help with the development of HPLC separation methods.

Appendix A. Supplementary data

Supplementary data to this article can be found online at <https://doi.org/10.1016/j.ejmech.2025.117496>.

Abbreviations Used

HDP, host-defense peptide; AMP, antimicrobial peptide; MRSA, Methicillin-resistant *Staphylococcus aureus*; HOBr, N-hydroxybenzotriazole; EDC, 1-(3-dimethylaminopropyl)-3-ethylcarbodiimide hydrochloride; DIPEA, *N,N*-diisopropylethylamine; DMF, dimethylformamide; SPPS, solid-phase peptide synthesis; CTC resin, 2-Chlorotriptylchloride resin; *S. aureus*, *Staphylococcus aureus*; ATCC, American type culture collection; MIC, minimum inhibitory concentrations; *E. gallinarum*, *Enterococcus gallinarum*; *E. faecalis*, *Enterococcus faecalis*; *E. coli*, *Escherichia coli*; *P. aeruginosa*, *Pseudomonas aeruginosa*; *A. baumannii*, *Acinetobacter baumannii*; RBCs, red blood cells; HC₅₀, 50 % hemolytic unit of complement; MTT, 3-(4,5-dimethylthiazol-2-yl)-2,5-diphenyltetrazolium bromide; PI, propidium iodide; SEM, scanning electron microscopy; H&E, hematoxylin and eosin; ELISA, enzyme-linked immunosorbent assay; TNF- α , tumor necrosis factor; IL-6, interleukin-6; HPLC, high-performance liquid chromatography; NMR, nuclear magnetic resonance; HRMS, high-resolution mass spectrometry; MALDI-TOF, matrix-assisted laser desorption ionization time of flight; DMSO, dimethyl sulfoxide; HCTU, 1-(bis(dimethylamino)methylene)-5-chloro-1H-benz[*d*] [1-3]triazole-1-ium 3-oxide; DIC, *N,N*'-diisopropylcarbodiimide; DCM, dichloromethane; TFA, trifluoroacetic acid; HFIP, 1,1,1,3,3,3-Hexafluoro-2-propanol; CLSI, Clinical and Laboratory Standards Institute; MHB, Hinton broth; MD, molecular dynamics; CFU, colony forming units; SD rat, Sprague-Dawley rat; PBS, phosphate buffered saline; IACUC, Institutional Animal Care and Use Committee; MH, Mueller-Hinton.

Data availability

No data was used for the research described in the article.

References

- [1] U. Theuretbacher, Challenges and strategies for addressing antibacterial drug resistance in LMICs, *Nat. Rev. Microbiol.* 22 (2024) 591–592.
- [2] Jim O'Neill, *Nat Rev Drug Dis* 15 (2016) 526, 526.
- [3] E.D. Brown, G.D. Wright, Antibacterial drug discovery in the resistance era, *Nature* 529 (2016) 336–343.
- [4] L.A. Mitscher, Bacterial topoisomerase inhibitors: quinolone and pyridone antibacterial agents, *Chem Rev* 105 (2005) 559–592.
- [5] H.A. Aziz, A.M. El-Saghier, M. badr, B.E.M. Elsadek, G.E.-D.A. Abou-Rahma, M. E. Shoman, Design, synthesis and mechanistic study of N-4-Piperazinyl Butyryl Thiazolidinedione derivatives of ciprofloxacin with Anticancer Activity via Topoisomerase I/II inhibition, *Sci. Rep.* 14 (2024) 24101.
- [6] Y.-Q. Hu, S. Zhang, Z. Xu, Z.-S. Lv, M.-L. Liu, L.-S. Feng, 4-Quinolone hybrids and their antibacterial activities, *Eur. J. Med. Chem.* 141 (2017) 335–345.
- [7] L.L. Shen, A.G. Pernet, Mechanism of inhibition of DNA gyrase by analogues of nalidixic acid: the target of the drugs is DNA, *Proc. Natl. Acad. Sci. USA* 82 (1985) 307–311.
- [8] B.D. Bax, P.F. Chan, D.S. Eggleston, A. Fosberry, D.R. Gentry, F. Gorrec, I. Giordano, M.M. Hann, A. Hennessy, M. Hibbs, J. Huang, E. Jones, J. Jones, K. K. Brown, C.J. Lewis, E.W. May, M.R. Saunders, O. Singh, C.E. Spitzfaden, C. Shen, A. Shillings, A.J. Theobald, A. Wohlkonig, N.D. Pearson, M.N. Gwynn, Type IIA topoisomerase inhibition by a new class of antibacterial agents, *Nature* 466 (2010) 935–940.
- [9] D.C. Hooper, Emerging mechanisms of fluoroquinolone resistance, *Emerg. Infect. Dis.* 7 (2001) 337–341.
- [10] J.H. Tran, G.A. Jacoby, Mechanism of plasmid-mediated quinolone resistance, *Proc. Natl. Acad. Sci. USA* 99 (2002) 5638–5642.

- [11] T.D.M. Pham, Z.M. Ziora, M.A.T. Blaskovich, Quinolone antibiotics, *MedChemComm* 10 (2019) 1719–1739.
- [12] M. Heidary, M. Shirani, M. Moradi, M. Goudarzi, R. Pouriran, T. Rezaeian, S. Khoshnood, Tuberculosis challenges: resistance, co-infection, diagnosis, and treatment, *Eur J Microbiol Immunol (Bp)* 12 (2022) 1–17.
- [13] L.E. Evans, A. Krishna, Y. Ma, T.E. Webb, D.C. Marshall, C.L. Tookey, J. Spencer, T. B. Clarke, A. Armstrong, A.M. Edwards, Exploitation of antibiotic resistance as a novel drug target: development of a β -lactamase-activated antibacterial prodrug, *J. Med. Chem.* 62 (2019) 4411–4425.
- [14] C.L. Ross, A. Lawer, K.J. Sircombe, D. Pletzer, A.B. Gamble, S. Hook, Site-specific antimicrobial activity of a dual-responsive ciprofloxacin prodrug, *J. Med. Chem.* 67 (2024) 9599–9612.
- [15] J. Meiers, E. Zahorska, T. Röhrig, D. Hauck, S. Wagner, A. Titz, Directing drugs to bugs: antibiotic-carbohydrate conjugates targeting biofilm-associated lectins of *Pseudomonas aeruginosa*, *J. Med. Chem.* 63 (2020) 11707–11724.
- [16] J. Meiers, K. Rox, A. Titz, Lectin-targeted prodrugs activated by *Pseudomonas aeruginosa* for self-destructive antibiotic release, *J. Med. Chem.* 65 (2022) 13988–14014.
- [17] P.P. Sedghizadeh, S. Sun, A.F. Junka, E. Richard, K. Sadrerafi, S. Mahabady, N. Bakhtshiani, N. Tjokro, M. Bartoszewicz, M. Oleksy, P. Szymczyk, M.W. Lundy, J.D. Neighbors, R.G.G. Russell, C.E. McKenna, F.H. Ebetino, Design, synthesis, and antimicrobial evaluation of a novel bone-targeting bisphosphonate-ciprofloxacin conjugate for the treatment of osteomyelitis biofilms, *J. Med. Chem.* 60 (2017) 2326–2343.
- [18] Y.-Y. Wang, X.-Y. Zhang, X.-L. Zhong, Y.-J. Huang, J. Lin, W.-M. Chen, Design and synthesis of 3-Hydroxy-pyridin-4(1H)-ones-Ciprofloxacin conjugates as dual antibacterial and antbiofilm agents against *Pseudomonas aeruginosa*, *J. Med. Chem.* 66 (2023) 2169–2193.
- [19] A. Pandey, C. Savino, S.H. Ahn, Z. Yang, S.G. Van Lanen, E. Boros, Theranostic gallium siderophore ciprofloxacin conjugate with broad spectrum antibiotic potency, *J. Med. Chem.* 62 (2019) 9947–9960.
- [20] A. Pandey, D. Śmiłowicz, E. Boros, Galbfoxacin: a xenometal-antibiotic with potent in vitro and in vivo efficacy against *S. aureus*, *Chem. Sci.* 12 (2021) 14546–14556.
- [21] M. Xiong, M.W. Lee, R.A. Mansbach, Z. Song, Y. Bao, R.M. Peek, C. Yao, L.-F. Chen, A.L. Ferguson, G.C.L. Wong, J. Cheng, Helical antimicrobial polypeptides with radial amphiphilicity, *Proc. Natl. Acad. Sci. U.S.A.* 112 (2015) 13155–13160.
- [22] D. Nagarajan, N. Roy, O. Kulkarni, N. Nanajkar, A. Datey, S. Ravichandran, C. Thakur, S. T. I.V. Aprameya, S.P. Samra, D. Chakravortty, N. Chandra, Q76: a designed antimicrobial peptide to combat carbapenem- and tigecycline-resistant *Acinetobacter baumannii*, *Sci. Adv.* 5 (2019) eaax1946.
- [23] M. Zasloff, Antimicrobial peptides of multicellular organisms, *Nature* 415 (2002) 389–395.
- [24] R.E. Hancock, H.G. Sahl, Antimicrobial and host-defense peptides as new anti-infective therapeutic strategies, *Nat. Biotechnol.* 24 (2006) 1551–1557.
- [25] C.D. Fjell, J.A. Hiss, R.E.W. Hancock, G. Schneider, Designing antimicrobial peptides: form follows function, *Nat. Rev. Drug Discov.* 11 (2012) 37–51.
- [26] B.P. Lazzaro, M. Zasloff, J. Rolff, Antimicrobial peptides: application informed by evolution, *Science* 368 (2020).
- [27] N. Mookherjee, M.A. Anderson, H.P. Haagsman, D.J. Davidson, Antimicrobial host defence peptides: functions and clinical potential, *Nat. Rev. Drug Discov.* 19 (2020) 311–332.
- [28] P. Teng, H. Shao, B. Huang, J. Xie, S. Cui, K. Wang, J. Cai, Small molecular mimetics of antimicrobial peptides as a promising therapy to combat bacterial resistance, *J. Med. Chem.* 66 (2023) 2211–2234.
- [29] H. Gong, X. Hu, M. Liao, K. Fa, D. Ciumac, L.A. Clifton, M.-A. Sani, S.M. King, A. Maestro, F. Separovic, T.A. Waigh, H. Xu, A.J. McBain, J.R. Lu, Structural disruptions of the outer membranes of gram-negative bacteria by rationally designed amphiphilic antimicrobial peptides, *ACS Appl. Mater. Inter.* 13 (2021) 16062–16074.
- [30] S. Gou, B. Li, X. Ouyang, Z. Ba, C. Zhong, T. Zhang, L. Chang, Y. Zhu, J. Zhang, N. Zhu, Y. Zhang, H. Liu, J. Ni, Novel broad-spectrum antimicrobial peptide derived from anoplins and its activity on bacterial pneumonia in mice, *J. Med. Chem.* 64 (2021) 11247–11266.
- [31] D.M. McGrath, E.M. Barbu, W.H.P. Driessens, T.M. Lasco, J.J. Tarrand, P. C. Okhuysen, D.P. Kontoyiannis, R.L. Sidman, R. Pasqualini, W. Arap, Mechanism of action and initial evaluation of a membrane active all-D-enantiomer antimicrobial peptidomimetic, *Proc. Natl. Acad. Sci. U.S.A.* 110 (2013) 3477–3482.
- [32] A. Ivankin, L. Livne, A. Mor, G.A. Caputo, W.F. DeGrado, M. Meron, B. Lin, D. Gidalevitz, Role of the conformational rigidity in the design of biomimetic antimicrobial compounds, *Angew. Chem. Int. Ed.* 49 (2010) 8462–8465.
- [33] D. Liu, S. Choi, B. Chen, R.J. Doerksen, D.J. Clements, J.D. Winkler, M.L. Klein, W. F. DeGrado, Nontoxic membrane-active antimicrobial arylamide oligomers, *Angew. Chem. Int. Ed.* 43 (2004) 1158–1162.
- [34] L.L. Ling, T. Schneider, A.J. Peoples, A.L. Spoering, I. Engels, B.P. Conlon, A. Mueller, T.F. Schäferle, D.E. Hughes, S. Epstein, M. Jones, L. Lazarides, V. A. Steadman, D.R. Cohen, C.R. Felix, K.A. Fetterman, W.P. Millett, A.G. Nitti, A. M. Zullo, C. Chen, K. Lewis, A new antibiotic kills pathogens without detectable resistance, *Nature* 517 (2015) 455–459.
- [35] K.A. Brodgen, Antimicrobial peptides: pore formers or metabolic inhibitors in bacteria? *Nat. Rev. Microbiol.* 3 (2005) 238–250.
- [36] B.H. Gan, J. Gaynor, S.M. Rowe, T. Deingruber, D.R. Spring, The multifaceted nature of antimicrobial peptides: current synthetic chemistry approaches and future directions, *Chem. Soc. Rev.* 50 (2021) 7820–7880.
- [37] M.A. Cook, G.D. Wright, The past, present, and future of antibiotics, *Sci. Transl. Med.* 14 (2022) eabo7793.
- [38] D.S.J. Ting, R.W. Beuerman, H.S. Dua, R. Lakshminarayanan, I. Mohammed, Strategies in translating the therapeutic potentials of host defense peptides, *Front. Immunol.* 11 (2020) 983.
- [39] B.L. Bray, Large-scale manufacture of peptide therapeutics by chemical synthesis, *Nat. Rev. Drug Discov.* 2 (2003) 587–593.
- [40] J. Wang, J. Song, Z. Yang, S. He, Y. Yang, X. Feng, X. Dou, A. Shan, Antimicrobial peptides with high proteolytic resistance for combating gram-negative bacteria, *J. Med. Chem.* 62 (2019) 2286–2304.
- [41] M. Magana, M. Pushpanathan, A.L. Santos, L. Leanne, M. Fernandez, A. Ioannidis, M.A. Giulianotti, Y. Apidianakis, S. Bradfute, A.L. Ferguson, A. Cherkasov, M. N. Seleem, C. Pinilla, C. de la Fuente-Nunez, T. Lazaridis, T. Dai, R.A. Houghton, R. E.W. Hancock, G.P. Tegos, The value of antimicrobial peptides in the age of resistance, *Lancet Infect. Dis.* 20 (2020) e216–e230.
- [42] M.A.T. Blaskovich, K.A. Hansford, Y. Gong, M.S. Butler, C. Muldoon, J.X. Huang, S. Ramu, A.B. Silva, M. Cheng, A.M. Kavanagh, Z. Ziora, R. Premraj, F. Lindahl, T. A. Bradford, J.C. Lee, T. Karoli, R. Pelingon, D.J. Edwards, M. Amado, A.G. Elliott, W. Phetsang, N.H. Daud, J.E. Deeeke, H.E. Sidjabat, S. Ramaologa, J. Zuegg, J. R. Betley, A.P.G. Beevers, R.A.G. Smith, J.A. Roberts, D.L. Paterson, M.A. Cooper, Protein-inspired antibiotics active against vancomycin- and daptomycin-resistant bacteria, *Nat. Commun.* 9 (2018) 22.
- [43] M.A.T. Blaskovich, K.A. Hansford, M.S. Butler, S. Ramu, A.M. Kavanagh, A. M. Jarrad, A. Prasetyoputri, M.E. Pitt, J.X. Huang, F. Lindahl, Z.M. Ziora, T. Bradford, C. Muldoon, P. Rajaratnam, R. Pelingon, D.J. Edwards, B. Zhang, M. Amado, A.G. Elliott, J. Zuegg, L. Coin, A.-K. Woischnig, N. Khanna, E. Breidenstein, A. Stincone, C. Mason, N. Khan, H.-K. Cho, M.J. Karau, K. E. Greenwood-Quaintance, R. Patel, M. Wootton, M.L. James, M.L. Hutton, D. Lyras, A.D. Ogunniyi, L.K. Mahdi, D.J. Trott, X. Wu, S. Niles, K. Lewis, J. R. Smith, K.E. Barber, J. Yim, S.A. Rice, M.J. Rybak, C.R. Ishmael, K.R. Hori, N. M. Bernthal, K.P. Francis, J.A. Roberts, D.L. Paterson, M.A. Cooper, A lipoglycopeptide antibiotic for Gram-positive biofilm-related infections, *Sci. Transl. Med.* 14 (2022) eabj2381.
- [44] E.A. Porter, B. Weisblum, S.H. Gellman, Mimicry of host-defense peptides by unnatural oligomers: antimicrobial β -peptides, *J. Am. Chem. Soc.* 124 (2002) 7324–7330.
- [45] L. Liu, K.C. Courtney, S.W. Huth, L.A. Rank, B. Weisblum, E.R. Chapman, S. H. Gellman, Beyond amphiphilic balance: changing subunit stereochemistry alters the pore-forming activity of nylon-3 polymers, *J. Am. Chem. Soc.* 143 (2021) 3219–3230.
- [46] Y. Qian, S. Deng, Z. Cong, H. Zhang, Z. Lu, N. Shao, S.A. Bhatti, C. Zhou, J. Cheng, S.H. Gellman, R. Liu, Secondary amine pendant β -peptide polymers displaying potent antibacterial activity and promising therapeutic potential in treating MRSA-induced wound infections and keratitis, *J. Am. Chem. Soc.* 144 (2022) 1690–1699.
- [47] W. Jiang, M. Zhou, Z. Cong, J. Xie, W. Zhang, S. Chen, J. Zou, Z. Ji, N. Shao, X. Chen, M. Li, R. Liu, Short guanidinium-functionalized poly(2-oxazoline)s displaying potent therapeutic efficacy on drug-resistant fungal infections, *Angew. Chem. Int. Ed.* 61 (2022) e202200778.
- [48] E. Lei, H. Tao, S. Jiao, A. Yang, Y. Zhou, M. Wang, K. Wen, Y. Wang, Z. Chen, X. Chen, J. Song, C. Zhou, W. Huang, L. Xu, D. Guan, C. Tan, H. Liu, Q. Cai, K. Zhou, J. Modica, S.-Y. Huang, W. Huang, X. Feng, Potentiation of vancomycin: creating cooperative membrane lysis through a “dermatization-for-sensitization” approach, *J. Am. Chem. Soc.* 144 (2022) 10622–10639.
- [49] W.X. Liang, Q. Yu, Z.X. Zheng, J.Y. Liu, Q.N. Cai, S.P. Liu, S.M. Lin, Design and synthesis of phenyl sulfide-based cationic amphiphiles as membrane-targeting antimicrobial agents against gram-positive pathogens, *J. Med. Chem.* 65 (2022) 14221–14236.
- [50] S. Lin, J.-J. Koh, T.T. Aung, W.L.W. Sin, F. Lim, L. Wang, R. Lakshminarayanan, L. Zhou, D.T.H. Tan, D. Cao, R.W. Beuerman, L. Ren, S. Liu, Semisynthetic flavone-derived antimicrobials with therapeutic potential against methicillin-resistant *Staphylococcus aureus* (MRSA), *J. Med. Chem.* 60 (2017) 6152–6165.
- [51] M. Zhou, M. Zheng, J. Cai, Small molecules with membrane-active antibacterial activity, *ACS Appl. Mater. Interfaces* 12 (2020) 21292–21299.
- [52] P. Teng, D. Huo, A. Nimmagadda, J. Wu, F. She, M. Su, X. Lin, J. Yan, A. Cao, C. Xi, Y. Hu, J. Cai, Small antimicrobial agents based on acylated reduced amide scaffold, *J. Med. Chem.* 59 (2016) 7877–7887.
- [53] W. Cheng, T. Xu, L. Cui, Z. Xue, J. Liu, R. Yang, S. Qin, Y. Guo, Discovery of amphiphilic xanthohumol derivatives as membrane-targeting antimicrobials against methicillin-resistant *Staphylococcus aureus*, *J. Med. Chem.* 66 (2023) 962–975.
- [54] R.P. Dewangan, D.P. Verma, N.K. Verma, A. Gupta, G. Pant, K. Mitra, S. Habib, J. K. Ghosh, Spermine-conjugated short proline-rich lipopeptides as broad-spectrum intracellular targeting antibacterial agents, *J. Med. Chem.* 65 (2022) 5433–5448.
- [55] Y. Niu, M. Wang, Y. Cao, A. Nimmagadda, J. Hu, Y. Wu, J. Cai, X.-S. Ye, Rational design of dimeric lysine N-alkylamides as potent and broad-spectrum antibacterial agents, *J. Med. Chem.* 61 (2018) 2865–2874.
- [56] V. Saini, D. Mehta, S. Gupta, S. Kumar, P. Rani, K. Rana, K. Rajput, D. Jain, G. Pal, B. Aggarwal, S. Pal, S.K. Gupta, Y. Kumar, V.S. Ramu, A. Bajaj, Targeting vancomycin-resistant enterococci (VRE) infections and van operon-mediated drug resistance using dimeric cholic acid-peptide conjugates, *J. Med. Chem.* 65 (2022) 15312–15326.
- [57] N. Shao, L. Yuan, P. Ma, M. Zhou, X. Xiao, Z. Cong, Y. Wu, G. Xiao, J. Fei, R. Liu, Heterochiral β -peptide polymers combating multidrug-resistant cancers effectively without inducing drug resistance, *J. Am. Chem. Soc.* 144 (2022) 7283–7294.
- [58] M. Wang, X. Feng, R. Gao, P. Sang, X. Pan, L. Wei, C. Lu, C. Wu, J. Cai, Modular design of membrane-active antibiotics: from macromolecular antimicrobials to small scorpionlike peptidomimetics, *J. Med. Chem.* 64 (2021) 9894–9905.

- [59] M. Wang, R. Gao, M. Zheng, P. Sang, C. Li, E. Zhang, Q. Li, J. Cai, Development of bis-cyclic imidazolidine-4-one derivatives as potent antibacterial agents, *J. Med. Chem.* 63 (2020) 15591–15602.
- [60] R. Zhong, H. Li, H. Li, S. Fang, J. Liu, Y. Chen, S. Liu, S. Lin, Development of amphiphilic coumarin derivatives as membrane-active antimicrobial agents with potent *in vivo* efficacy against gram-positive pathogenic bacteria, *ACS Infect. Dis.* 7 (2021) 2864–2875.
- [61] S. Choi, A. Isaacs, D. Clements, D. Liu, H. Kim, R.W. Scott, J.D. Winkler, W. F. DeGrado, De novo design and *in vivo* activity of conformationally restrained antimicrobial arylamide foldamers, *Proc. Natl. Acad. Sci. U.S.A.* 106 (2009) 6968–6973.
- [62] C. Ghosh, G.B. Manjunath, P. Akkapeddi, V. Yarlagadda, J. Hoque, D.S. Uppu, M. M. Konai, J. Haldar, Small molecular antibacterial peptoid mimics: the simpler the better, *J. Med. Chem.* 57 (2014) 1428–1436.
- [63] J.B. Bremner, P.A. Keller, S.G. Pyne, T.P. Boyle, Z. Brkic, D.M. David, A. Garas, J. Morgan, M. Robertson, K. Somphol, M.H. Miller, A.S. Howe, P. Ambrose, S. Bhavnani, T.R. Fritsche, D.J. Biedenbach, R.N. Jones, R.W. Buckheit Jr., K. M. Watson, D. Baylis, J.A. Coates, J. Deadman, D. Jeevarajah, A. McCracken, D. I. Rhodes, Binaphthyl-based dicationic peptoids with therapeutic potential, *Angew. Chem. Int. Ed.* 49 (2010) 537–540.
- [64] E. Bonvin, H. Personne, T. Paschoud, J. Reusser, B.-H. Gan, A. Luscher, T. Köhler, C. van Delden, J.-L. Reymond, Antimicrobial peptide-peptoid hybrids with and without membrane disruption, *ACS Infect. Dis.* 9 (2023) 2593–2606.
- [65] H. Personne, T. Paschoud, S. Fulgencio, S. Baeriswyl, T. Köhler, C. van Delden, A. Stocker, S. Javor, J.-L. Reymond, To Fold or not to fold: diastereomeric optimization of an α -helical antimicrobial peptide, *J. Med. Chem.* 66 (2023) 7570–7583.
- [66] B. Li, X. Ouyang, Z. Ba, Y. Yang, J. Zhang, H. Liu, T. Zhang, F. Zhang, Y. Zhang, S. Gou, J. Ni, Novel β -hairpin antimicrobial peptides containing the β -turn sequence of -rrrf- having high cell selectivity and low incidence of drug resistance, *J. Med. Chem.* 65 (2022) 5625–5641.
- [67] Y. Hu, H. Li, R. Qu, T. He, X. Tang, W. Chen, L. Li, H. Bai, C. Li, W. Wang, G. Fu, G. Luo, X. Xia, J. Zhang, Lysine stapling screening provides stable and low toxic cationic antimicrobial peptides combating multidrug-resistant bacteria *in vitro* and *in vivo*, *J. Med. Chem.* 65 (2022) 579–591.
- [68] K.K. Sharma, I.K. Maurya, S.I. Khan, M.R. Jacob, V. Kumar, K. Tikoo, R. Jain, Discovery of a membrane-active, ring-modified histidine containing ultrashort amphiphilic peptide that exhibits potent inhibition of cryptococcus neoformans, *J. Med. Chem.* 60 (2017) 6607–6621.
- [69] A.J. Tague, P. Putsatit, K.A. Hammer, S.M. Wales, D.R. Knight, T.V. Riley, P. A. Keller, S.G. Pyne, Cationic biaryl 1,2,3-triazolyl peptidomimetic amphiphiles: synthesis, antibacterial evaluation and preliminary mechanism of action studies, *Eur. J. Med. Chem.* 168 (2019) 386–404.
- [70] C. Ghosh, G.B. Manjunath, P. Akkapeddi, V. Yarlagadda, J. Hoque, D.S.S.M. Uppu, M.M. Konai, J. Haldar, Small molecular antibacterial peptoid mimics: the simpler the better, *J. Med. Chem.* 57 (2014) 1428–1436.
- [71] J. Hoque, M.M. Konai, S. Gonuguntla, G.B. Manjunath, S. Samaddar, V. Yarlagadda, J. Haldar, Membrane active small molecules show selective broad spectrum antibacterial activity with no detectable resistance and eradicate biofilms, *J. Med. Chem.* 58 (2015) 5486–5500.
- [72] H. Kong, S. Qin, D. Yan, B. Shen, T. Zhang, M. Wang, S. Li, M. Ampomah-Wireko, M. Bai, E. Zhang, J. Cai, Development of aromatic-linked diamino acid antimicrobial peptide mimics with low hemolytic toxicity and excellent activity against methicillin-resistant *Staphylococcus aureus* (MRSA), *J. Med. Chem.* 66 (2023) 7756–7771.
- [73] J.B. Patel, M.P. Weinstein, G.M. Eliopoulos, S.G. Jenkins, J.S. Lewis, B.M. Limbagi, A.J. Mathers, T. Mazzulli, R. Patel, S.S. Richter, M.J. Satlin, J.M. Swenson, M. Traczewski, J. Turnidge, B.L. Zimmer, Performance Standards for Antimicrobial Susceptibility Testing, 2019.
- [74] Y. Guo, E. Hou, T. Wen, X. Yan, M. Han, L.-P. Bai, X. Fu, J. Liu, S. Qin, Development of membrane-active honokiol/magnolol amphiphiles as potent antibacterial agents against methicillin-resistant *Staphylococcus aureus* (MRSA), *J. Med. Chem.* 64 (2021) 12903–12916.
- [75] M. Vaara, New polymyxin derivatives that display improved efficacy in animal infection models as compared to polymyxin B and colistin, *Med. Res. Rev.* 38 (2018) 1661–1673.
- [76] M. Berney, F. Hammes, F. Bosshard, H.-U. Weilenmann, T. Egli, Assessment and interpretation of bacterial viability by using the LIVE/DEAD BacLight kit in combination with flow cytometry, *Appl. Environ. Microb.* 73 (2007) 3283–3290.
- [77] X. Li, W. Wang, Q. Gao, S. Lai, Y. Liu, S. Zhou, Y. Yan, J. Zhang, H. Wang, J. Wang, Y. Feng, R. Yang, J. Su, B. Li, Y. Liao, Intelligent bacteria-targeting ZIF-8 composite for fluorescence imaging-guided photodynamic therapy of drug-resistant superbug infections and burn wound healing, *Exploration* 4 (2024) 20230113.
- [78] Y. Li, H. Wu, P. Teng, G. Bai, X. Lin, X. Zuo, C. Cao, J. Cai, Helical antimicrobial sulfono- γ -AApeptides, *J. Med. Chem.* 58 (2015) 4802–4811.
- [79] M. Bugnon, M. Goullioux, U.F. Röhrig, M.A.S. Perez, A. Daina, O. Michelin, V. Zoete, SwissParam 2023: a modern web-based tool for efficient small molecule parametrization, *J. Chem. Inf. Model.* 63 (2023) 6469–6475.
- [80] E.L. Wu, X. Cheng, S. Jo, H. Rui, K.C. Song, E.M. Dávila-Contreras, Y. Qi, J. Lee, V. Monje-Galvan, R.M. Venable, J.B. Klauda, W. Im, CHARMM-GUI Membrane Builder toward realistic biological membrane simulations, *J. Comput. Chem.* 35 (2014) 1997–2004.
- [81] J. Lee, X. Cheng, J.M. Swails, M.S. Yeom, P.K. Eastman, J.A. Lemkul, S. Wei, J. Buckner, J.C. Jeong, Y. Qi, S. Jo, V.S. Pande, D.A. Case, C.L. Brooks III, A. D. MacKerell Jr., J.B. Klauda, W. Im, CHARMM-GUI input generator for NAMD, GROMACS, AMBER, OpenMM, and CHARMM/OpenMM simulations using the CHARMM36 additive force field, *J. Chem. Theory Comput.* 12 (2016) 405–413.
- [82] D. Van Der Spoel, E. Lindahl, B. Hess, G. Groenhof, A.E. Mark, H.J.C. Berendsen, GROMACS: fast, flexible, and free, *J. Comput. Chem.* 26 (2005) 1701–1718.